

# Development of an Analytical Model of Erbium Doped Silicon Laser Diode

A thesis submitted to the Department of Electrical and Electronic Engineering (EEE)

of

Bangladesh University of Engineering and Technology (BUET)

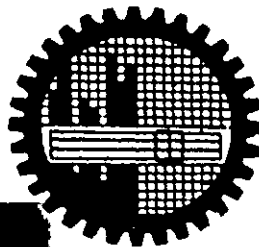
in partial fulfillment of the requirements for

the degree of

**MASTER OF SCIENCE IN ELECTRICAL AND ELECTRONIC ENGINEERING**

by

**Md. Zahid Hossain**




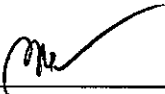


**DEPARTMENT OF ELECTRICAL AND ELECTRONIC ENGINEERING  
BANGLADESH UNIVERSITY OF ENGINEERING AND TECHNOLOGY**

July 2006

The thesis entitled “**Development of an Analytical Model of Erbium Doped Silicon Laser Diode**” submitted by Md. Zahid Hossain, Roll No.: 040406245P, Session: April 2004 has been accepted as satisfactory in partial fulfillment of the requirement for the degree of MASTER OF SCIENCE IN ELECTRICAL AND ELECTRONIC ENGINEERING on July 23, 2006.

## **BOARD OF EXAMINERS**

1.   
\_\_\_\_\_  
Dr. Md. Quamrul Huda  
Professor  
Department of Electrical and Electronic Engineering  
BUET, Dhaka-1000, Bangladesh.  
Chairman  
(Supervisor)
  
2.   
\_\_\_\_\_  
Dr. Satya Prasad Majumder  
Professor & Head  
Department of Electrical and Electronic Engineering  
BUET, Dhaka-1000, Bangladesh.  
Member  
(Ex-officio)
  
3.   
\_\_\_\_\_  
Dr. A. B. M. Harun-ur-Rashid  
Professor  
Department of Electrical and Electronic Engineering  
BUET, Dhaka-1000, Bangladesh.  
Member
  
4.   
\_\_\_\_\_  
Dr. Md. Abu Hashan Bhuyian  
Professor  
Department of Physics  
BUET, Dhaka-1000, Bangladesh.  
Member  
(External)

## Declaration

I hereby declare that this thesis or any part of it has not been submitted elsewhere for the award of any degree or diploma.

Signature of the candidate



---

(Md. Zahid Hossain)

## **Dedication**

Those who inspired me in the quest of  
knowledge

# Acknowledgements

I would like to express my sincere gratitude and profound respect to my supervisor Dr. Md. Quamrul Huda, Professor, Department of Electrical and Electronic Engineering (EEE), Bangladesh University of Engineering and Technology (BUET), Bangladesh for his continuous guidance and advice during every stage of this work. I am grateful to him for his continual inspiration and support without which it is impossible for me to complete the work. I am also indebted to him for acquainting me to the advanced research world.

I want to thank the Head, Department of EEE, BUET for giving me the opportunity to use the Robert Noyce Simulation Lab. I am also thankful to all personnel of simulation laboratory and departmental library.

I am grateful to my family members for their encouragement and blessing. I remain indebted to my friends and colleagues who inspired me and gave valuable suggestions to complete this thesis.

# CONTENTS

<b>Declaration</b>	iii
<b>Dedication</b>	iv
<b>Acknowledgements</b>	v
<b>List of Figures</b>	viii
<b>Abstract</b>	xi
<b>Chapter One – Introduction</b>	
1.1 Silicon Photonics	1
1.2 Luminescence in Silicon from Erbium	2
1.3 Literature Review	3
1.4 Objective of the Thesis	5
1.5 Organization of the Thesis	5
<b>Chapter Two – Luminescence from Silicon</b>	
2.1 Direct and Indirect Bandgap	7
2.2 Erbium in Silicon	8
2.3 Transition of Er <sup>3+</sup> at 1.54 $\mu\text{m}$	9
2.4 Excitation Mechanism of Erbium in Silicon	9
2.5 De-excitation Mechanism of Erbium in Silicon	10
2.6 Shockley-Read-Hall (SRH) Generation-Recombination Kinetics	13
2.7 Occupation Probability of Erbium Site	14
<b>Chapter Three – Laser Fundamentals</b>	
3.1 Emission and Absorption of Radiation	16
3.2 Einstein Relations	18
3.3 Absorption of Radiation	20
3.4 Population Inversion	21
3.5 Optical Feedback	21
3.6 Threshold Condition for Laser Oscillation	22

## **Chapter Four – Mathematical Model of Erbium Doped Silicon Laser**

4.1	Rate equation for Si:Er Laser	24
4.2	Threshold Gain and Current Density	28
4.3	Power vs. Current Density Characteristics	30
4.3.1	Condition (i): Below Threshold	31
4.3.2	Condition (ii): Above Threshold	32
4.4	Direct Current Modulation of Si:Er Diode Laser	34
4.4.1	Optical Gain	35
4.4.2	Steady State Characteristics	35
4.4.3	Small Signal Analysis	37
4.5	Large Signal Analysis and Transient Behavior	41

## **Chapter Five – Results and Discussion**

5.1	Parameters for Erbium Incorporated Silicon	42
5.2	Excited Erbium Atom and Laser Operation	43
5.2.1	Effect of Internal Loss Coefficient	44
5.2.2	Effect of Erbium Radiative Lifetime	45
5.2.3	Effect of Doping Concentration	47
5.2.4	Effect of Spectral Width	47
5.3	Power-Current Characteristics	49
5.4	Effect of Injection Dependent Loss Coefficient	54
5.5	Frequency Response	54
5.6	Transient Characteristics	59

## **Chapter Six – Conclusion**

6.1	<u>Recommendation for future work</u>	64
-----	---------------------------------------	----

<b>APPENDIX – A</b>	Derivation of injected carrier density at threshold	65
---------------------	---	----

<b>APPENDIX – B</b>	Derivation of EDS Laser Output Power	68
---------------------	--------------------------------------	----

<b>APPENDIX – C</b>	EDS Laser Frequency Response	75
---------------------	------------------------------	----

<b>APPENDIX – D</b>	Flowchart for transient characteristics	84
---------------------	---	----

<b>References</b>		85
-------------------	--	----

## List of Figures

Fig. 2.1 E-k diagram for direct and indirect bandgap material.	8
Fig. 2.2 Schematic representation of the Er <sup>3+</sup> intra 4f energy levels.	9
Fig. 2.3 Schematic representation of impurity Auger de-excitation processes for Er in Si: (a) Auger de-excitation with free electrons (b) Auger de-excitation with free holes, (c) Auger de-excitation with bound electrons and (d) Auger de-excitation with bound holes.	11
Fig. 2.4 Schematic representation of energy back transfer process	12
Fig. 2.5 Schematic diagram of SRH generation-recombination processes: (a) electron capture, (b) electron emission, (c) hole capture and (d) hole emission.	14
Fig. 3.1 Two energy level system.	17
Fig. 3.2 Energy state diagram showing (a) stimulated absorption, (b) spontaneous emission and (c) stimulated emission. The black dot indicates the electron which takes part in the transition between the energy levels.	17
Fig. 3.1 Radiation passing through a volume element of length $\Delta x$ and unit cross sectional area.	20
Fig. 3.2 Schematic representation of the Fabry-Perot optical cavity. The shadowed bars indicate the end mirrors.	22
Fig. 4.1 Model for the excitation and de-excitation of Er in Si.	25
Fig. 4.2 Model used in the rate equation analysis of erbium doped silicon laser.	25
Fig. 4.3 Photon is passing through the cavity medium of gain $g$ . The length of the cavity element is $L$ and time for a photon to travel this distance is $\Delta t$ .	27
Fig. 4.4 Variation of output power $P(t)$ with the variation of injection current density $J(t)$ where $P_0$ and $J_0$ are the bias values for direct current modulation of EDS laser.	34
Fig. 5.1 Excited Er atom as a function of excess carrier density for different values of loss coefficient ( $\alpha$ ) with $N_{Er} = 10^{19} \text{ cm}^{-3}$ .	44
Fig. 5.2 Excited Er atom as a function of excess carrier density for different values of loss coefficient ( $\alpha$ ) with $N_{Er} = 10^{20} \text{ cm}^{-3}$ .	45
Fig. 5.3 Excited erbium atom as a function of excess carrier density for different values of Er radiative lifetime with $N_{Er} = 10^{19} \text{ cm}^{-3}$ .	46



<b>Fig. 5.4</b> Excited Er atom as a function of excess carrier density for different values of Er radiative life time with $N_{Er} = 10^{20} \text{ cm}^{-3}$ .	46
<b>Fig. 5.5</b> Excited erbium atom as a function of excess carrier density for different values of doping concentration with $N_{Er} = 10^{19} \text{ cm}^{-3}$ .	47
<b>Fig. 5.6</b> Excited Er atom as a function of excess carrier density for different values of spectral width of emission with $N_{Er} = 10^{19} \text{ cm}^{-3}$ .	48
<b>Fig. 5.7</b> Excited Er atom as a function of excess carrier density for different values of spectral width of emission with $N_{Er} = 10^{20} \text{ cm}^{-3}$ .	48
<b>Fig. 5.8</b> Output power vs injection current density of EDS laser for different values of loss coefficient with $N_{Er} = 10^{19} \text{ cm}^{-3}$ .	49
<b>Fig. 5.9</b> Output power vs injection current density of EDS laser for different values loss coefficient with $N_{Er} = 10^{20} \text{ cm}^{-3}$ .	50
<b>Fig. 5.10</b> Output power vs injection current density of EDS laser for different erbium life time with Er concentration of $N_{Er} = 10^{19} \text{ cm}^{-3}$ .	51
<b>Fig. 5.11</b> Output power vs injection current density of EDS laser for different erbium lifetime. The inset shows only the spontaneous power. In this case, erbium concentration is $N_{Er} = 10^{20} \text{ cm}^{-3}$ .	51
<b>Fig. 5.12</b> Output power vs injection current density of EDS laser for different values of background doping concentration with $N_{Er} = 10^{19} \text{ cm}^{-3}$ .	52
<b>Fig. 5.13</b> Output power vs injection current density of EDS laser for different spectral width. The doped Er concentration is $10^{20} \text{ cm}^{-3}$ .	53
<b>Fig. 5.14</b> Output power vs injection current density of EDS laser for different silicon lifetime. The erbium concentration is $10^{19} \text{ cm}^{-3}$ .	53
<b>Fig. 5.15</b> Effect of injected carrier dependent absorption loss coefficient on the EDS laser output power.	54
<b>Fig. 5.16</b> Semi-log plot of frequency response of erbium doped silicon laser for different output powers.	55
<b>Fig. 5.17</b> Plot of relaxation oscillation frequency and the 3-dB bandwidth of EDS laser for different output power.	56
<b>Fig. 5.18</b> Plot of relaxation frequency ( $f_r$ ) and actual peak frequency of resonance ( $f_p$ ) for different output power.	56

<b>Fig. 5.19</b> Effect of output power on the damping coefficient ( $\gamma$ ) and relaxation resonance frequency ( $f_r$ ).	57
<b>Fig. 5.20</b> Normalized magnitude of the peak of the modulation response as a function of output power.	58
<b>Fig. 5.21</b> Transient response of excited erbium atoms of EDS laser for step input current density $J=27.6\text{A/cm}^2$ (carrier concentration $10^{19}\text{cm}^{-3}$ ). After transient state, the excited erbium atoms clamp to its threshold value $N_{Erth}^*$ .	60
<b>Fig. 5.22</b> Transient response for photon density of EDS laser for step input current density $J=27.6\text{A/cm}^2$ .	60
<b>Fig. 5.23</b> Transient response of excited erbium atoms of EDS laser for step input current density $J=276\text{A/cm}^2$ (carrier concentration $10^{20}\text{cm}^{-3}$ ).	61
<b>Fig. 5.24</b> Transient response of photon density of EDS laser for step input current density $J=276\text{A/cm}^2$ .	61
<b>Fig. 5.25</b> Transient response of excited erbium atoms of EDS laser for step input current density $J=1380\text{A/cm}^2$ (carrier concentration $5 \times 10^{20}\text{cm}^{-3}$ ). Here oscillation dies out quickly.	62
<b>Fig. 5.26</b> Transient response of photon density of EDS laser for step input current density $J=1380\text{A/cm}^2$ .	62

## Abstract

An analytical model is developed for laser operation from erbium doped silicon. The mechanism of erbium excitation through Shockley-Read-Hall (SRH) recombination process in silicon is analyzed for conditions of achieving the lasing threshold. Stimulated and spontaneous emission and the stimulated absorption of light by erbium under different conditions are determined. The effects of erbium concentration, background doping, erbium lifetime, loss coefficient, carrier lifetime etc. are investigated on the light output. Enhancement of the absorption coefficient of light with the increase of carrier injection is studied. Rate equations for the excited erbium atom and photon density are solved for determining the dynamic characteristics of laser. The steady state values for excited erbium atom and photon density are determined as a function of the excitation current. Sinusoidal small signal variation is added to the steady state current density and modulation transfer function is determined to evaluate the frequency response characteristics and 3-dB cutoff points. It is found that bandwidth of erbium doped silicon laser is of the order of hundred MHz range, which increases with the output power level. Numerical solution of the rate equations for large signal is done for studying the transient behavior and turn-on time of the laser. The laser turn-on time is found to reduce with the increasing excitation level.



# CHAPTER ONE

## Introduction

### 1.1 Silicon Photonics

Silicon is the most important semiconductor material in today's microelectronics technology. Because of its good mechanical, chemical and electrical properties and continuous improvement in scale integration, this semiconductor has proved to be the best choice in satisfying the increasing demand for more complex integrated circuits. But with the increase of scale integration, the number of devices per chip increases by reducing the device size and increasing the chip area and also there is an increase in clock frequency. As the chip size and complexity increase, interconnection needs more space and difficult to accommodate which is a bottleneck towards the miniaturization and high speed operation of integrated circuit. So a complete integration of optoelectronic devices on silicon IC chip may be an effective solution to overcome these hurdles. In this scheme, electrical signal is converted by light emitter to optical form and transferred to another part of the chip. The optical signal is then detected at the receiving end and converted back to the electrical signal by a photodetector. Optical system offers enormous bandwidth which is suitable for high speed data transmission. Optical transmission is free from any ambient electrical noise, electromagnetic interference, and echoes or cross-talk. Thus optical interconnection offers a high degree of flexibility and versatility.

Silicon devices constitute most of the integrated circuits in present day technology. But using conventional IC technology, integration of group III-V heterojunction LED/LASER on silicon chip is complicated and very expensive. Hybrid solutions are expensive and often become ineffective. Furthermore, compound semiconductors fail to grow epitaxially on crystalline silicon. If silicon be considered as light emitting components, problems of monolithic integration between optoelectronics and



microelectronics will be removed. But due to the indirect nature of its energy band structure, bulk silicon is indeed not a good light emitter. Achievement of efficient light emission from crystalline silicon is now being considered as one of the most crucial steps towards the development of fully silicon-based optoelectronics functionality. Several optical functions such as laser, amplifier and optical modulator have been shown to be achievable from silicon [1].

## 1.2 Luminescence in Silicon from Erbium

The issue of silicon as light source is still at elementary stage. Several different approaches such as band gap engineering, addition of isovalent impurities, use of porous silicon, etc. are being attempted to overcome this drawback. Incorporation of rare earth element erbium into silicon is considered to be one of the most promising approaches in order to obtain light from silicon. The erbium ion, when incorporated in Si in the trivalent charge state shows an intra- $4f$  shell atomic transition between the first excited state  $^4I_{13/2}$  and the ground state  $^4I_{15/2}$  and emits photon at a wavelength of  $1.54\mu\text{m}$ . This wavelength matches to the minimum of the light absorption spectra in silica-based optical fibers. Again, silicon band gap energy is much higher than the photon energy at this wavelength and hence silicon becomes transparent. This avoids the cross-link effect on device performances.

Although erbium doped silicon shows above mentioned promising results, this field remained unexplored for several years due to the lack of room temperature (RT) luminescence. Erbium also suffers low solubility limit in silicon. Problem of limited solid solubility has been overcome by the use of solid phase epitaxial recrystallization following the ion implantation process [2]. Recently observation of photoluminescence [3] and electroluminescence [4] at room temperature has opened up the renewed enthusiasm on erbium doped silicon devices. Prospect of erbium doped silicon laser has little bit explored. Since erbium has longer decay lifetime from  $^4I_{13/2}$  state to the ground state, it has a scope of population inversion. For optimized conditions of pumping actions and minimized non-radiative competition, it may be possible to achieve population inversion and lasing action in erbium doped silicon [1]. Thus the rare earth element erbium may play an important role in the development of silicon based laser and other optoelectronic devices capable of operating at GHz frequency level.

### 1.3 Literature Review

Light emission from silicon is a long quest for the last few years and extensive research works have been done on this issue. In 1983, Ennen et al. [5] have pointed out the potential applications of rare earth elements in semiconductor materials particularly in silicon for the development of light-emitting diodes and lasers. They also showed that erbium is a promising dopant of all rare earth elements because it shows a sharp atomic-like luminescence at 1.54  $\mu\text{m}$  wavelength and this luminescence was fairly independent of the host material. This phenomenon makes the Si:Er system very attractive for silicon based optoelectronics.

Ennen et al. [6] and Tang et al. [7] carried out photo emission analysis from erbium in silicon. They demonstrated that most of the optically active  $\text{Er}^{3+}$  ions have tetrahedral or lower site symmetries on interstitial lattice sites in Si. Enhancement of luminescence in the presence of impurities such as O, C, N, F or Br has been found by a number of authors. Michel et al. [3] found a large enhancement of luminescence intensity by introducing oxygen. They also showed that erbium photoluminescence vary for FZ and CZ materials at higher annealing temperatures. By using Extended X-ray Absorption Fine Spectroscopy (EXAFS) analysis, Alder et al. [8] found that the impurities modify the chemical surrounding of Er in Si and form erbium impurity complex. Since O activates erbium optically, researches are very much interested in Si:Er system with O co-dopant.

Erbium has demonstrated to present donor behavior in silicon [9]. It was pointed out that oxygen co-implant enhances Er activity [10-11]. They suggested that this donor behavior might be the result of the formation of Er-O complexes in EDS. Based on these results, Priolo et al. [11] suggested that electrical and optical activation of Er in Si could be correlated, i.e., the Er donor behavior might be associated with the  $\text{Er}^{3+}$  state. Coffa et al. [12] also showed that incorporation of oxygen increases the electrical and optical activation of Er in Si. Lombardo et al. [13] evaluated erbium luminescence both under forward and reverse biased condition using electrical excitation. They pointed out that luminescence intensity under reverse bias is higher than under forward bias.

One of the major limitations of Si:Er system is that its intensity falls sharply with increasing temperature. This phenomenon is called temperature quenching. Libertino et al. [10], by using DLTS and SRP measurements showed that only 1% of the total amount of erbium ions introduce a level at 0.15 eV below the silicon conduction band while most of them introduce much shallower level. These shallow levels are hindrance to achieve erbium luminescence at high temperature. Coffa et al. [12] demonstrated that emission of electron from the erbium trap level to the conduction band is responsible for reduced erbium luminescence. Priolo et al. [14] demonstrated that the dissociation of bound excitons results temperature quenching.

Kik et al. [15] performed luminescence decay measurement within the temperature range of 12K to 170K. They observed that the luminescence intensity decreases by three orders of magnitude as temperature rises from 12 to 150K. They pointed out that thermalization of bound excitons and non-radiative energy back transfer process is responsible for temperature quenching.

Priolo et al. [14] and Coffa et al. [12] demonstrated that co-doping with impurities such as O, C or F reduced temperature quenching significantly. They showed that different impurities produce a different reduction in the concentration of erbium-related deep levels. Since these deep levels act as efficient recombination centers for carriers, reduction of these levels would produce an increase in the lifetime and hence a reduced temperature quenching.

Franzo et al. [4] observed room temperature electroluminescence from Er and O co-doped crystalline p-n Si diodes under both forward and reverse biased conditions. They suggested that Er excitation occur through electron-hole mediated processes under forward biased conditions and through impact excitation under reverse biased condition. They found that temperature quenching could be significantly reduced while operating under reverse biased condition.

Shin et al. [16] showed the effect of short excitation pulse on erbium luminescence. They demonstrated that erbium atom continues to excite for some times even after the excitation pulse is turned off. From this phenomenon, they concluded that  $\text{Er}^{3+}$  ions in Si

are excited by recombination of carriers trapped at a state in the forbidden gap of Si and supported the involvement of bound exciton for erbium excitation in silicon host.

To the best of our knowledge, no work has been done on the possible achievement of laser action from erbium doped silicon. Xie et al. [1] studied the stimulated emission and light amplification for erbium doped silicon structure. They showed that the threshold population inversion for laser action is theoretically possible to achieve in overly optimistic case.

## **1.4 Objective of the Thesis**

The goal of this work is to develop an analytical model for erbium doped silicon laser diode. Possibility of laser operation from EDS medium will be investigated. Threshold current density for lasing will be determined. Power output versus current density characteristics of EDS laser will be developed from time independent rate equations. Effect of erbium concentration, background doping, erbium lifetime, carrier lifetime, loss coefficient etc. on light output will be discussed. At high level of carrier injection, loss coefficient does not remain constant. This effect will be analyzed on light output. Rate equations will be solved for small-signal in order to evaluate the performance of EDS laser as a direct analog modulator. Numerical simulations of the rate equations will also be done to get a look of the transient behaviors.

## **1.5 Organization of the Thesis**

This thesis consists of six chapters. Chapter one describes the necessity of silicon based optoelectronic devices and objectives of the present work.

Chapter two deals with band structure of materials, optical properties of erbium in silicon, literature review on erbium doped silicon (EDS) system, excitation and de-excitation mechanism of erbium ions, Shockley-Read-Hall recombination kinetics and probability of electron occupied erbium site.

Chapter three discusses the elementary theory of semiconductor laser, population inversion, condition of lasing threshold etc.



In chapter four, mathematical model for erbium doped silicon laser has been developed. Output power and small signal modulation transfer function have been determined. The derivations present an understanding of the important parameters in the model.

Chapter five demonstrates the result for the model equations presented in chapter four. Effects of various parameters have been explained with graphical presentation.

Chapter six gives a short outlook of the result presented in chapter five and proposes some recommendations for future works in this area.

# CHAPTER TWO

## Erbium Luminescence

In this chapter, an introduction is given about silicon with erbium doping for light emission and the resulting energy levels with the possible atomic transitions. Direct and indirect bandgap structure, excitation and de-excitation mechanism of erbium atoms in silicon host, Shockley-Read-Hall (SRH) generation-recombination kinetics etc. are discussed in brief. Steady state and time dependent probability of erbium site occupied by electron are presented.

### 2.1 Direct and Indirect Bandgap

Depending on the energy band structure ( $E$ - $k$  diagram), semiconductor materials are classified into two types: direct bandgap and indirect bandgap semiconductor. The energy vs. propagation constant curve ( $E$ - $k$ ) for two typical cases is shown in Fig. 2.1. In direct bandgap semiconductor, the minimum of the conduction band lies directly above the maximum of the valence band in  $k$ -space. Here, an electron at the conduction-band minimum can recombine directly with a hole at the valence band maximum and conserve momentum. The energy of the recombination across the bandgap will be emitted in the form of a photon. This is radiative recombination and also called spontaneous emission. InP, GaAs, InAs etc. are the examples of direct band gap materials and suitable for light emitting devices.

In indirect bandgap semiconductors, the conduction band minimum and valence band maximum have different propagation constant  $k$ . Here direct transition across the bandgap does not conserve momentum and is forbidden. Recombination occurs with the involvement of a third particle like phonon or a crystallographic defect which allows for the conservation of momentum. The recombination will often release the bandgap energy

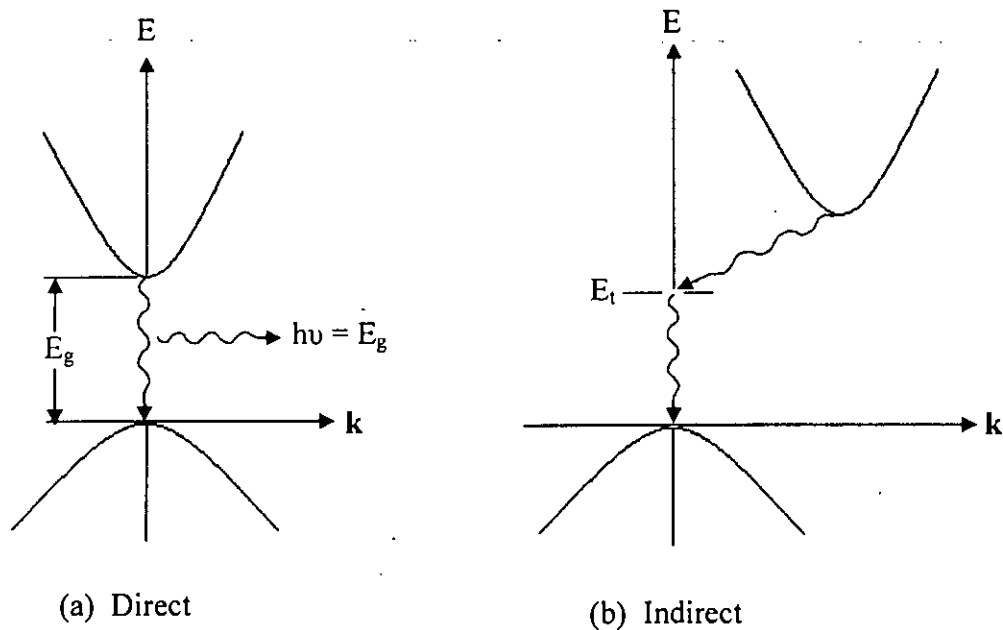


Fig. 2.1 E-k diagram for direct and indirect bandgap material.

as phonons instead of photons. So, light emission from indirect semiconductors is very inefficient and weak. Examples for indirect material include Si, Ge, and AlAs etc.

## 2.2 Erbium in Silicon

Erbium is a rare earth element belonging to the lanthanide group and it is so far the best optical dopant in silicon for efficient light emission. It generally has the trivalent charge state  $\text{Er}^{3+}$  when embedded in a solid, losing two electrons from the outermost  $6s$  shell and one electron from the  $4f$  shell and it has then an electronic configuration of Xenon  $[\text{Xe}]4f^{11}$ . The incompletely filled  $4f$ -shell of the  $\text{Er}^{3+}$  ion allows different electronic configurations with different energies due to spin-spin and spin-orbit interactions. For a free  $\text{Er}^{3+}$  ion, the radiative transitions between most of these energy levels are forbidden. But when Er is incorporated in a solid, for example silicon, perturbation of the  $4f$  wave functions by the surrounding material occurs which cause Stark-splitting of the different energy levels. This result in a broadening of the optical transitions making radiative transitions weakly allowed. The schematic energy level diagram of Fig. 2.2 shows the Stark-splitting of  $\text{Er}^{3+}$  ion embedded in silicon.

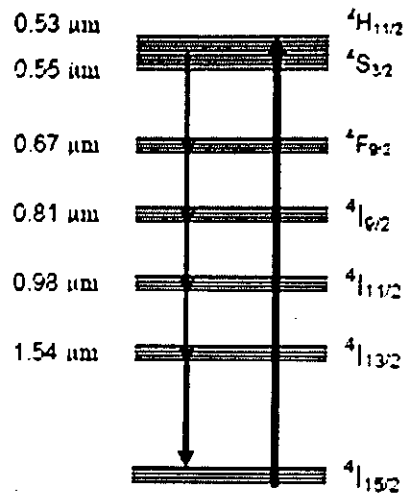


Fig. 2.2 Schematic representation of the  $\text{Er}^{3+}$  intra  $4f$  energy levels.

### 2.3 Transition from $\text{Er}^{3+}$ at $1.54 \mu\text{m}$

The transition from the first excited state of  $\text{Er}^{3+}$  ( ${}^4I_{13/2}$ ) to the ground state ( ${}^4I_{15/2}$ ) gives a photon of wavelength  $1.54 \mu\text{m}$  which is represented by the small thick arrow in Fig. 2.2. As the  $4f$ -shell is shielded from its surrounding by  $5s$  and  $5p$  shells, this emission wavelength is not very sensitive to the host material. The decay time for the  $1.54 \mu\text{m}$  transition is long which is about a few milliseconds. Once the Er is excited to one of its higher levels, it then rapidly decays to the  ${}^4I_{13/2}$  level via multi-phonon emissions. The long decay time of the first excited state  ${}^4I_{13/2}$  provides the possibility of having population inversion and constructing a laser from erbium doped silicon structure. However, the probability for stimulated emission is quite small because of low optical gain. Also there are several non-radiative processes competing with the radiative de-excitation which are explained in the section 2.6. The large transition energy (0.8 eV) of the first excited state of Er makes the multi-phonon emission unlikely and efficient emission at  $1.54 \mu\text{m}$  may be possible.

### 2.4 Excitation Mechanism of Erbium in Silicon

Exact mechanism of erbium excitation from ground state ( ${}^4I_{15/2}$ ) to the first excited state ( ${}^4I_{13/2}$ ) is yet to be unknown. When erbium is doped with an impurity, a trap level is formed at 0.15 eV below the conduction band. This trap level acts as recombination centre for erbium excitation. It has been suggested that excitation of Er atoms from silicon host is a carrier mediated process [16-22]. Palm et al. [19] proposed that electron-

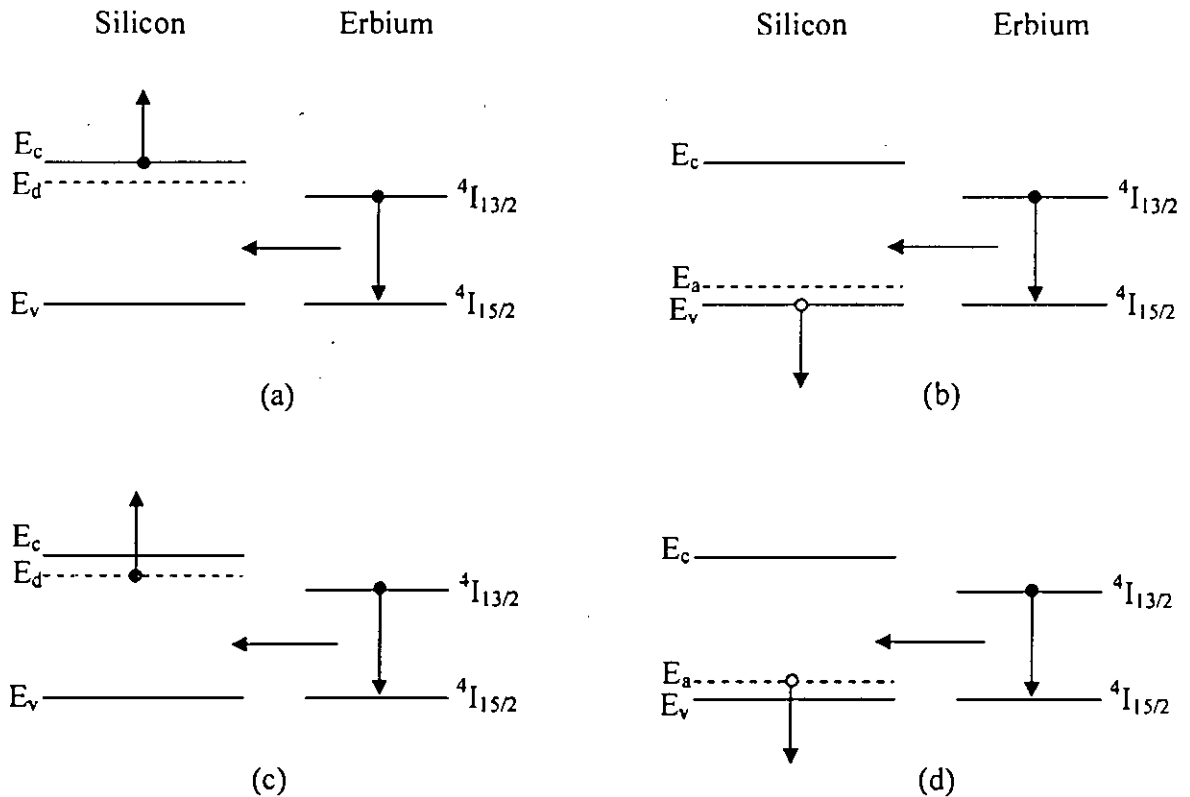
hole pair forms bound exciton due to coulomb attraction between them. Recombination of the bound exciton near the erbium related level gives up energy which is responsible for erbium excitation. The same excitation mechanism has also been suggested by Shin et al. [16] and Coffa et al. [20]. Huda et al. [21] proposed another excitation model of erbium luminescence based on Shockley-Read-Hall (SRH) recombination kinetics. According to their model, after the generation of excess carrier either by optical or electrical excitation, electrons from the conduction band recombine with holes from the valence band via erbium related trap levels. The energy given up due to recombination excites erbium atom. The erbium atom can then decay radiatively, resulting in 1.54  $\mu\text{m}$  luminescence.

Franzo et al. [22] proposed a different excitation mechanism of erbium atom in reverse-biased p-n junction diode. At reverse bias, the  $\text{Er}^{3+}$  ions are excited by the hot carrier impact excitation mechanism. When the p-n junction is reversed biased, the electrons tunnel from the p-side of the junction to the n-side if the applied field is high enough. Then they will get accelerated at the other side of the depletion layer by the applied electric field and become hot electrons. When a hot electron with kinetic energy higher than the energy difference between the ground state ( $^4I_{15/2}$ ) and the first excited state ( $^4I_{13/2}$ ) of  $\text{Er}^{3+}$  collides with another  $\text{Er}^{3+}$  ion, the second  $\text{Er}^{3+}$  can be excited by this impact process.

## 2.5 De-excitation Mechanism of Erbium in Silicon

There are two kinds of possible de-excitation mechanisms for the excited erbium atom to come to the ground state ( $^4I_{15/2}$ ). The first one is radiative de-excitation with a life time of approximately 1 ms [1]. This de-excitation process is responsible for light emission. The second one is non-radiative de-excitation which does not produce any light. Here instead of emitting a photon, the energy given up due to transition is wasted as heat. The radiative de-excitation between the first excited state ( $^4I_{13/2}$ ) and the ground state ( $^4I_{15/2}$ ) of  $\text{Er}^{3+}$  ions emits photon at wavelength of 1.54  $\mu\text{m}$ . This transition level is required in our device and this is the active level where the laser action may take place. Thus to have an efficient luminescence, it is important to suppress the competing non-radiative de-excitation processes which limit the light emission from erbium because of the long decay time of the  $^4I_{13/2}$  state.

Depending on the way of de-excitation, non-radiative de-excitation of erbium in silicon has been categorized into two different classes such as (i) impurity Auger de-excitation and (ii) energy back transfer. Fig. 2.3 demonstrates the various impurity Auger de-excitation processes.



**Fig. 2.3** Schematic representation of impurity Auger de-excitation processes for Er in Si: (a) Auger de-excitation with free electrons, (b) Auger de-excitation with free holes, (c) Auger de-excitation with bound electrons, and (d) Auger de-excitation with bound holes.

**(i) Impurity Auger De-excitation:** In this process, excited  $\text{Er}^{3+}$  ion de-excites by giving its energy to a free electron in the conduction band or to a hole in the valence band or carriers bound to shallow donor or acceptor level. By absorbing this energy, free carriers or bound carriers go to the higher energy state. Depending on the recipient of the energy, Auger process can be classified into following two groups.

**(a) Impurity Auger de-excitation with free carriers:** The de-excitation probability of erbium atoms through this process is proportional to the concentration of free carriers. So a lifetime corresponding to this process is defined as inversely proportional to the free carriers. Priolo et al. [17] has mathematically expressed this process by

$$\frac{1}{\tau_{Af}} = C_{Ac} n \quad \text{for n-type Si}$$

$$\frac{1}{\tau_{Af}} = C_{Ah} p \quad \text{for p-type Si}$$

where  $\tau_{Af}$  is the decay lifetime,  $C_{Ac}$  and  $C_{Ah}$  are Auger coefficient for free carriers,  $n$  and  $p$  are the free electron and hole concentrations respectively.

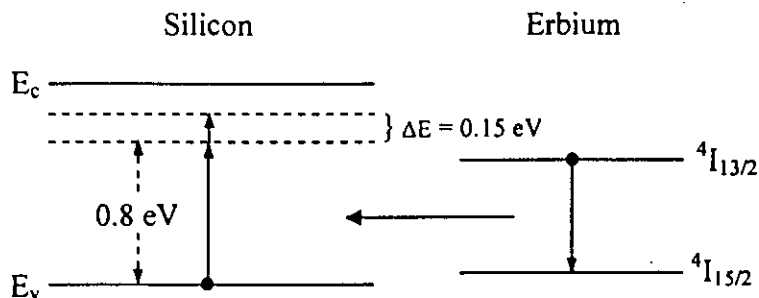
**(b) Impurity Auger de-excitation with bound carriers:** In this case the de-excitation rate is directly proportional to the number of carriers bound to shallow donor or acceptor level. So as before this effect can be expressed as

$$\frac{1}{\tau_{Ab}} = C_{Abe} n_b \quad \text{for n-type Si}$$

$$\frac{1}{\tau_{Ab}} = C_{Abh} p_b \quad \text{for p-type Si}$$

where  $C_{Abe}$  and  $C_{Abh}$  are Auger coefficients for bound carriers, and  $n_b$  and  $p_b$  are the concentration of carriers bound to donor and acceptor levels respectively.

**(ii) Energy Back Transfer:** In this process, the energy given up by the non-radiative decay of excited erbium atom promotes an electron from the valence band to the erbium related level in the silicon bandgap. This process is exactly the reverse of excitation and hence has been named energy back transfer since energy is being transferred back through the same path. The extra energy needed to complete this process ( $\Delta E$ ) is given by phonons. Fig. 2.4 illustrates the energy back transfer mechanism.



**Fig. 2.4** Schematic representation of energy back transfer process

The phonon participation makes this non-radiative process thermally activated. The energy back transfer process is characterized by activation energy of 0.15 eV and hence must always be completed by thermalization of electron trapped at Er-related level to the conduction band [17]. Priolo et al. [17] has mathematically expressed this process by defining a lifetime related to energy back transfer process as follows

$$\frac{1}{\tau_{bt}} = W_0 \exp\left(-\frac{0.15eV}{kT}\right)$$

where  $W_0$  is the fitting parameter per second.

All these non-radiative de-excitation processes are expressed all together by a non-radiative decay lifetime  $\tau_{nonrad}$  as follows

$$\frac{1}{\tau_{nonrad}} = \frac{1}{\tau_{Af}} + \frac{1}{\tau_{Ab}} + \frac{1}{\tau_{bt}} \quad (2.1)$$

All the above-mentioned non-radiative decay processes lower the amount of Er atoms in the excited state. Hence one needs to increase the number of excess carriers by increasing the injection current or optical excitation in order to get a population inversion and have laser action.

## 2.6 Shockley-Read-Hall (SRH) Generation-Recombination Kinetics

According to Shockley-Read-Hall (SRH) recombination kinetics, there are basically four processes involving generation and recombination of electron-hole pairs [23]. These processes are as bellows:

(i) **Electron capture:** The rate of electron capture from the conduction band to the trap level is proportional to the number of electrons available for capture and the density of the empty trap level. If the probability of a trap level filled by an electron is  $f_t$ , then probability of a trap level to be empty is  $(1-f_t)$ . The recombination rate for the electron is given by

$$R_n = c_n n N_t (1 - f_t)$$

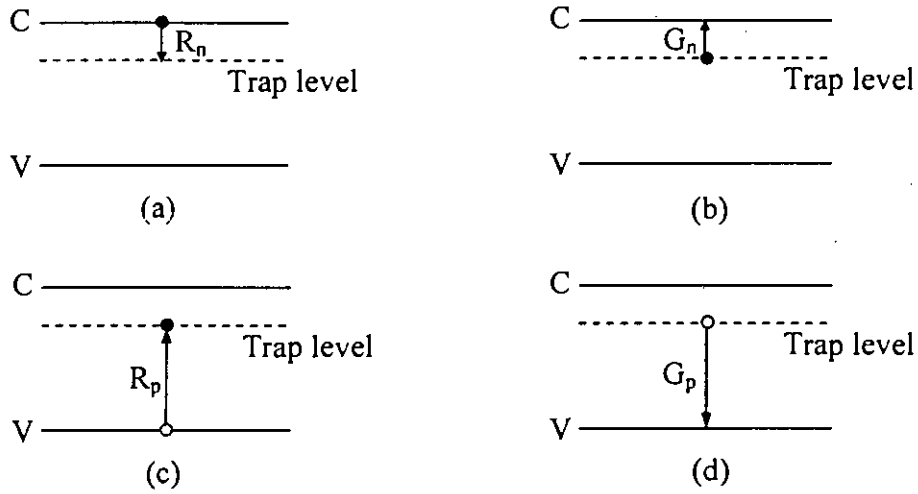
where  $c_n$  is the capture coefficient for electrons,  $n$  is the free electron concentration and  $N_t$  is the total trap level per unit volume.



(ii) **Electron emission:** The rate of electron emission from the trap level to the conduction band is proportional to the trap levels that are filled by electron. Thus the rate of free electron generation is given by

$$G_n = e_n N_t f_t$$

where  $e_n$  is the emission coefficient.



**Fig. 2.5** Schematic diagram of SRH generation-recombination processes: (a) electron capture, (b) electron emission, (c) hole capture and (d) hole emission.

(iii) **Hole Capture:** The rate of recombination of holes at the trap levels is proportional to number of holes available and number of traps occupied by electron. This rate is given by

$$R_p = c_p N_t (1 - f_t)$$

where  $c_p$  is the hole capture coefficient.

(iv) **Hole Emission:** The generation rate for this process is proportional to the density of the traps that are empty and is given by

$$G_p = e_p N_t f_t$$

where  $e_p$  is the emission coefficient for holes.

## 2.7 Occupation Probability of Erbium Site

Let,

$N_{Er}$  = total number of active Er sites per unit volume.

$n_{Er}$  = total number of active Er sites filled by electron at steady state.

Now from the discussion in section 2.6, we can write

$$\text{Electron emission rate} = (e_n + c_p p)n_{Er}$$

$$\text{Electron capture rate} = (e_p + c_n n)(N_{Er} - n_{Er})$$

At steady state, electron emission rate = electron capture rate.

$$\therefore (e_n + c_p p)n_{Er} = (e_p + c_n n)(N_{Er} - n_{Er})$$

Thus the fraction of erbium sites occupied by electron at steady state is given by [21]

$$f_i = \frac{n_{Er}}{N_{Er}} = \frac{e_p + c_n n}{e_n + e_p + c_n n + c_p p} \quad (2.2)$$

When an optical excitation pulse is applied to an erbium doped silicon sample, excess electron-hole pairs are generated almost instantaneously. However, rate of capture and emission of carriers through erbium sites are controlled by corresponding emission and capture coefficients. As a result, a finite amount of time is needed for the excited erbium atoms to reach to the steady state value. In this case, both the number of electron occupied erbium sites and that of the excited erbium atoms are function of time. We can write,

$$\text{Electron emission rate} = (e_n + c_p p)n_{Er}(t)$$

$$\text{Electron capture rate} = (e_p + c_n n)(N_{Er} - n_{Er}(t))$$

So the rate of change of electron occupied trap density at time  $t$  is given by

$$\frac{dn_{Er}(t)}{dt} = (e_p + c_n n)(N_{Er} - n_{Er}(t)) - (e_n + c_p p)n_{Er}(t)$$

The solution of the above differential equation is

$$n_{Er}(t) = \frac{b}{a} N_{Er} (1 - e^{-at}) \quad (2.3)$$

where  $a = e_n + e_p + c_n n + c_p p$

$$b = e_p + c_n n$$

So, time varying probability of electron occupied erbium site is

$$f_i(t) = \frac{n_{Er}(t)}{N_{Er}} = \frac{b}{a} (1 - e^{-at}) \quad (2.4)$$

# CHAPTER THREE

## Laser Fundamentals

Laser is an acronym for “Light Amplification by Stimulated Emission of Radiation.” It is a source of highly directional, monochromatic and coherent light and hence widely used for optical communications. In this chapter, the basic concepts of semiconductor laser are given. Population inversion, lasing threshold condition etc. are also discussed in brief.

### 3.1 Emission and Absorption of Radiation

The interaction of light with matter takes place in discrete packets of energy or quanta called photons. Quantum theory suggests that electrons exist only in certain discrete energy states. So absorption and emission of light causes the electrons to make a transition from one discrete energy state to another. The frequency of the emitted or absorbed photon is defined by  $\nu = \Delta E/h$  where  $\Delta E$  is the energy difference between the two levels concerned and  $h$  is the Planck’s constant. Let us consider the electron transitions which may occur between the two energy levels of the atomic system shown in Fig. 3.1.

If an electron is initially at lower energy state  $E_1$  shown in Fig. 3.2(a), the electron will remain in this state unless get excited. When a photon with energy  $\Delta E = E_2 - E_1$  is incident on this electron, there is a finite probability that the electron will absorb the incident energy and jump to energy level  $E_2$ . This process is called stimulated absorption. Alternatively, if the electron is in the upper level  $E_2$ , it may return to the lower energy state  $E_1$  with the emission of a photon. This emission can occur in two ways:

(a) by spontaneous emission in which the atom returns to the lower energy state  $E_1$  in an entirely random manner.

(b) by stimulated emission when a photon having an energy equal to the energy difference between the two states ( $E_2 - E_1$ ) interacts with an electron in the upper energy state causing it to return to the lower state with the creation of another photon.

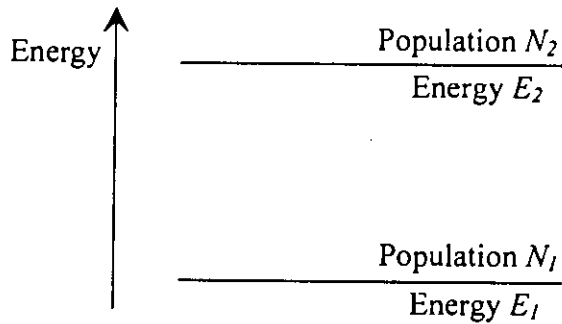


Fig. 3.1 Two energy level system.

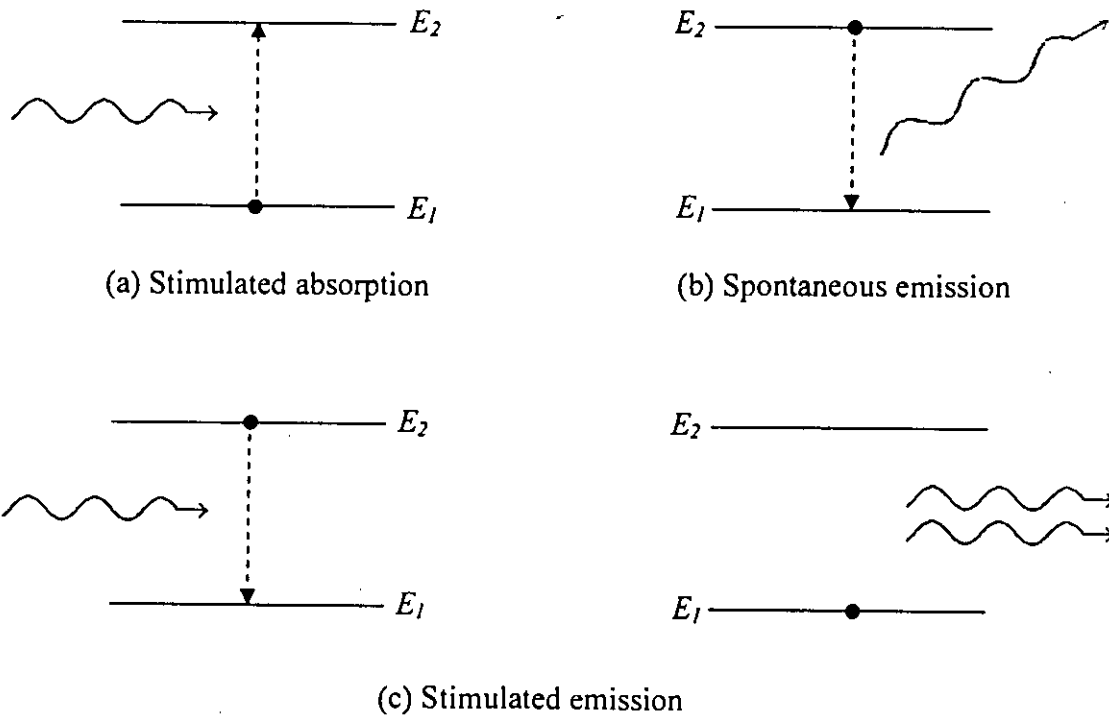


Fig. 3.2 Energy state diagram showing (a) stimulated absorption, (b) spontaneous emission and (c) stimulated emission. The black dot indicates the electron which takes part in the transition between the energy levels.

The spontaneous and stimulated emission processes are shown in Fig. 3.2(b) and (c) respectively. Normally the number of atoms at lower energy levels is larger than atoms at higher energy levels and the probability of occurrence of spontaneous process is much

higher than that of the stimulated process. The random nature of the spontaneous emission process from a large number of atoms gives incoherent radiation. But the stimulated emission process results in coherent radiation since both the stimulating and stimulated photons have identical frequencies, are in phase, have the same state of polarization and travel in the same direction. So the amplitude of the incident photon can increase by stimulated emission as it passes through a collection of excited atoms.

### 3.2 Einstein Relations

If the density of atoms in the lower or ground energy state  $E_1$  is  $N_1$ , the rate of upward transition ( $E_1 \rightarrow E_2$ ) or absorption is proportional to both  $N_1$  and energy density  $\rho_\nu$ . So the upward transition rate is given by

$$R_{12} = N_1 \rho_\nu B_{12} \quad (3.1)$$

where  $B_{12}$  is proportionality constant and is known as the Einstein coefficient of absorption and  $\rho_\nu = N_p h \nu$ . Here  $N_p$  is the photon density having frequency  $\nu$ .

Atoms at higher energy state undergo downward transitions either spontaneously or through stimulation by the radiation field. If the density of atoms within the system with energy  $E_2$  is  $N_2$ , the spontaneous emission rate is given by  $N_2 A_{21}$  where  $A_{21}$  is the spontaneous emission coefficient. The rate of stimulated transition from energy level 2 to level 1 is given by  $N_2 \rho_\nu B_{21}$  where  $B_{21}$  is the Einstein coefficient of stimulated emission. The total transition rate from level 2 to level 1 is the sum of spontaneous and stimulated contribution. Hence:

$$R_{21} = N_2 A_{21} + N_2 \rho_\nu B_{21} \quad (3.2)$$

For a system with thermal equilibrium, the upward and downward rates must be equal.

So,

$$N_1 \rho_\nu B_{12} = N_2 A_{21} + N_2 \rho_\nu B_{21} \quad (3.3)$$

or

$$\rho_\nu = \frac{A_{21} / B_{21}}{\frac{B_{12}}{B_{21}} \frac{N_1}{N_2} - 1} \quad (3.4)$$

The populations of various energy levels of a system in thermal equilibrium are given by Boltzmann statistics to be:

$$N_j = \frac{g_j N_0 \exp(-E_j / kT)}{\sum g_i \exp(-E_i / kT)} \quad (3.5)$$

where  $N_j$  is the population density of the energy level  $E_j$ ,  $N_0$  is the total population density and  $g_j$  is the degeneracy of the  $j$ -th level. So population of two levels associated with energy  $E_1$  and  $E_2$  is given by

$$\frac{N_1}{N_2} = \frac{g_1}{g_2} \exp((E_2 - E_1) / kT) \quad (3.6)$$

Substituting Eq. (3.6) into Eq. (3.4) gives

$$\rho_\nu = \frac{A_{21} / B_{21}}{\frac{B_{12}}{B_{21}} \frac{g_1}{g_2} \exp(h\nu / kT) - 1} \quad (3.7)$$

Since the atomic system under consideration is in thermal equilibrium, it produces a radiation density which is identical to the black body radiation. This radiation density can be expressed as

$$\rho_\nu = \frac{8\pi h \nu^3}{c^3} \left( \frac{1}{\exp(h\nu / kT) - 1} \right) \quad (3.8)$$

Comparing Eq. (3.7) with Eq. (3.8), we obtain the Einstein relations:

$$B_{12} = \left( \frac{g_2}{g_1} \right) B_{21} \quad (3.9)$$

and

$$\frac{A_{21}}{B_{21}} = \frac{8\pi h \nu^3}{c^3} \quad (3.10)$$

The ratio  $g_1 / g_2$  is generally in the order of unity and hence ignored. Thus taking refractive index of the medium into account, we get

$$B_{12} = B_{21} = \frac{A_{21} c^3}{8\pi h \nu^3 n^3} \quad (3.11)$$

where  $n$  is the refractive index of the medium.

### 3.3 Absorption of Radiation

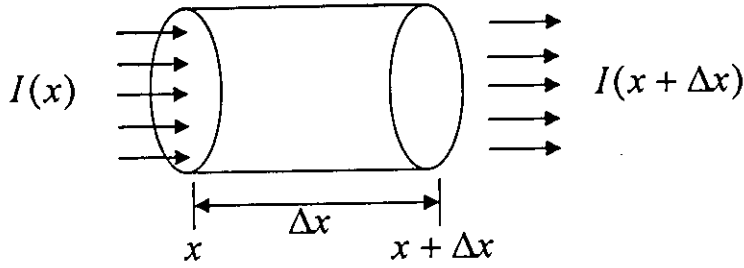


Fig. 3.1 Radiation passing through a volume element of length  $\Delta x$  and unit cross sectional area.

Let us consider a collimated beam of perfectly monochromatic radiation of unit cross sectional area passing through an absorbing medium. We assume that there is only one relevant electron transition which occurs between the energy  $E_1$  and  $E_2$ . The change in irradiance of the beam as a function of distance is given by

$$\Delta I(x) = I(x + \Delta x) - I(x) \quad (3.12)$$

For a homogeneous medium,  $\Delta I(x)$  is proportional to both the distance traveled and to  $I(x)$ . That is  $\Delta I(x) = -\alpha I(x) \Delta x$ . The proportionality constant  $\alpha$  is called absorption coefficient. The negative sign indicates the reduction in beam irradiance due to absorption as  $\alpha$  is a positive quantity. Writing this expression as a differential equation we get

$$\frac{dI(x)}{dx} = -\alpha I(x) \quad (3.13)$$

Integrating this equation, we have

$$I = I_0 \exp(-\alpha x) \quad (3.14)$$

where  $I_0$  is the incident irradiance.

So, due to absorption the irradiance decreases exponentially with distance. If we can make  $\alpha$  negative, then  $(-\alpha x)$  in the exponent of Eq. (3.14) becomes positive. So the beam irradiance grows as it propagates through the medium in accordance with the equation

$$I = I_0 \exp(gx) \quad (3.15)$$

where  $g = -\alpha$  is called small signal gain coefficient. The expression of  $\alpha$  is given by [24]

$$\alpha = \left( \frac{g_2}{g_1} N_1 - N_2 \right) \frac{B_{21} h \nu n}{c} \quad (3.16)$$

where  $n$  is the refractive index of the medium. The expression of  $g$  is given by

$$g = \left( N_2 - \frac{g_2}{g_1} N_1 \right) \frac{B_{21} h \nu n}{c} \quad (3.17)$$

So in order to make small signal gain  $g$  positive,  $N_2$  must be greater than  $\frac{g_2}{g_1} N_1$ .

### 3.4 Population Inversion

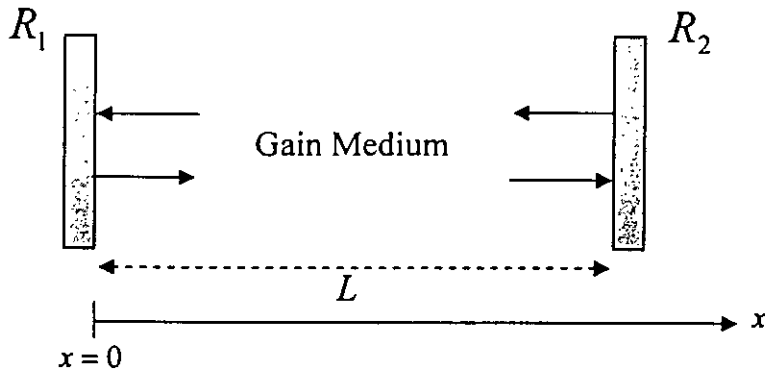
Under the conditions of thermal equilibrium given by the Boltzmann distribution (Eq. 3.6), the lower energy level  $E_1$  contains more atoms than the upper energy level  $E_2$ . Again at thermal equilibrium, although stimulated emission/absorption and spontaneous emission are going on in the same time, the stimulated absorption dominates over stimulated emission and the incident photon cannot be amplified in this case. To obtain optical amplification, it is necessary to create a nonequilibrium distribution of atoms such that population of upper energy level is greater than that of the lower energy level (i.e.,  $N_2 > N_1$ ). This condition is called population inversion. So to achieve population inversion, we need to excite the atoms from lower level to the upper level. This excitation process is called pumping. In our EDS laser, the population inversion is achieved by injecting current into the device. Continuous capture of electrons and holes pumps erbium atoms from ground state to the first excited state and then achieve population inversion.

### 3.5 Optical Feedback

Light amplification in the laser occurs when a photon interacts with an electron in the excited state and causes the stimulated emission of the second photon. Continuation of this process produces more photons. When all these photons are in phase, amplified coherent emission is obtained. To achieve this laser action, it is necessary to contain photons within the laser medium. This is accomplished by placing the laser medium between a pair of mirrors which form optical cavity like Fabry-Perot resonator shown in



Fig. 3.2. The cavity provides positive feedback for the photons. The light signal gets amplified as it passes through the medium and feeds back by the mirrors. A stable output is obtained at saturation when the gain provided by the medium exactly matches the losses incurred during a complete round trip. The gain per unit length of most active media is so small that very little amplification of the signal results from a single pass through the medium. But after multiple passes which the signal undergoes when the medium is placed within a cavity, the amplification is substantial.



**Fig. 3.2** Schematic representation of the Fabry-Perot optical cavity. The shadowed bars indicate the end mirrors.

### 3.6 Threshold Condition for Laser Oscillation

Steady state level of laser oscillation is achieved when gain of the amplifying medium exactly balances all losses. While population inversion between the energy levels is a necessary condition for laser action, it is not alone sufficient because the gain coefficient must be large enough to overcome the losses and sustain oscillation. Let us include all losses except those due to transmission through the mirrors in a single loss coefficient  $\alpha$ , per unit length. If  $g$  be the gain coefficient per unit length then radiation intensity of the light beam varies exponentially with the distance  $x$  as it travels along the lasing cavity according to the relationship

$$I(x) = I(0) \exp\{(g - \alpha)x\} \quad (3.18)$$

We can determine the threshold gain by considering the change in radiation intensity of a light beam undergoing a round trip within the laser cavity. We assume that gain medium is placed between the two mirrors which have reflectances  $R_1$  and  $R_2$  and a separation  $L$ .

After one roundtrip ( $x = 2L$ ), only the fractions  $R_1$  and  $R_2$  of the optical radiation are reflected from the end mirrors. Thus Eq. (3.18) becomes

$$I(2L) = I(0)R_1R_2 \exp\{(g - \alpha_i)2L\} \quad (3.19)$$

At the lasing threshold, a steady state oscillation takes place and the magnitude and phase of the returned wave after a round trip must be equal to those of the original wave. This gives the condition for the amplitude is

$$I(2L) = I(0) \quad (3.20)$$

The threshold gain may be obtained by using Eqs. (3.19) and (3.20) and rearranging them to give:

$$g_{th} = \alpha_i + \frac{1}{2L} \ln\left(\frac{1}{R_1R_2}\right) \quad (3.21)$$

The second term on the right hand side of Eq. (3.21) represents the transmission loss through the mirrors. For lasing action to be easily achieved, it is essential to have high threshold gain in order to balance the losses from the cavity.

# CHAPTER FOUR

## Mathematical Model of Erbium Doped Silicon Laser

In this chapter, the mathematical model for erbium doped silicon (EDS) diode laser is developed. In the course of this development, several appendices are being referred for mathematical analysis. Rate equations for excited erbium atom and photon density are described. The threshold gain of lasing is studied next and it is found to be the gain needed to compensate the losses in the cavity. The current needed to achieve this gain is called threshold current and is determined. The below threshold and above threshold limit to the steady state solutions of the rate equations are considered to determine the operating characteristics of the laser. The rate equations are solved for a modulated current and small signal intensity modulation transfer function is determined. The optical modulation response is found to have a resonance and falls off quickly above this resonance frequency. Finally, computer/numerical simulations are done to observe the transient characteristics for excited erbium atoms and photon density for different excitation conditions.

### 4.1 Rate Equations for Si:Er Laser

Figs. 4.1 and 4.2 represent the model used to develop the rate equations for EDS laser. Each arrow in the model represents the numbers of particles flowing per unit volume per second. The rate equation for excited Er atom is given by

$$\frac{dN_{Er}^*}{dt} = R_{ex} - R_{dex} \quad (4.1)$$

where  $R_{ex}$  is the rate of excited Er atoms or pumping rate from the ground state ( $^4I_{15/2}$ ) to the first excited state ( $^4I_{13/2}$ ) and  $R_{dex}$  is the rate of de-excitation of the excited Er atoms from the  $^4I_{13/2}$  state to the ground state  $^4I_{15/2}$ .

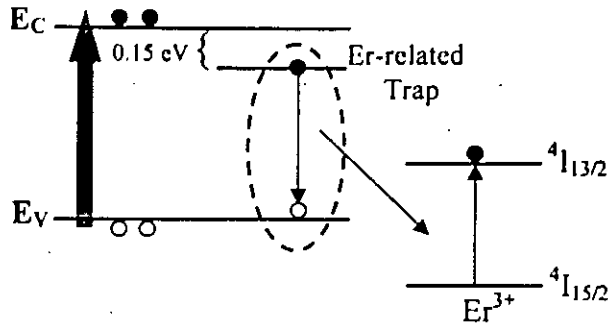


Fig. 4.1 Model for the excitation and de-excitation of Er in Si.

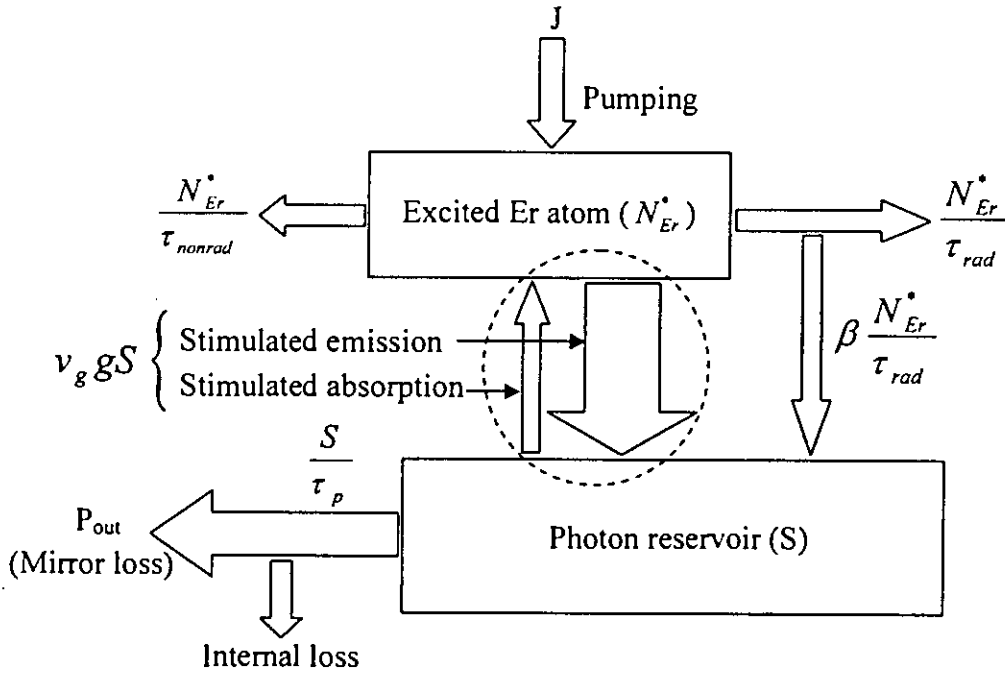


Fig. 4.2 Model used in the rate equation analysis of erbium doped silicon laser.

Excitation of erbium atoms in silicon host is an electron-hole mediated process. Successive capture of an electron and a hole in an Er-related trap level releases the recombination energy which is responsible for erbium excitation. If  $N_{Er}^*$  is the number of erbium atoms in the excited state, number of Er atoms available for excitation is given by  $(N_{Er} - N_{Er}^*)$ . The rate of useful recombination of electron-hole pairs through erbium sites is then given by electronic excitation rate [25],

$$R_{ex} = f_i c_p p (N_{Er} - N_{Er}^*) \quad (4.2)$$

The recombination process of excited erbium atoms is somewhat complicated and involves several mechanisms. There is radiative recombination process which is largely

independent of the host materials and the excitation conditions. The non-radiative recombination process consists of impurity Auger de-excitation through free and bound carriers and also the energy back transfer. These processes are dependent on the excitation level. The decay of excited Er atoms also occurs through stimulated processes. Thus, we can write the de-excitation or recombination rate as

$$R_{deex} = R_{rad} + R_{nonrad} + R_{st} \quad (4.3)$$

where,  $R_{st}$  represents net rate of de-excitation through both stimulated emission and absorption. This is a gain process for photon if stimulated emission dominates over the stimulated absorption otherwise it is a loss process. The first two terms on the right side of Eq. (4.3) indicate the natural or un-stimulated decay of excited Er atoms. This decay is characterized by the Er decay lifetime  $\tau_{Er}$  of the  $^4I_{13/2}$  state to the ground state. Now Eq. (4.3) can be re-written as

$$R_{deex} = \frac{N_{Er}^*}{\tau_{Er}} + R_{st} \quad (4.4)$$

where,

$$R_{rad} = \frac{N_{Er}^*}{\tau_{rad}} \quad (4.5a)$$

$$R_{nonrad} = \frac{N_{Er}^*}{\tau_{nonrad}} \quad (4.5b)$$

$$\text{and } \frac{1}{\tau_{Er}} = \frac{1}{\tau_{rad}} + \frac{1}{\tau_{nonrad}} \quad (4.5c)$$

The rate equation for excited Er atoms therefore becomes

$$\frac{dN_{Er}^*}{dt} = f_i c_p p (N_{Er} - N_{Er}^*) - \frac{N_{Er}^*}{\tau_{Er}} - R_{st} \quad (4.6)$$

The photon density  $S$  is increased by the stimulated emission ( $R_{st}$ ) and by the fraction  $\beta$  of spontaneously emitted photons that enter into the lasing mode. The factor  $\beta$  is usually very small ( $\sim 10^{-4}$ ) and spontaneous emission can often be neglected above the lasing threshold. The density  $S$  is reduced from the cavity by internal absorption and scattering losses ( $\alpha_i$ ) and also by emission through end mirrors ( $\alpha_m$ ). These photon losses are characterized by the photon life time  $\tau_p$  where [23]

$$1/\tau_p = v_g (\alpha_i + \alpha_m) \quad (4.7)$$

Therefore, the rate equation for photon can be written as

$$\frac{dS}{dt} = R_{st} + \beta \frac{N_{ir}^*}{\tau_{rad}} - \frac{S}{\tau_p} \quad (4.8)$$

Let's consider a laser cavity of length  $L$  and  $S$  be the incoming photon density. After passing through the medium of net gain  $g$  due to stimulated emission and stimulated absorption per unit length, the photon density becomes  $S + \Delta S$ . Then

$$S + \Delta S = S e^{gL}$$

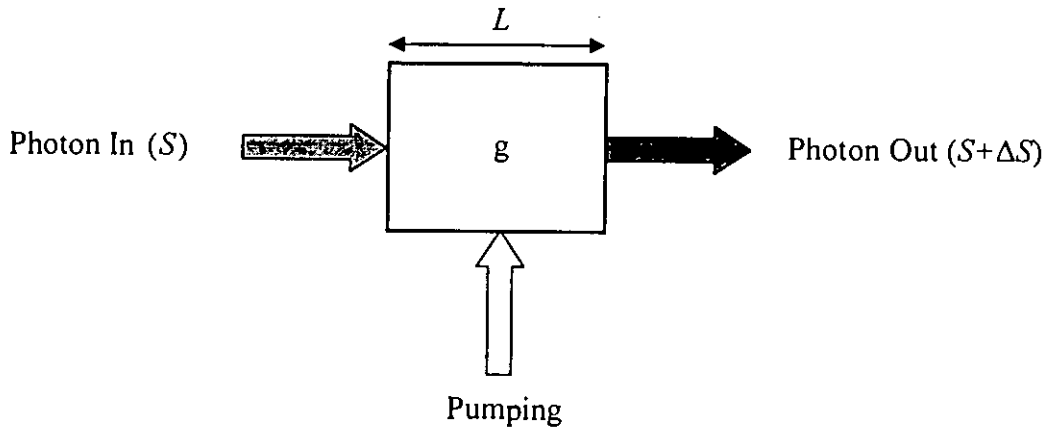


Fig. 4.3 Photon is passing through the cavity medium of gain  $g$ . The length of the cavity element is  $L$  and time for a photon to travel this distance is  $\Delta t$ .

As  $L$  is sufficiently small,  $e^{gL} \approx 1 + gL$

$$\begin{aligned} \therefore S + \Delta S &= S(1 + gL) \\ \Rightarrow \Delta S &= SgL \end{aligned}$$

Inside the cavity, the velocity of light is  $v_r = \frac{c}{N_r}$ , where  $c$  is the speed of light in free space and  $N_r$  is the refractive index of the cavity. Let  $\Delta t$  be the time of a photon to travel the distance  $L$ . So

$$\begin{aligned} L &= v_r \Delta t \\ \therefore \Delta S &= v_r g \Delta t S \end{aligned}$$

Therefore, the generation term for  $dS/dt$  is given by

$$\left(\frac{dS}{dt}\right)_{gen} = R_{st} = \frac{\Delta S}{\Delta t} = \nu_g g S \quad (4.9)$$

Thus, rate equations for excited Er atom and photon density can be written as

$$\frac{dN_{Er}^*}{dt} = f_i c_p p (N_{Er} - N_{Er}^*) - \frac{N_{Er}^*}{\tau_{Er}} - \nu_g g S \quad (4.10)$$

$$\frac{dS}{dt} = \nu_g g S + \beta \frac{N_{Er}^*}{\tau_{rad}} - \frac{S}{\tau_p} \quad (4.11)$$

## 4.2 Threshold Gain and Current Density

Since only a small fraction of spontaneous emission enters into lasing mode, under steady state conditions with vanishing  $\beta$ , Eq. (4.11) becomes

$$\nu_g g S = \frac{S}{\tau_p}$$

$$\text{or, } g = \alpha_i + \alpha_m \quad (4.12)$$

At this condition, there is a balance between gain and optical losses in the cavity and this is called threshold gain, which is expressed as

$$\begin{aligned} g_{th} &= \alpha_i + \alpha_m \\ &= \alpha_i + \frac{1}{2L} \log_e (1/R_1 R_2) \end{aligned} \quad (4.13)$$

Below the threshold level, the value of photon density  $S$  can be neglected as lasing has not yet occurred. Under this condition, the excitation rate remains the same as before in Eq. (4.2) but the de-excitation rate presented by Eq. (4.4) becomes

$$R_{dex} = \frac{N_{Er}^*}{\tau_{Er}} \quad (4.14)$$

At steady state, the rate of excitation and de-excitation must be equal.

$$f_i c_p p (N_{Er} - N_{Er}^*) = \frac{N_{Er}^*}{\tau_{Er}} \quad (4.15)$$

So, at equilibrium, the number of erbium atoms in the excited state is given by

$$N_{Er}^* = \frac{f_t c_p p}{f_t c_p p + \frac{1}{\tau_{Er}}} N_{Er} \quad (4.16)$$

Eq. (4.16) gives the excited erbium atoms as a function of excess carrier density in the absence of any optical feedback in the cavity. But when stimulated transition occurs, the excited Er atoms clamp to its threshold level  $N_{Er}^*$ . The gain of the cavity medium also depends upon the excited Er atom. So, when threshold occurs, gain also becomes constant at its threshold value  $g_{th}$ . Using Eq. (2.1) and (4.5c) in Eq. (4.15), we get

$$f_t c_p p (N_{Er} - N_{Er}^*) = N_{Er}^* \left( \frac{1}{\tau_{rad}} + \frac{1}{\tau_{Af}} + \frac{1}{\tau_{Ab}} + \frac{1}{\tau_{bt}} \right) \quad (4.17)$$

We have assumed that erbium is doped in the p-region of diode laser. For p-type material,

$$\frac{1}{\tau_{Af}} = C_{Ah} p \quad \text{and} \quad \frac{1}{\tau_{Ab}} = C_{Abh} N_A.$$

Substituting these values in Eq. (4.17), we obtain

$$f_t c_p p (N_{Er} - N_{Er}^*) = N_{Er}^* \left( \frac{1}{\tau_{rad}} + C_{Ah} p + C_{Abh} N_A + \frac{1}{\tau_{bt}} \right) \quad (4.18)$$

At low temperature (below 100K), energy back transfer effect can be neglected. Then above equation becomes

$$f_t c_p p (N_{Er} - N_{Er}^*) = N_{Er}^* \left( \frac{1}{\tau_{rad}} + C_{Ah} p + C_{Abh} N_A \right) \quad (4.19)$$

The occupation probability of erbium trap is given by [21]

$$f_t = \frac{e_p + c_n n}{e_p + e_n + c_n n + c_p p} \quad (4.20)$$

Combining Eqs. (4.19) and (4.20) and converting hole concentration into electron concentration by putting  $p = n + N_A$ , where  $N_A$  is the background doping and  $n$  and  $p$  are the injected electron and hole concentration respectively, we get

$$\frac{(e_p + c_n n)}{e_n + e_p + c_n n + c_p (n + N_A)} c_p (n + N_A) (N_{Er} - N_{Er}^*) = N_{Er}^* \left[ \frac{1}{\tau_{rad}} + C_{Ah} n + (C_{Ah} + C_{Abh}) N_A \right] \quad (4.21)$$



At the onset of threshold,

$$N_{Er}^* = N_{Erth}^*$$

$$\text{and, } n = n_{thrs}$$

Then at threshold, Eq. (4.21) becomes

$$\frac{(e_p + c_n n_{thrs})}{e_n + e_p + c_n n_{thrs} + c_p (n_{thrs} + N_A)} c_p (n_{thrs} + N_A) (N_{Er} - N_{Erth}^*) = N_{Erth}^* \left[ \frac{1}{\tau_{rad}} + C_{Ah} n_{thrs} + (C_{Ah} + C_{Abh}) N_A \right] \quad (4.22)$$

Therefore the excess or injected carrier density at which excited erbium atoms reach to the threshold level of population inversion is (Detailed derivation is given in Appendix-A)

$$n_{thrs} = \frac{1}{2 \{ N_{Erth}^* C_{Ah} (c_n + c_p) - c_n c_p (N_{Er} - N_{Erth}^*) \}} \times \left( \left[ \left[ N_{Erth}^* C_{Ah} (e_n + e_p + c_p N_A) + N_{Erth}^* (c_n + c_p) \left\{ \frac{1}{\tau_{rad}} + (C_{Ah} + C_{Abh}) N_A \right\} \right]^2 - \left( 4 \{ N_{Erth}^* C_{Ah} (c_n + c_p) - c_n c_p (N_{Er} - N_{Erth}^*) \} \left\{ N_{Erth}^* (e_n + e_p + c_p N_A) \left[ \frac{1}{\tau_{rad}} + (C_{Ah} + C_{Abh}) N_A \right] \right\} \right) \right] \right)^{1/2} - \left[ N_{Erth}^* C_{Ah} (e_n + e_p + c_p N_A) + N_{Erth}^* (c_n + c_p) \left\{ \frac{1}{\tau_{rad}} + (C_{Ah} + C_{Abh}) N_A \right\} \right] \quad (4.23)$$

The threshold current density is given by

$$J_{th} = \frac{n_{thrs}}{\tau_{si}} L_{eq} q \quad (4.24)$$

where  $\tau_{si}$  is the silicon lifetime and  $L_{eq}$  is the thickness of erbium doped region.

### 4.3 Power vs. Current Density Characteristics

The rate equations (4.9) and (4.10) are valid both above and below the threshold condition. In both cases, output power is proportional to the photon density which is given by [23]

$$\text{Power} = \left( \begin{array}{c} \text{Energy of} \\ \text{a photon} \end{array} \right) \times \left( \begin{array}{c} \text{Photon} \\ \text{density} \end{array} \right) \times \left( \begin{array}{c} \text{Cavity} \\ \text{volume} \end{array} \right) \times \left( \begin{array}{c} \text{Escape rate} \\ \text{of a photon} \end{array} \right) \quad (4.25)$$

The energy of a photon is  $h\nu$ . If the mirror loss term is  $\alpha_m$ , then escape rate of the photons through the mirrors is  $v_g\alpha_m$  [23]. So the output power emitted through both mirrors is given by

$$\text{Power} = h\nu S(\text{Vol}^m)v_g\alpha_m \quad (4.26)$$

### 4.3.1 Condition (i): Below Threshold

When the current density is bellow the threshold level ( $J < J_{th}$ ), low intensity light is generated due to spontaneous emission. Neglecting the stimulated transition term from Eq. (4.10), at steady state we get,

$$S = \beta \frac{\tau_p}{\tau_{rad}} N_{Er}^* \quad (J < J_{th}) \quad (4.27)$$

This is the photon density inside the cavity due to spontaneous emission. From Eq. (4.14) we get,

$$\begin{aligned} N_{Er}^* &= \frac{f_i c_p p}{f_i c_p p + \frac{1}{\tau_{Er}}} N_{Er} \\ &= \frac{P_{01} + P_{02}J + P_{03}J^2}{P_{04} + P_{05}J + P_{06}J^2} N_{Er} \end{aligned} \quad (4.28)$$

(Detailed derivation is given in Appendix-B)

where

$$P_{01} = e_p c_p N_A (L_{eq} q)^2$$

$$P_{02} = \tau_{si} L_{eq} q c_p (e_p + c_n N_A)$$

$$P_{03} = c_n c_p \tau_{si}^2$$

$$P_{04} = \left\{ N_A c_p \left( e_p + \frac{1}{\tau_{rad}} \right) + \frac{1}{\tau_{rad}} (e_n + e_p) + N_A (e_n + e_p) (C_{Ah} + C_{Abh}) + c_p N_A^2 (C_{Ah} + C_{Abh}) \right\} (L_{eq} q)^2$$

$$P_{05} = \tau_{si} L_{eq} q \left\{ e_p c_n + N_A (c_n c_p + c_n C_{Ah} + 2C_{Ah} c_p) + C_{Abh} N_A (c_n + c_p) + \frac{1}{\tau_{rad}} (c_n + c_p) + C_{Ah} (e_n + e_p) \right\}$$

$$P_{06} = \tau_{si}^2 \left\{ c_n c_p + C_{Ah} (c_n + c_p) \right\}$$

Substituting from Eqs. (4.27) and (4.28) in Eq. (4.26), we get the spontaneous emission power

$$\begin{aligned}
 P_{spont} &= h\nu\beta \frac{\tau_p}{\tau_{rad}} N_{Er}^* (Vol^m) v_g \alpha_m \\
 &= h\nu\beta \frac{1}{v_g (\alpha_i + \alpha_m) \tau_{rad}} \left( \frac{P_{01} + P_{02}J + P_{03}J^2}{P_{04} + P_{05}J + P_{06}J^2} \right) N_{Er} (Vol^m) v_g \alpha_m \\
 &= \frac{\alpha_m}{(\alpha_i + \alpha_m)} h\nu \frac{\beta}{\tau_{rad}} N_{Er} (Vol^m) \left( \frac{P_{01} + P_{02}J + P_{03}J^2}{P_{04} + P_{05}J + P_{06}J^2} \right) \quad (4.29)
 \end{aligned}$$

Now, by defining

$$H_{spont} = \frac{\alpha_m}{(\alpha_i + \alpha_m)} h\nu \frac{\beta}{\tau_{rad}} N_{Er} (Vol^m) \quad (4.30)$$

we can simplify Eq. (4.29) to be

$$P_{spont} = H_{spont} \frac{P_{01} + P_{02}J + P_{03}J^2}{P_{04} + P_{05}J + P_{06}J^2} \quad (4.31)$$

The spontaneous emission power depends upon the excited Er atoms. At threshold, the spontaneous emission clamps as the excited erbium atoms  $N_{Er}^*$  clamp to its threshold value  $N_{Erth}^*$ . Thus, as the current density is increased above threshold ( $J > J_{th}$ ), the spontaneous power remains constant at the value of Eq. (4.31) with  $J = J_{th}$ .

### 4.3.2 Condition (ii): Above Threshold

After the threshold level ( $J > J_{th}$ ), the stimulated emission plays the dominant role than spontaneous emission and gain becomes constant at its threshold value  $g_{th}$ . At steady state condition, photon density can be obtained from Eq. (4.10) as

$$S = \frac{f_i c_p p (N_{Er} - N_{Erth}^*) - \frac{N_{Erth}^*}{\tau_{Er}}}{v_g g_{th}} \quad (4.32)$$

Now,

$$f_i c_p p = \frac{(e_p + c_n n) c_p p}{e_n + e_p + c_n n + c_p p}$$

$$= \frac{P_{07} + P_{08}J + P_{09}J^2}{P_{10} + P_{11}J} \quad [\text{Appendix-B}] \quad (4.33)$$

where

$$\begin{aligned} P_{07} &= e_p c_p N_A L_{eq}^2 q^2 \\ P_{08} &= \tau_{si} L_{eq} q c_p (e_p + c_n N_A) \\ P_{09} &= c_n c_p \tau_{si}^2 \\ P_{10} &= L_{eq}^2 q^2 (e_n + e_p + N_A c_p) \\ P_{11} &= \tau_{si} L_{eq} q (c_n + c_p) \end{aligned}$$

Erbium (Er) life time:

$$\begin{aligned} \frac{1}{\tau_{Er}} &= \frac{1}{\tau_{rad}} + \frac{1}{\tau_{nonrad}} \\ &= P_{12} + P_{13}J \quad [\text{Appendix-B}] \end{aligned} \quad (4.34)$$

where

$$\begin{aligned} P_{12} &= \frac{1}{\tau_{rad}} + N_A (C_{Ah} + C_{Abh}) \\ P_{13} &= \frac{C_{Ah} \tau_{si}}{L_{eq} q} \end{aligned}$$

Substituting Eqs. (4.33) and (4.34) into Eq. (4.32), the photon density inside the cavity after threshold is given by

$$S = \frac{(P_{07} + P_{08}J + P_{09}J^2)(N_{Er} - N_{Erth}^*) - N_{Erth}^* (P_{10} + P_{11}J)(P_{12} + P_{13}J)}{v_g g_{th} (P_{10} + P_{11}J)}$$

or

$$\begin{aligned} S &= \left[ \frac{\{e_p c_p N_A L_{eq}^2 q^2 + \tau_{si} L_{eq} q c_p (e_p + c_n N_A)J + c_n c_p \tau_{si}^2 J^2\} (N_{Er} - N_{Erth}^*)}{-N_{Erth}^* \{L_{eq}^2 q^2 (e_n + e_p + N_A c_p) + \tau_{si} L_{eq} q (c_n + c_p)\}} \left( \frac{1}{\tau_{rad}} + N_A (C_{Ah} + C_{Abh}) + \frac{C_{Ah} \tau_{si}}{L_{eq} q} J \right) \right] \\ &\quad \times \left[ \frac{1}{v_g g_{th} [L_{eq}^2 q^2 (e_n + e_p + N_A c_p) + \{\tau_{si} L_{eq} q (c_n + c_p)\}J]} \right] \end{aligned} \quad (4.35)$$



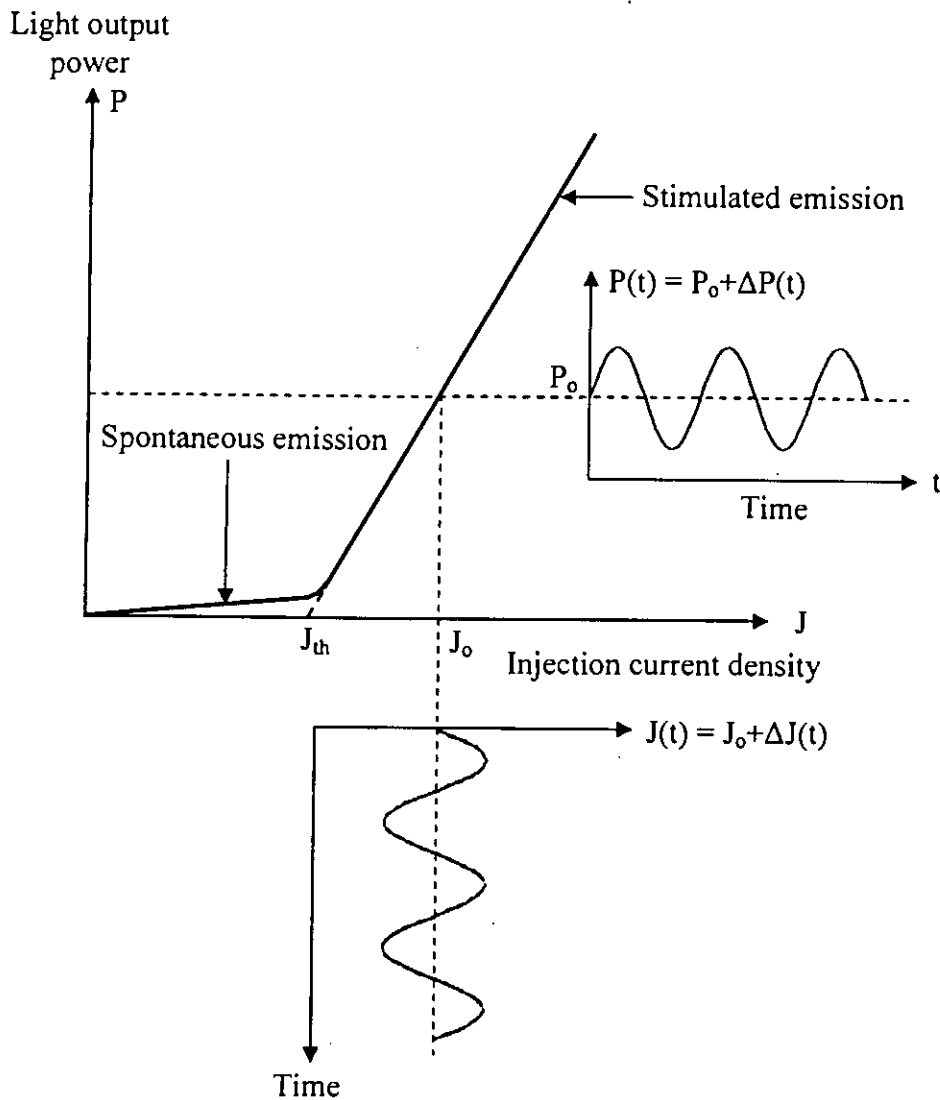
So the laser output power after threshold is

$$P_{out} = S * v_g * \alpha_m * h\nu * Vol \quad (J > J_{th}) \quad (4.36)$$

Eq. (4.36) represents the total output power of both mirrors. If the mirrors have equal reflectivity, then exactly half will be emitted through each mirror.

#### 4.4 Direct Current Modulation of Si:Er Diode Laser

The main application of semiconductor laser is as the source for optical communication systems. So the problem of high-speed modulation of their output by the high-data-rate information is one of the great technological importances.



**Fig. 4.4** Variation of output power  $P(t)$  with the variation of injection current density  $J(t)$  where  $P_0$  and  $J_0$  are the bias values for direct current modulation of EDS laser.

The light-output current-density (P-J) curve for a typical semiconductor laser is shown in Fig. 4.4 [28]. The figure shows that almost linear light output is obtained above the threshold current density  $J_{th}$ . Now if the current density is varied by an amount  $\Delta J$  around an operating point  $J_0$ , then power output will also vary in a synchronous fashion. However, the performance of the communication systems is highly dependent on the bandwidth. Thus our problem is to ascertain the frequency response of Si:Er laser. We do this by examining the interplay between the stimulated emission and injected current density.

#### 4.4.1 Optical Gain

The gain of the cavity medium depends on the excited Er atom which is proportional to the difference between stimulated emission and absorption. When population inversion occurs, stimulated emission is higher than stimulated absorption and gain is positive. But in the absence of population inversion, stimulated emission is negligible and gain is negative. We assume that photon density  $S$  is not very high. So, effect of output power on gain can be neglected and we have a simplified gain model for small signal analysis [1]

$$g(N_{Er}^*) = g_0(2N_{Er}^* - N_{Er}) \quad (4.37)$$

where,  $g_0$  is the gain cross-section. It is an intrinsic property of EDS and given by

$$g_0 = \frac{\lambda^4}{8\pi N_r^2 \tau_{rad} c \Delta\lambda} \quad (4.38)$$

#### 4.4.2 Steady State Characteristics

Rewriting the rate Eqs. (4.10) and (4.11) using Eq. (4.37) for gain, we get

$$\frac{dN_{Er}^*(t)}{dt} = f_i c_p p (N_{Er} - N_{Er}^*(t)) - \frac{N_{Er}^*(t)}{\tau_{Er}} - v_g g_0 (2N_{Er}^*(t) - N_{Er}) v_g S(t) \quad (4.39)$$

$$\frac{dS(t)}{dt} = v_g g_0 (2N_{Er}^*(t) - N_{Er}) g S(t) + \beta \frac{N_{Er}^*(t)}{\tau_{rad}} - \frac{S(t)}{\tau_p} \quad (4.40)$$

Using Eqs. (2.1) and (4.5c), Eq. (4.39) becomes

$$\frac{dN_{Er}^*(t)}{dt} = f_i c_p p (N_{Er} - N_{Er}^*(t)) - N_{Er}^*(t) \left( \frac{1}{\tau_{rad}} + \frac{1}{\tau_{Af}} + \frac{1}{\tau_{Ab}} + \frac{1}{\tau_{bl}} \right) - v_g g_0 (2N_{Er}^*(t) - N_{Er}) S(t) \quad (4.41)$$

At low temperature, energy back transfer can be neglected i.e.,  $1/\tau_{bt} \approx 0$ . We assume that Er is doped into the p-type silicon. Then Eq. (4.41) becomes

$$\frac{dN_{Er}^*(t)}{dt} = f_i c_p p (N_{Er} - N_{Er}^*(t)) - N_{Er}^*(t) C_{Ah} p - N_{Er}^*(t) \left( \frac{1}{\tau_{rad}} + \frac{1}{\tau_{Ab}} \right) - v_g g_0 (2N_{Er}^*(t) - N_{Er}) S(t) \quad (4.42)$$

At high level of excitation, we can assume  $n \approx p$ . Occupation probability of Er-trap  $f_i$  is a function of time in case of ac excitation. For simplicity, at high excitation condition, assuming that  $f_i$  is constant. Using  $n = \frac{\tau_{si}}{L_{eq} q} J$  in Eq. (4.42), we get

$$\begin{aligned} \frac{dN_{Er}^*(t)}{dt} &= f_i c_p \frac{\tau_{si}}{L_{eq} q} J (N_{Er} - N_{Er}^*(t)) - N_{Er}^*(t) C_{Ah} \frac{\tau_{si}}{L_{eq} q} J - N_{Er}^*(t) \left( \frac{1}{\tau_{rad}} + \frac{1}{\tau_{Ab}} \right) - v_g g_0 (2N_{Er}^*(t) - N_{Er}) S(t) \\ &= A_{01} J (N_{Er} - N_{Er}^*(t)) - A_{02} J N_{Er}^*(t) - A_{03} N_{Er}^*(t) - v_g g_0 (2N_{Er}^*(t) - N_{Er}) S(t) \end{aligned} \quad (4.43)$$

where,

$$\begin{aligned} A_{01} &= f_i c_p \frac{\tau_{si}}{L_{eq} q} \\ A_{02} &= \frac{C_{Ah} \tau_{si}}{L_{eq} q} \quad \text{and} \\ A_{03} &= \left( \frac{1}{\tau_{rad}} + \frac{1}{\tau_{Ab}} \right) \end{aligned}$$

At steady state, time variation of  $N_{Er}^*(t)$  is zero i.e.,  $\frac{dN_{Er}^*(t)}{dt} = 0$ . Again above the threshold,  $N_{Er}^*(t)$  becomes fixed to its threshold value  $N_{Erth}^*$ . Using these conditions in Eq. (4.43), we obtain,

$$\begin{aligned} A_{01} J_0 (N_{Er} - N_{Erth}^*) - A_{02} J_0 N_{Erth}^* - A_{03} N_{Erth}^* - v_g g_0 (2N_{Erth}^* - N_{Er}) S_0 &= 0 \\ \Rightarrow A_{01} J_0 (N_{Er} - N_{Erth}^*) &= A_{02} J_0 N_{Erth}^* + A_{03} N_{Erth}^* + v_g g_0 (2N_{Erth}^* - N_{Er}) S_0 \end{aligned} \quad (4.44)$$

At steady state, from Eq. (4.40), we get

$$\begin{aligned} \frac{dS(t)}{dt} &= 0 \\ \Rightarrow v_g g_0 (2N_{Erth}^* - N_{Er}) S_0 + \beta \frac{N_{Erth}^*}{\tau_{rad}} &= \frac{S_0}{\tau_p} \end{aligned} \quad (4.45)$$

$$\Rightarrow v_g g_0 (2N_{Erth}^* - N_{Er}^*) S_0 = \frac{S_0}{\tau_p} - \beta \frac{N_{Erth}^*}{\tau_{rad}} \quad (4.46)$$

$$\Rightarrow 2v_g g_0 N_{Erth}^* = \frac{1}{\tau_p} + v_g g_0 N_{Er}^* - \beta \frac{N_{Erth}^*}{\tau_{rad} S_0} \quad (4.47)$$

The subscript 0 in those above equations refers to the DC or steady-state values of all parameters. Eq. (4.45) states that the sum of the stimulated and spontaneous rates is equal to the photon loss rate. Again Eq. (4.47) which is a minor rewrite of Eq. (4.45) points out that spontaneous emission (third term on the right side) becomes less and less important as the photon density  $S_0$  gets larger.

### 4.4.3 Small Signal Analysis

Let us assume that the Si:Er laser is biased above threshold by DC current  $J_0 > J_{th}$  and time-varying current  $\Delta J(t)$  is added:

$$J(t) = J_0 + \Delta J(t) \quad (4.48)$$

Then under steady state conditions, the excited Er atom and photon density would respond similarly with the drive current and are given by

$$N_{Er}^*(t) = N_{Erth}^* + \Delta N_{Er}^*(t) \quad (4.49)$$

$$S(t) = S_0 + \Delta S(t) \quad (4.50)$$

Let us assume that  $\Delta J(t)$ ,  $\Delta N_{Er}^*(t)$  and  $\Delta S(t)$  are much smaller than their respective dc values  $J_0$ ,  $N_{Erth}^*$  and  $S_0$ . This small signal case allows the nonlinear rate equations to be linearized and solved analytically.

Now substituting these equations into Eq. (4.43) and Eq. (4.40), we obtain

$$\begin{aligned} \frac{d}{dt} [N_{Erth}^* + \Delta N_{Er}^*(t)] &= A_{01} [J_0 + \Delta J(t)] [N_{Er}^* - N_{Erth}^* - \Delta N_{Er}^*(t)] - A_{02} [J_0 + \Delta J(t)] [N_{Erth}^* + \Delta N_{Er}^*(t)] \\ &\quad - v_g g_0 [2N_{Erth}^* + 2\Delta N_{Er}^*(t) - N_{Er}^*] [S_0 + \Delta S(t)] - A_{03} [N_{Erth}^* + \Delta N_{Er}^*(t)] \end{aligned} \quad (4.51)$$

Assuming the  $\Delta J(t)\Delta N_{Er}^*(t) \approx 0$ , Eq. (4.51) then becomes



$$\begin{aligned} \frac{d}{dt} [\Delta N_{Er}^*(t)] = & A_{01} A_{05} J_0 + A_{01} A_{05} \Delta J(t) - A_{01} J_0 \Delta N_{Er}^*(t) - A_{02} J_0 N_{Erth}^* - A_{02} J_0 \Delta N_{Er}^*(t) - A_{02} N_{Erth}^* \Delta J(t) \\ & - A_{06} v_g g_0 S_0 - 2v_g g_0 S_0 \Delta N_{Er}^*(t) - A_{06} v_g g_0 \Delta S(t) - A_{03} N_{Erth}^* - A_{03} \Delta N_{Er}^*(t) \end{aligned}$$

(Detailed derivation in Appendix-C) (4.52)

Using Eq. (4.44), we get from Eq. (4.52)

$$\frac{d}{dt} [\Delta N_{Er}^*(t)] = A_{07} \Delta J(t) - A_{08} \Delta S(t) - A_{09} \Delta N_{Er}^*(t) \quad (4.53)$$

where

$$A_{05} = N_{Er} - N_{Erth}^*$$

$$A_{06} = 2N_{Erth}^* - N_{Er}$$

$$A_{07} = A_{01} A_{05} - A_{02} N_{Erth}^*$$

$$A_{08} = A_{06} v_g g_0$$

$$A_{09} = 2v_g g_0 S_0 + (A_{01} + A_{02}) J_0 + A_{03}$$

and

$$\begin{aligned} \frac{d}{dt} [S_0 + \Delta S(t)] = & v_g g_0 [2N_{Erth}^* + 2\Delta N_{Er}^*(t) - N_{Er}] [S_0 + \Delta S(t)] + \frac{\beta}{\tau_{rad}} [N_{Erth}^* + \Delta N_{Er}^*(t)] - \frac{1}{\tau_p} [S_0 + \Delta S(t)] \end{aligned} \quad (4.54)$$

Again assuming  $\Delta S(t) \Delta N_{Er}^*(t) \approx 0$ , Eq. (4.54) becomes

$$\begin{aligned} \frac{d}{dt} [\Delta S(t)] = & v_g g_0 (2N_{Erth}^* - N_{Er}) S_0 + 2v_g g_0 S_0 \Delta N_{Er}^*(t) + v_g g_0 (2N_{Erth}^* - N_{Er}) \Delta S(t) + \frac{\beta}{\tau_{rad}} N_{Erth}^* \\ & + \frac{\beta}{\tau_{rad}} \Delta N_{Er}^*(t) - \frac{1}{\tau_p} S_0 - \frac{1}{\tau_p} \Delta S(t) \end{aligned} \quad (4.55)$$

Combining Eq. (4.46) and Eq. (4.55), we get

$$\frac{d}{dt} [\Delta S(t)] = A_{10} \Delta N_{Er}^*(t) + A_{11} \Delta S(t) \quad (4.56)$$

where

$$A_{10} = \frac{\beta}{\tau_{rad}} + 2v_g g_0 S_0$$

$$\text{and } A_{11} = A_{06} v_g g_0 - \frac{1}{\tau_p}$$

Differentiating Eq. (4.56) again

$$\frac{d^2}{dt^2}[\Delta S(t)] = A_{10} \frac{d}{dt}[\Delta N_{ir}^*(t)] + A_{11} \frac{d}{dt}[\Delta S(t)] \quad (4.57)$$

Using Eqs. (4.53), (4.56) and (4.57), we obtain

$$\frac{d^2}{dt^2}[S(t)] + A_{12} \frac{d}{dt}[\Delta S(t)] + A_{13} \Delta S(t) = A_{14} \Delta J(t) \quad (4.58)$$

where

$$A_{12} = A_{09} - A_{11}$$

$$A_{13} = A_{08} A_{10} - A_{09} A_{11}$$

$$A_{14} = A_{07} A_{10}$$

In order to evaluate the small signal transfer function, let

$$\Delta J(t) = \Delta J(\omega) e^{j\omega t} \quad (4.59)$$

$$\text{and } \Delta S(t) = \Delta S(\omega) e^{j\omega t} \quad (4.60)$$

Putting these in Eq. (4.58), we obtain

$$\begin{aligned} \frac{d^2}{dt^2}[\Delta S(\omega) e^{j\omega t}] + A_{12} \frac{d}{dt}[\Delta S(\omega) e^{j\omega t}] + A_{13} \Delta S(\omega) e^{j\omega t} &= A_{14} \Delta J(\omega) e^{j\omega t} \\ \Rightarrow [(A_{13} - \omega^2) + j\omega A_{12}] \Delta S(\omega) &= A_{14} \Delta J(\omega) \end{aligned} \quad (4.61)$$

The modulation response function therefore can be written as

$$M(\omega) = \frac{\Delta S(\omega)}{\Delta J(\omega)} = \frac{A_{14}}{(A_{13} - \omega^2) + j\omega A_{12}} \quad (4.62)$$

The zero frequency (DC) response is

$$M(0) = \frac{A_{14}}{A_{13}} \quad (4.63)$$

Therefore the frequency response of Si:Er laser normalized to the response at zero frequency is

$$\begin{aligned} H(\omega) &= \frac{M(\omega)}{M(0)} = \frac{A_{13}}{(A_{13} - \omega^2) + j\omega A_{12}} \\ &= \frac{\omega_r^2}{(\omega_r^2 - \omega^2) + j\omega\gamma} \end{aligned} \quad (4.64)$$

where

$$\omega_r = \sqrt{A_{13}}$$

$$= \left[ \frac{v_g g_0 (2N_{Erth}^* - N_{Er}) \left\{ \frac{\beta}{\tau_{rad}} + 2v_g g_0 S_0 \right\} - \left\{ v_g g_0 (2N_{Erth}^* - N_{Er}) - \frac{1}{\tau_p} \right\}}{2v_g g_0 S_0 + \frac{1}{\tau_{rad}} + \frac{1}{\tau_{Ab}} + (f_i c_p + C_{Ah}) \left[ \frac{\left( \frac{1}{\tau_{rad}} + \frac{1}{\tau_{Ab}} \right) N_{Erth}^* + v_g g_0 (2N_{Erth}^* - N_{Er}) S_0}{f_i c_p (N_{Er} - N_{Erth}^*) - C_{Ah} N_{Erth}^*} \right]} \right]^{\frac{1}{2}} \quad (4.65)$$

and

$$\begin{aligned} \gamma &= A_{12} \\ &= 2v_g g_0 S_0 - v_g g_0 (2N_{Erth}^* - N_{Er}) + \frac{1}{\tau_{rad}} + \frac{1}{\tau_{Ab}} + \frac{1}{\tau_p} \\ &\quad + (f_i c_p + C_{Ah}) \left[ \frac{\left( \frac{1}{\tau_{rad}} + \frac{1}{\tau_{Ab}} \right) N_{Erth}^* + v_g g_0 (2N_{Erth}^* - N_{Er}) S_0}{f_i c_p (N_{Er} - N_{Erth}^*) - C_{Ah} N_{Erth}^*} \right] \end{aligned} \quad (4.66)$$

$\omega_r$  is the relaxation oscillation frequency and  $\gamma$  is the damping constant of the relaxation oscillation respectively. These two terms play an important role in governing the dynamic characteristics of Si:Er laser. The resonance peak  $f_p$  is obtained by setting the first derivative of  $|H(\omega)|$  to zero. The analytic expression of  $f_p$  is

$$f_p = \frac{1}{2\pi} \left( \omega_r^2 - \frac{\gamma^2}{2} \right)^{\frac{1}{2}} \quad (4.67)$$

The 3-dB modulation bandwidth  $f_{3dB}$  is defined as the frequency at which  $|H(\omega)|$  is reduced by 3 dB from its DC value. Eq. (4.64) provides the following analytic expression for  $f_{3dB}$ :

$$f_{3dB} = \frac{1}{2\pi} \left( \frac{(2\omega_r^2 - \gamma^2) + \sqrt{(\gamma^2 - 2\omega_r^2)^2 + 4\omega_r^4}}{2} \right)^{\frac{1}{2}} \quad (4.68)$$

or,

$$f_{3dB} = \frac{1}{2\pi} \left( \omega_p^2 + (\omega_r^4 + \omega_r^4)^{\frac{1}{2}} \right)^{\frac{1}{2}} \quad (4.69)$$

The amplitude of the resonance peak  $H_p$ , which occurs at frequency  $\omega_p (= 2\pi f_p)$  is obtained by inserting Eq. (4.65) into Eq. (4.62):

$$H_p = \left[ \frac{1}{\left(\frac{\gamma}{\omega_r}\right)^2 - \frac{1}{4}\left(\frac{\gamma}{\omega_r}\right)^4} \right]^{\frac{1}{2}} \quad (4.70)$$

## 4.5 Large-Signal Analysis and Transient Behavior

The rate equations presented in section 4.4.2 are valid for both small signal and large signal modulation. They hold continuously below threshold and above threshold. If the laser is always kept above threshold, the excited erbium atom density does not change by a large amount due to carrier clamping. To determine the transient behavior of EDS laser for large-signal inputs, we need to solve the rate equations. But the problem for large signal is that the rate equations can not be linearized and solved analytically like small signal case. They need to be solved numerically. Numerical solutions to the rate equations are found by iterating from one rate equation to the other using a small increment of time and results are presented in the next chapter. (Flowchart is given in APPENDIX-D)

# CHAPTER FIVE

## Results and Discussion

The mathematical expressions to illustrate the various characteristics of erbium doped silicon diode laser have been derived in the previous chapter. The analysis has been done for both steady state and time varying conditions and assumed that erbium is doped into the p-region of the p-n junction diode. In this chapter, the analytical equations are calculated to demonstrate the model utility. A computer program is developed based on these derived equations to generate numerical data. These data are plotted in this chapter to study the effects of various parameters like loss coefficient, doping concentration, Er lifetime, carrier lifetime etc. and their significance.

### 5.1 Parameters for Er Incorporated Si

We know that when silicon is doped with an impurity, a trap level is formed inside the silicon band gap. Past studies showed [10,14,16,17] that erbium introduces a trap level, which is 0.15eV below the silicon conduction band. This trap level acts as a recombination center for erbium excitation. So 0.15eV has been used as activation energy [17]. The values of electron emission coefficient and hole emission coefficient have been calculated from the paper of Libertino et al. [10]. The electron emission rate and hole emission rate are given as follows:

$$e_n = Ae^{-\frac{E_a}{kT}}$$
$$e_p = Ae^{-\frac{(E_g - E_a)}{kT}}$$

where,

$E_g$  = Silicon bandgap energy, 1.1 eV

$E_a$  = Activation energy, 0.15 eV

$k$  = Boltzmann constant, eV / K

$T$  = Temperature, K

$A$  = constant depends on the property of the trap semiconductor,  $7.43 \times 10^{10}/s$ .

The electron capture coefficient,  $c_n = \sigma_n V_{th}$

The hole capture coefficient,  $c_p = \sigma_p V_{th}$

where,

$$V_{th} = \text{thermal velocity} = \sqrt{\frac{3kT}{m^*}}$$

$\sigma_n$  = electron capture cross-section area,  $cm^2$

$\sigma_p$  = hole capture cross-section area,  $cm^2$

$k$  = Boltzmann constant,  $eV / K$

$m^*$  = effective mass of electron or hole

The electron and hole capture cross sections have been taken as  $5 \times 10^{-19} cm^2$  [25]. The electron and hole effective masses are taken as  $m_e^* = 1.1m_0$  and  $m_h^* = 0.56m_0$  where  $m_0$  is the electron rest mass,  $9.1095 \times 10^{-31} Kg$ .

Values of other parameters used are,

$$\tau_{rad} = 1ms [1]$$

$$C_{Ar} = 4.4 \times 10^{-13} cm^3 s^{-1}$$

$$C_{Abe} = 1.9 \times 10^{-14} cm^3 s^{-1}$$

$$C_{Ah} = 4.4 \times 10^{-13} cm^3 s^{-1}$$

$$C_{Abh} = 6.5 \times 10^{-15} cm^3 s^{-1}$$

$$W_0 = 10^9 s^{-1}$$

The laser cavity is characterized by: Volume =  $300\mu m \times 300\mu m \times 1\mu m$ . Mirror reflectivities are  $R_1=R_2=90\%$ . Unless otherwise stated, the following values have been used for our analysis  $T=10K$ ,  $N_{Er} = 10^{19}/cm^3$  and  $N_A = 10^{16}/cm^3$ .

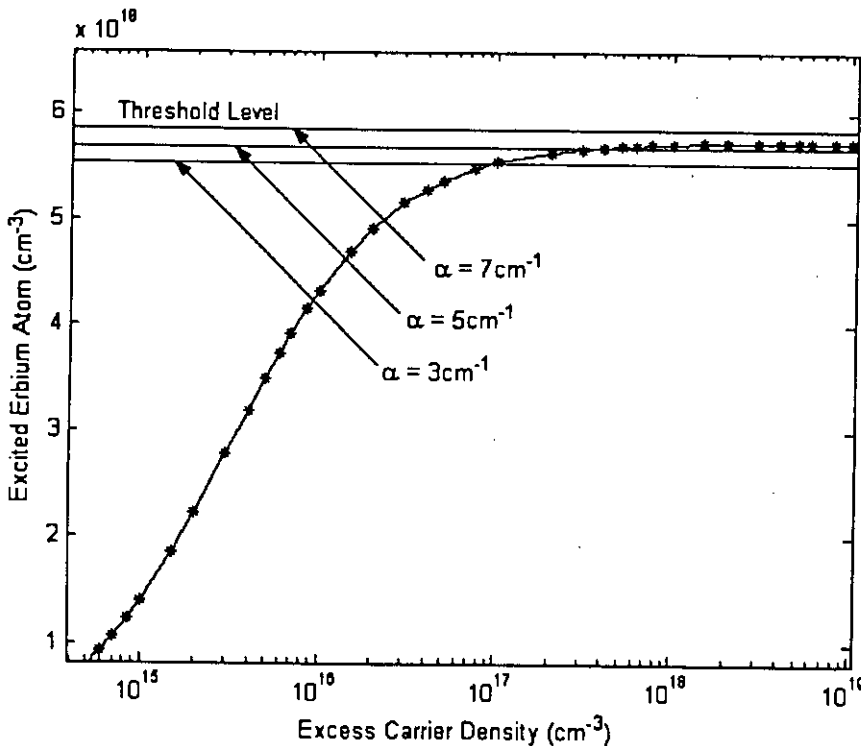
## 5.2 Excited Erbium Atom and Laser Operation

The lasing operation from erbium doped silicon (EDS) is highly dependent on device parameters and proper design. In this section, we have investigated how much amount of erbium atoms can be excited from the ground level to the  $^4I_{13/2}$  state in the absence of any

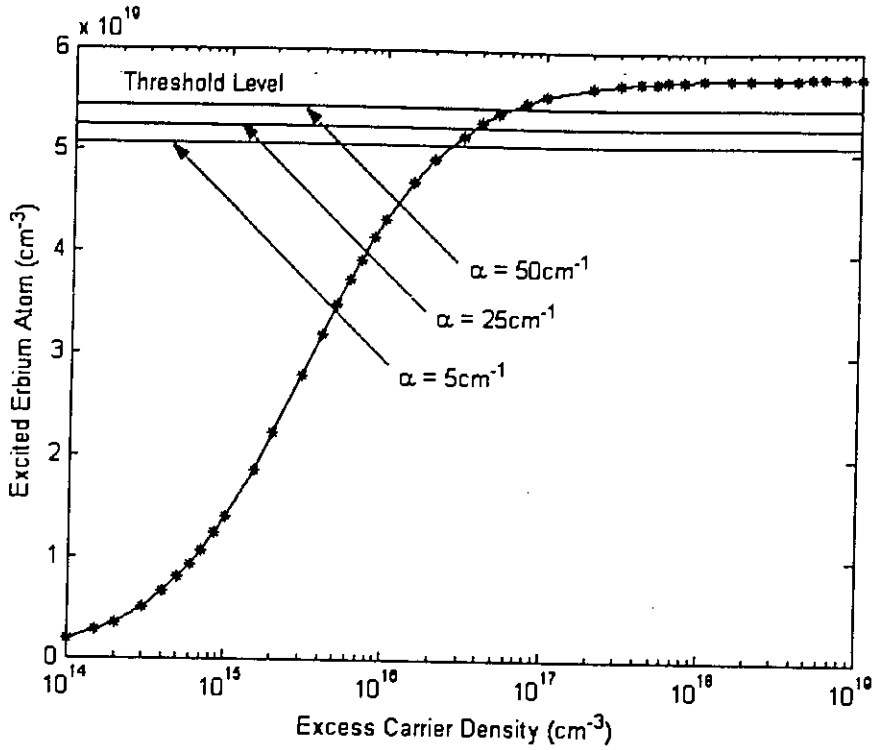
optical feedback for different excitation conditions, lifetime and doping level. We have also calculated the threshold value of population inversion for the lasing condition [25]. If the amount of erbium atoms in the excited state exceeds this threshold level, laser operation is possible. But when lasing occurs, the excited erbium atoms clamps to its threshold value due to stimulated transition which has been shown in the last part of this chapter.

### 5.2.1 Effect of Internal Loss Coefficient ( $\alpha$ )

Fig. 5.1 shows the curve of excited erbium atom as a function of excess carrier density with Er concentration of  $10^{19} \text{ cm}^{-3}$ . The asterisk curve illustrates that Er excitation in spontaneous emission is independent of loss coefficient ( $\alpha$ ). Horizontal lines show the corresponding threshold level of Er excitation. The curve shows that with the change of loss coefficient, the threshold level of population inversion for lasing condition changes. For  $\alpha = 3 \text{ cm}^{-1}$  and  $\alpha = 5 \text{ cm}^{-1}$ , the excited atoms can exceed the required threshold level for lasing operation but for  $\alpha = 7 \text{ cm}^{-1}$ , threshold level cannot be reached. But if the doping concentration of erbium is increased up to  $10^{20} \text{ cm}^{-3}$ , threshold level is possible to achieve even at higher absorption loss coefficient as shown in Fig. 5.2.



**Fig. 5.1** Excited Er atom as a function of excess carrier density for different values of loss coefficient ( $\alpha$ ) with  $N_{Er} = 10^{19} \text{ cm}^{-3}$ .



**Fig. 5.2** Excited Er atom as a function of excess carrier density for different values of loss coefficient ( $\alpha$ ) with  $N_{Er} = 10^{20} \text{ cm}^{-3}$ .

It is also observed that with the increase of loss coefficient, excess carrier density needed to achieve the threshold level of  $N_{Er}^*$  also increases indicating the higher threshold current density.

### 5.2.2 Effect of Er Radiative Lifetime ( $\tau_{rad}$ )

Figs. 5.3 and 5.4 show the excited erbium atom for different radiative lifetime of erbium atom. The amount of excited erbium atoms is almost same in three different cases but threshold level is different for different lifetime as before. For doping concentration of  $N_{Er} = 10^{19} \text{ cm}^{-3}$ , it is possible to achieve the threshold level for lifetime up to 1ms. Beyond this value, threshold level is not possible to achieve indicating that erbium doped silicon laser does not lase. But if the concentration of Er is increased to  $N_{Er} = 10^{20} \text{ cm}^{-3}$ , excited erbium atoms can reach the threshold level at higher lifetime as shown in Fig. 5.4.



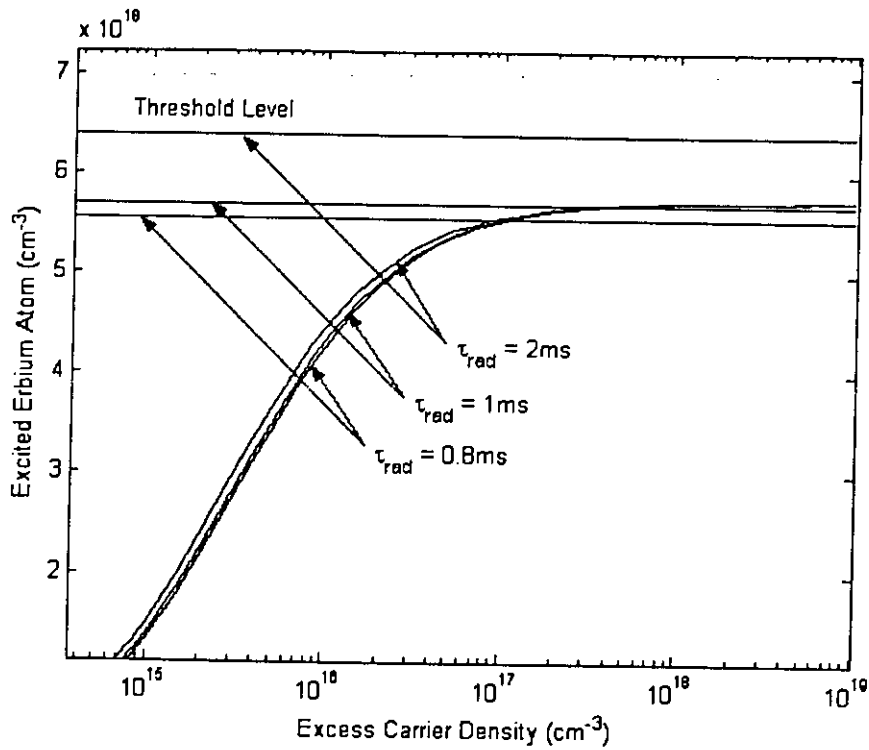


Fig. 5.3 Excited erbium atom as a function of excess carrier density for different values of Er radiative lifetime with  $N_{Er} = 10^{19} \text{ cm}^{-3}$ .

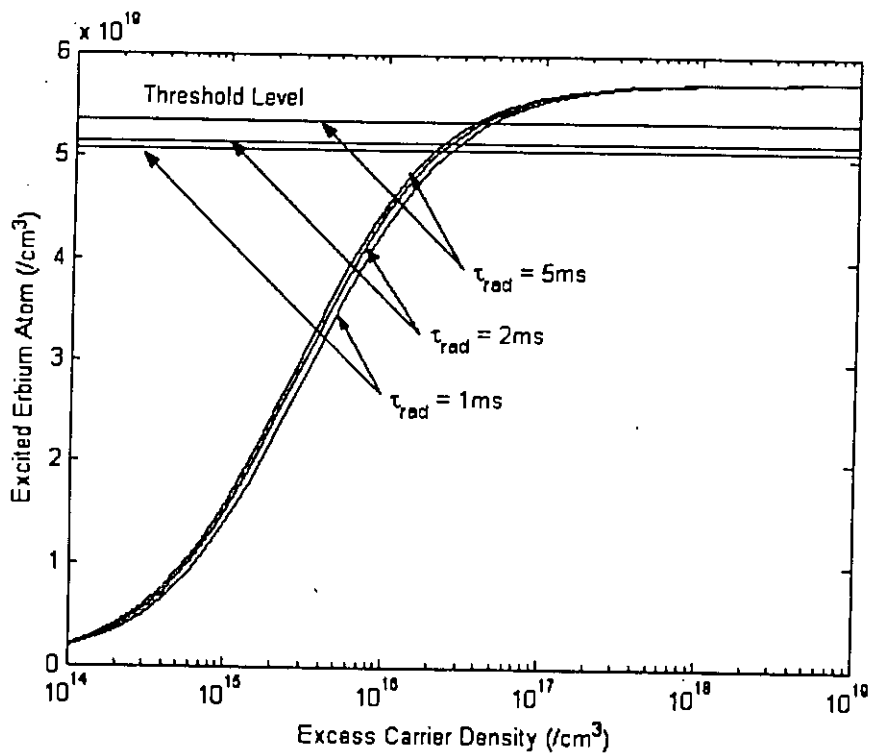


Fig. 5.4 Excited Er atom as a function of excess carrier density for different values of Er radiative lifetime with  $N_{Er} = 10^{20} \text{ cm}^{-3}$ .

### 5.2.3 Effect of Doping Concentration ( $N_A$ )

Fig. 5.5 describes the effects of background doping on the density of Er atoms in the excited state. Erbium atoms can be excited up to or slightly above the threshold level even at higher background concentration. But excess carrier density needed to achieve the required threshold level (shown in dotted line) for lasing operation increases with the increase of doping concentration. This is because Auger effect with bound carriers increases with the increase of doping concentration. Thus higher background doping causes weaker excitation of Er atoms and thereby requires a larger carrier injection for lasing threshold.

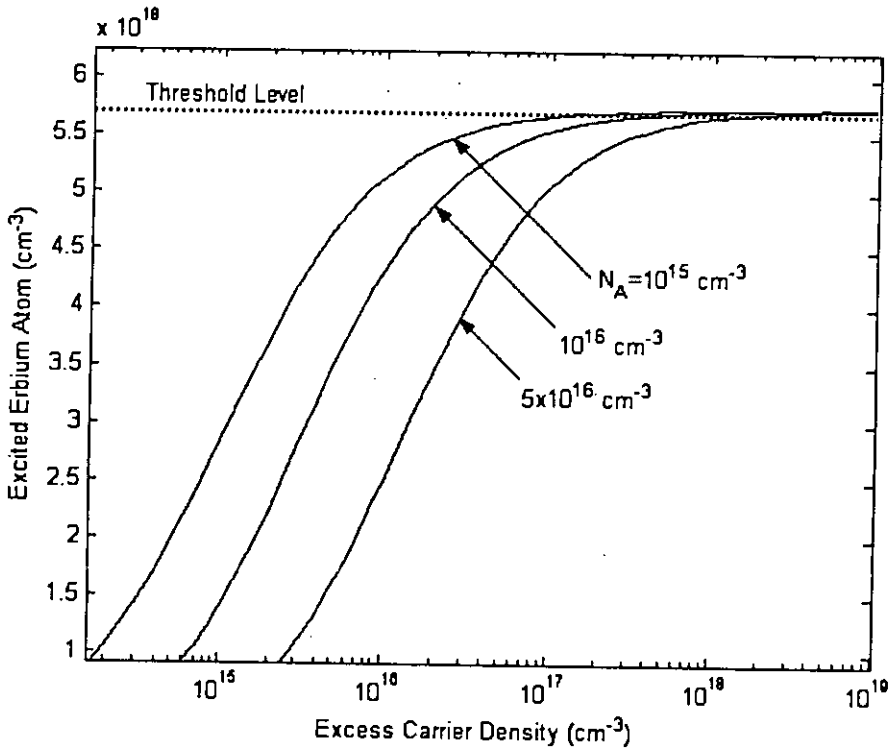


Fig. 5.5 Excited erbium atom as a function of excess carrier density for different values of doping concentration with  $N_{Er} = 10^{19} \text{ cm}^{-3}$ .

### 5.2.4 Effect of Spectral Width ( $\Delta\lambda$ )

Figs. 5.6 and 5.7 show the effect of spectral width on the Er atom excitation as a function of excess carrier density. The asterisk curve indicates that Er atoms in the excited state do not change with changing the spectral width but the threshold level changes with different spectral width. When erbium concentration is  $N_{Er} = 10^{19} \text{ cm}^{-3}$ , threshold can be achieved at  $\Delta\lambda = 1 \text{ \AA}$  and below  $1 \text{ \AA}$ . But if the erbium concentration is increased to  $N_{Er} = 10^{20} \text{ cm}^{-3}$ , threshold is possible to achieve even at higher spectral width.

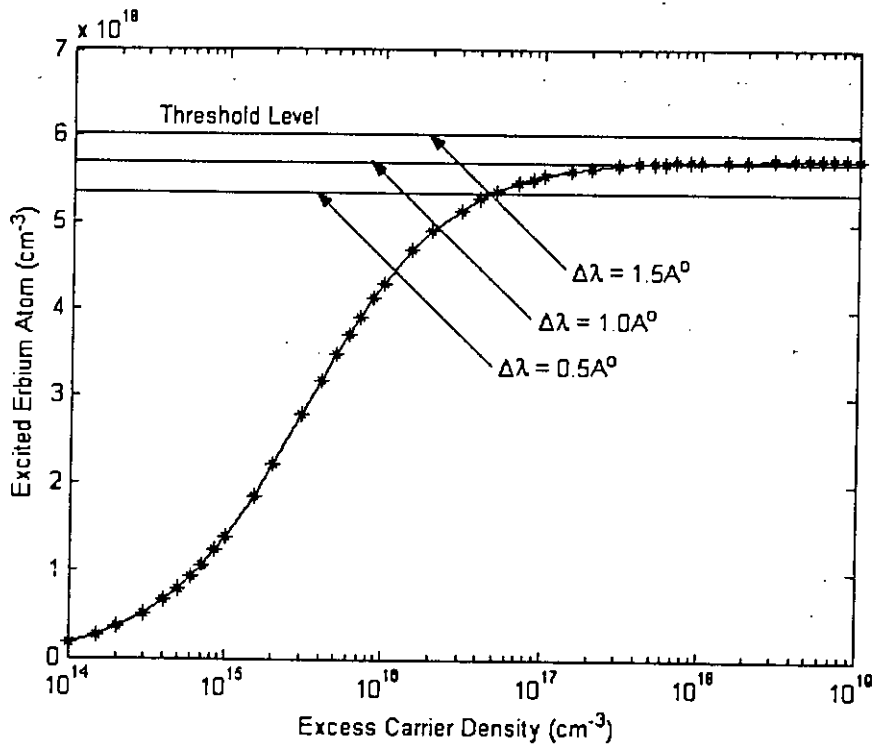


Fig. 5.6 Excited Er atom as a function of excess carrier density for different values of spectral width of emission with  $N_{Er} = 10^{19} \text{ cm}^{-3}$ .

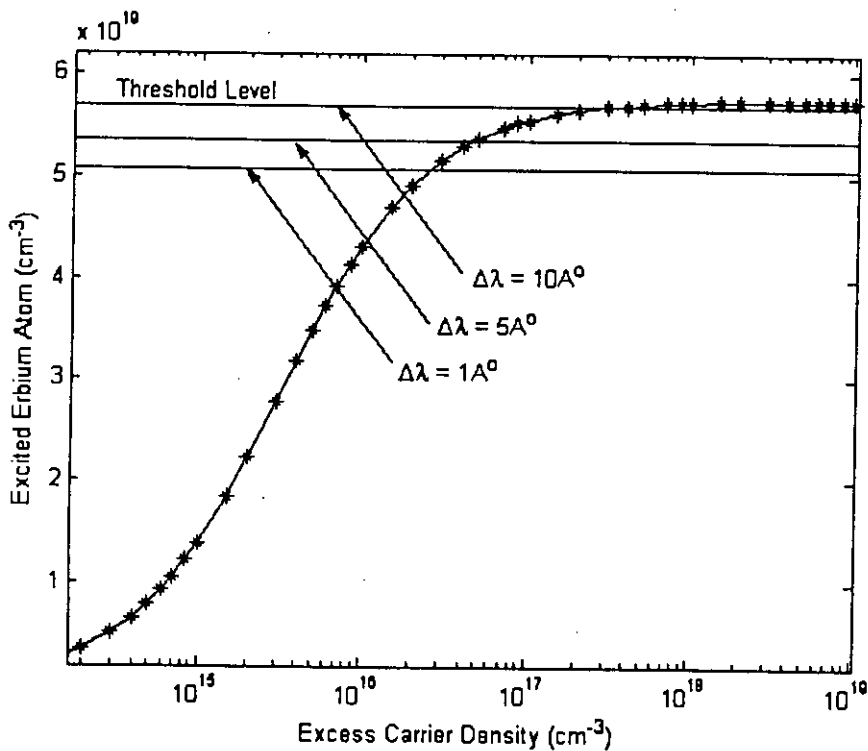


Fig. 5.7 Excited Er atom as a function of excess carrier density for different values of spectral width of emission with  $N_{Er} = 10^{20} \text{ cm}^{-3}$ .

### 5.3 Power-Current Characteristics

In this section we will discuss the output power of erbium doped silicon laser as a function of injection current and effect of various parameters on the output power. Below threshold, ignoring the photon density  $S$  inside the cavity, we have calculated the value of excess carrier density at threshold,  $n_{thr}$  using Eq. (4.22) and then calculated the value of current density  $J_{thr}$  using Eq. (4.23). Figs. 5.8 to 5.14 show the output power of EDS laser for different device parameters.

Figs. 5.8 and 5.9 show the effect of loss coefficient ( $\alpha$ ) on the output power for two different Er concentrations of  $10^{19} \text{ cm}^{-3}$  and  $10^{20} \text{ cm}^{-3}$  respectively. In all the cases, below threshold, there is no stimulated emission and output power is only due to spontaneous emission. This power is very small because only a small fraction of the spontaneous emission enters into lasing mode. When the current density  $J$  exceeds  $J_{thr}$ , stimulated emission dominates the spontaneous emission and power output increases almost linearly with the injection current density. Although the above threshold power is different at different  $\alpha$ , the spontaneous power is same. Because erbium excitation does not depend

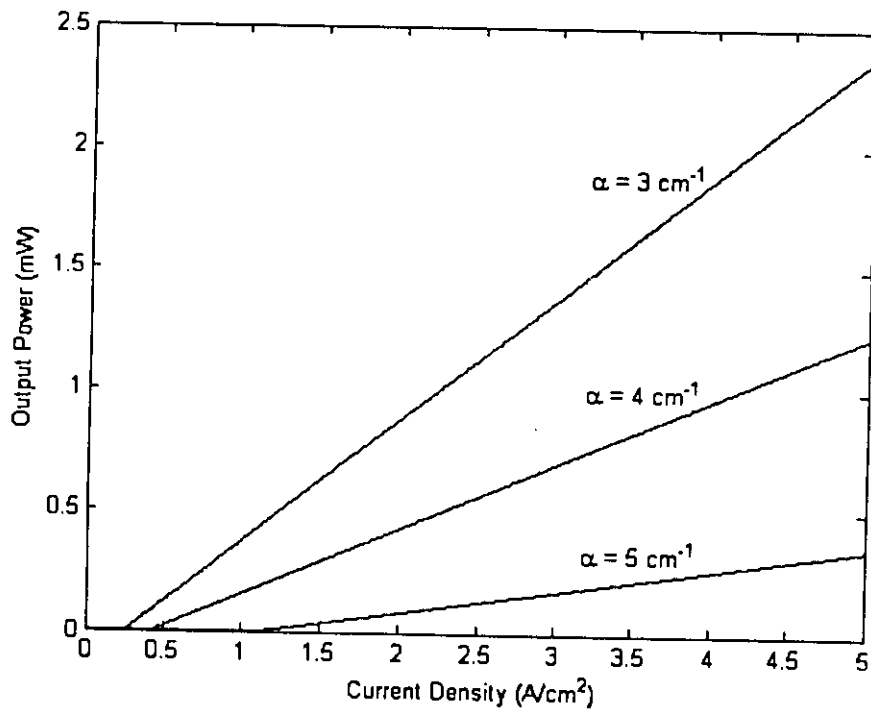
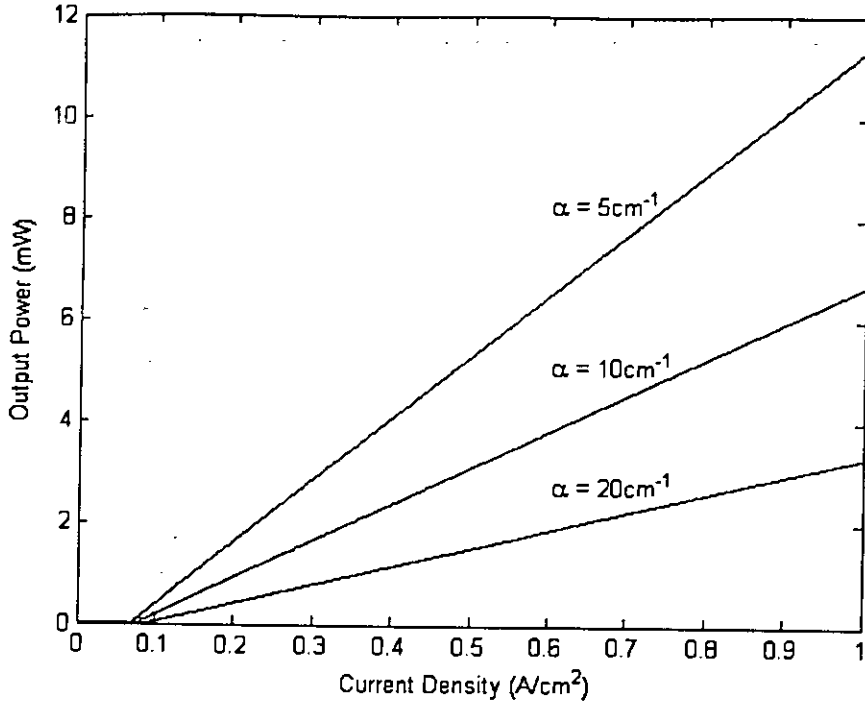


Fig. 5.8 Output power vs injection current density of EDS laser for different values of loss coefficient with  $N_{Er} = 10^{19} \text{ cm}^{-3}$ .



**Fig. 5.9** Output power vs injection current density of EDS laser for different values loss coefficient with  $N_{Er} = 10^{20} \text{ cm}^{-3}$ .

on  $\alpha$ . But with the increase of  $\alpha$ , threshold gain increases causing more carriers to be injected for achieving the threshold excitation of erbium atom. So at higher value of  $\alpha$ , threshold current density is also higher.

Figs. 5.10 and 5.11 show the effect of radiative lifetime of erbium atom on P-J curve. From figures, we can see that at lower lifetime, more power is obtained than the higher lifetime. Here below threshold, spontaneous power changes with the change of lifetime shown in the inset of Fig. 5.11. This is reasonable because spontaneous power is inversely proportional to the radiative lifetime. It is also observed that when Er concentration is  $N_{Er} = 10^{20} \text{ cm}^{-3}$ , threshold current density is reduced and consequently output power is increased compared to the Er concentration of  $10^{19} \text{ cm}^{-3}$ .

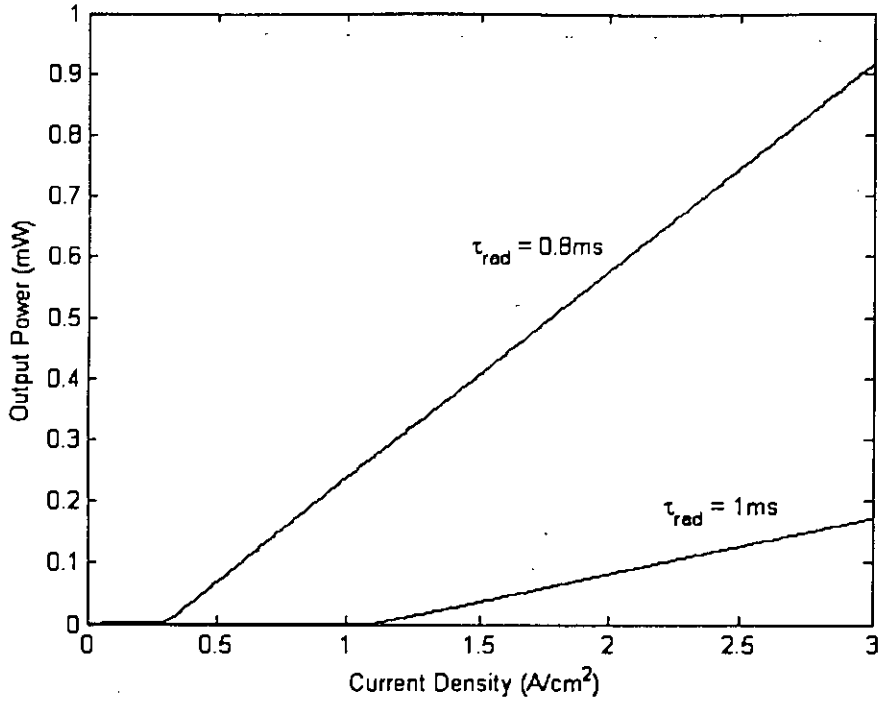


Fig. 5.10 Output power vs injection current density of EDS laser for different erbium life time with Er concentration of  $N_{Er} = 10^{19} \text{ cm}^{-3}$ .

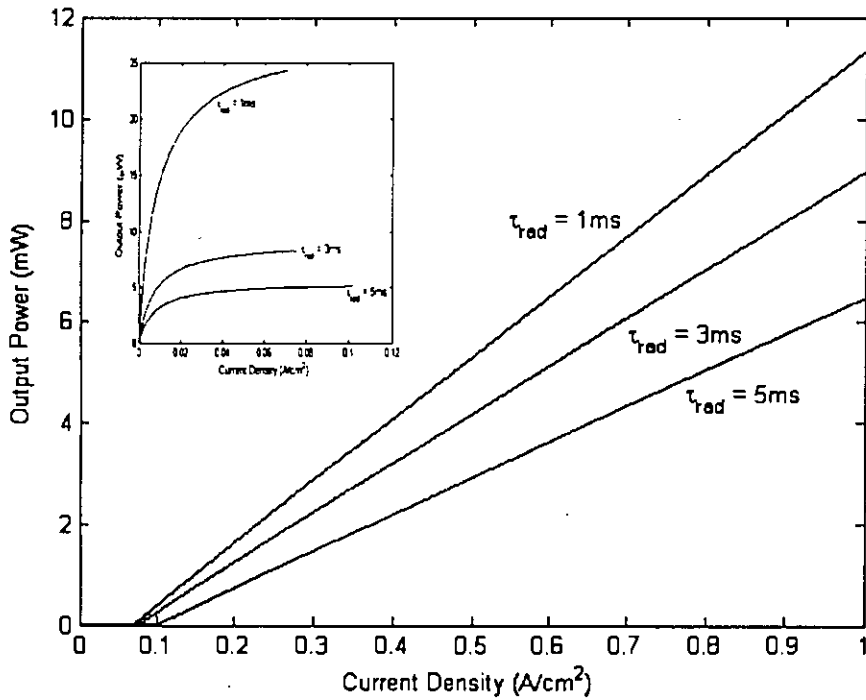
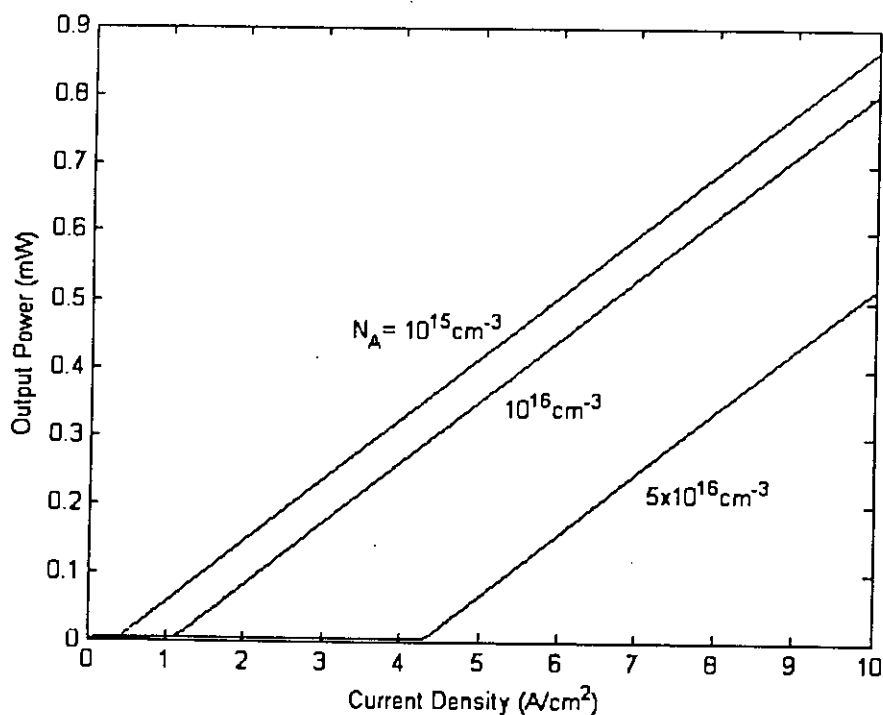


Fig. 5.11 Output power vs injection current density of EDS laser for different erbium lifetime. The inset shows only the spontaneous power. In this case, erbium concentration is  $N_{Er} = 10^{20} \text{ cm}^{-3}$ .

Effect of background doping and spectral width on the laser output power is shown in Figs. 5.12 and 5.13. With the increase of acceptor doping, Auger recombination with bound carrier increases. So non-radiative decay of erbium atom increases and output power is reduced. Fig. 5.13 is plotted for erbium concentration of  $10^{20} \text{ cm}^{-3}$ . It is seen that with the increase of spectral width, output power is reduced.



**Fig. 5.12** Output power vs injection current density of EDS laser for different values of background doping concentration with  $N_{Er} = 10^{19} \text{ cm}^{-3}$ .

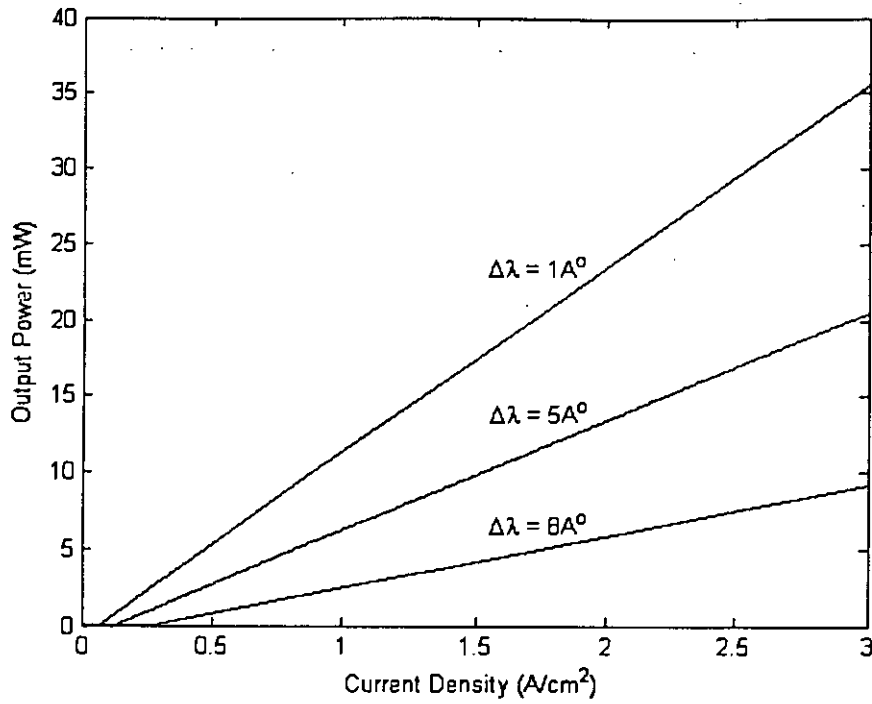


Fig. 5.13 Output power vs injection current density of EDS laser for different spectral width. The doped Er concentration is  $10^{20} \text{ cm}^{-3}$ .

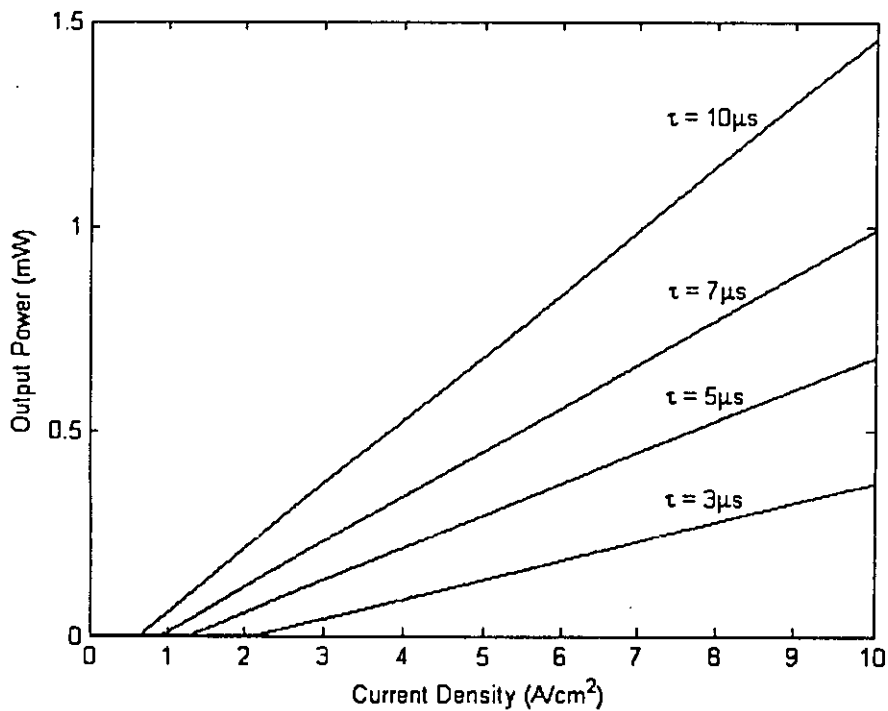


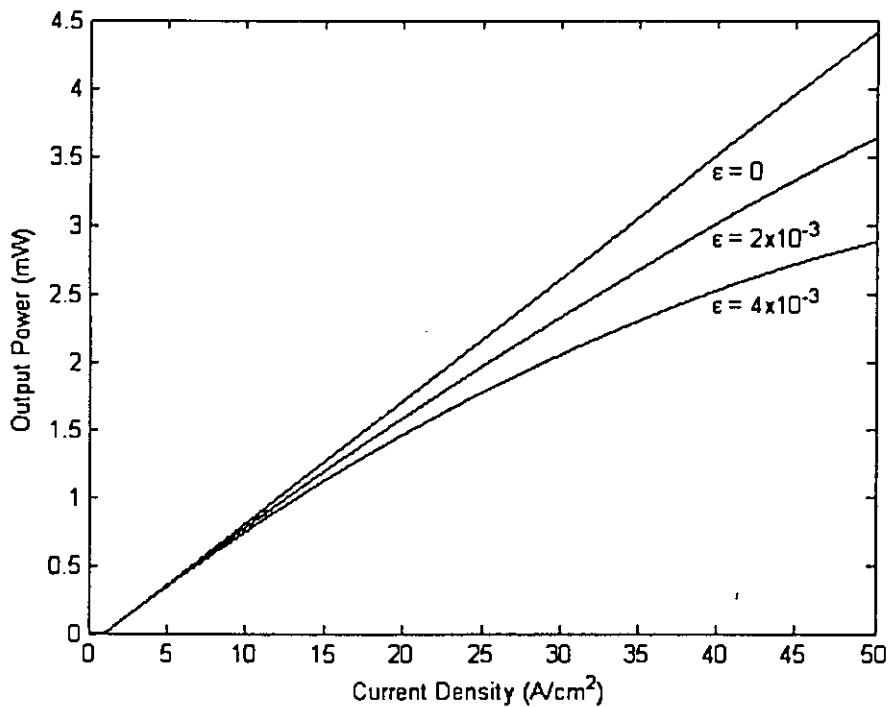
Fig. 5.14 Output power vs injection current density of EDS laser for different silicon (carrier) lifetime. The erbium concentration is  $10^{19} \text{ cm}^{-3}$ .



In Fig. 5.14, the effect of carrier lifetime ( $\tau$ ) on the output power has been demonstrated. It can be seen from the figure that output power increases with the increase of carrier lifetime. For certain current density, if the carrier lifetime increases, more carriers are recombined. As a result, excitation rate of erbium atoms increases and results the higher output power.

#### 5.4 Effect of Injection Dependent Loss Coefficient

We have assumed that internal loss coefficient  $\alpha$  is constant irrespective of the injection level. But practically, this value increases with the increase of current density. We have assumed that  $\alpha$  increases with current density like this  $\alpha = \alpha_0 + \epsilon J$ . Fig. 5.15 shows the effect of carrier dependent loss coefficient on laser output power. From figure, we see that output power is reduced with the increase of  $\alpha$ .



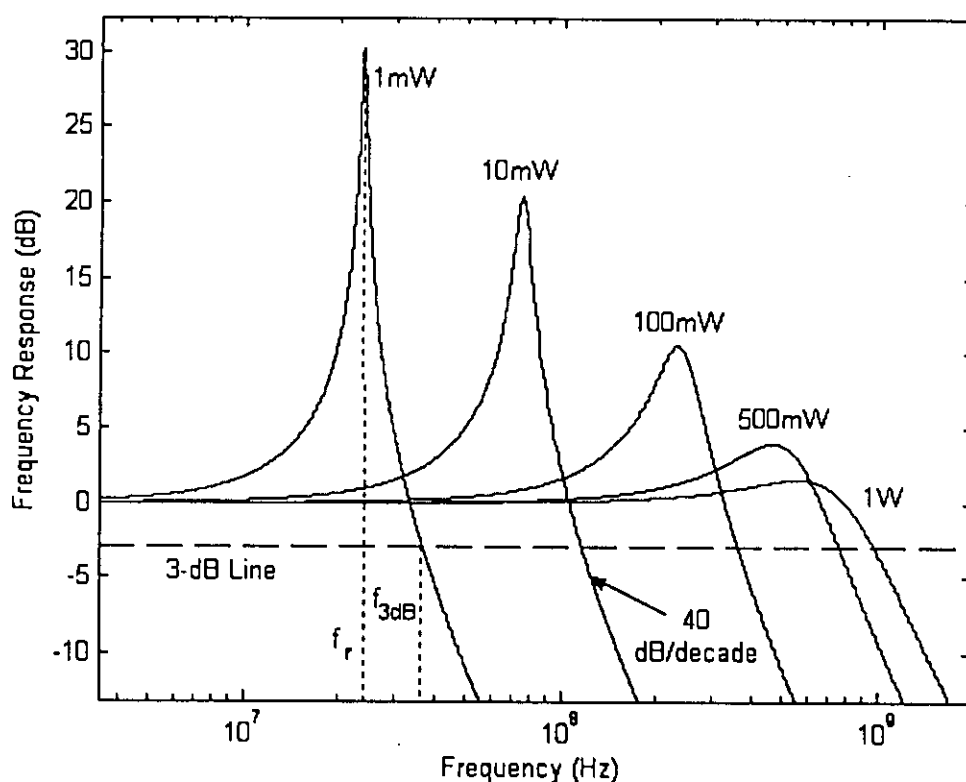
**Fig. 5.15** Effect of injected carrier dependent absorption loss coefficient on the EDS laser output power.

#### 5.5 Frequency Response

One of the main objectives of this thesis is to determine the frequency response of erbium doped silicon laser. The normalized intensity modulation transfer function  $H(\omega)$

derived in chapter four is plotted in Fig. 5.16 for different optical output powers as a function of modulation frequency. The figure shows the pattern of a low pass filter. The intensity modulation can follow the current modulation up to frequencies near  $f_r$  with an abrupt increased response. Above the resonance peak, the response drops off rapidly with a slope of  $-40\text{dB/decade}$ . The curves in Fig. 5.16 also reveal that resonance peak flattens and broadens out with increasing output power.

The 3-dB modulation bandwidth  $f_{3dB}$  is defined as the frequency at which  $|H(\omega)|$  is reduced by 3-dB from its DC value. The variation of  $f_{3dB}$  and the variation of  $f_r$  are shown in Fig. 5.17 as a function of output power. Note that the modulation bandwidth increases with the increase of output power. The response characteristic becomes maximum at frequency  $f_p$ . The variation of  $f_p$  and  $f_r$  are shown in Fig. 5.18. When the power level is small, damping coefficient is small and  $f_p$  is approximately equal to the resonance frequency  $f_r$ . But with the increase of power, damping coefficient increases and  $f_p \neq f_r$ .



**Fig. 5.16** Semi-log plot of frequency response of erbium doped silicon laser for different output powers.

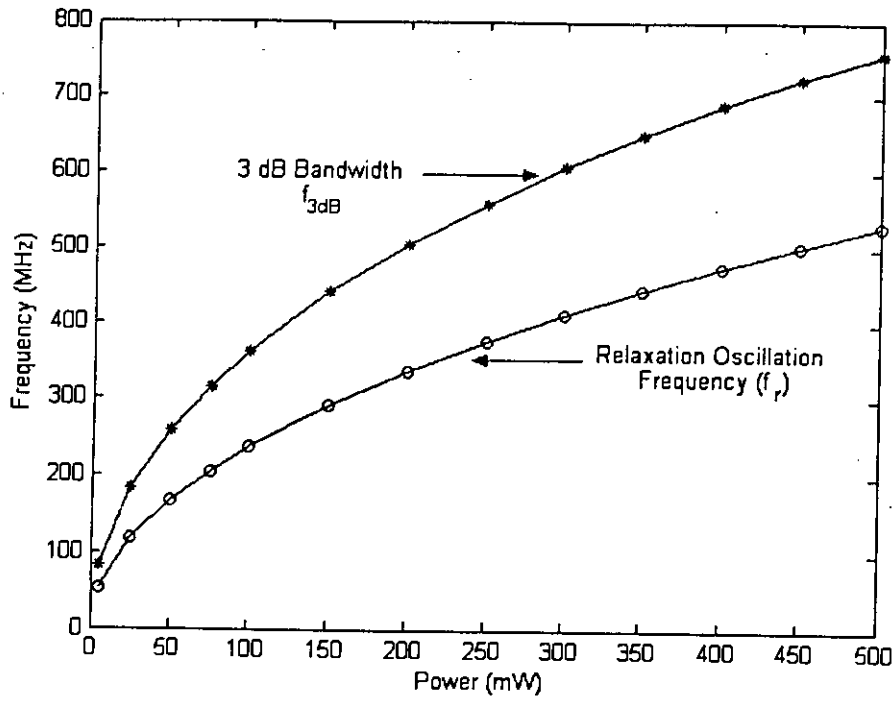


Fig. 5.17 Plot of relaxation oscillation frequency and the 3-dB bandwidth of EDS laser for different output power.

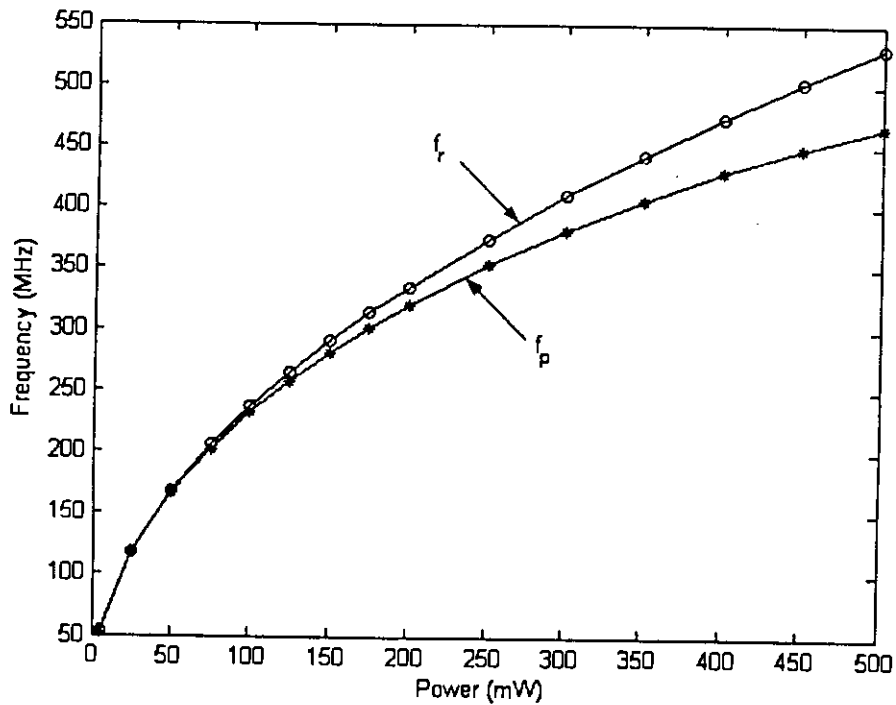
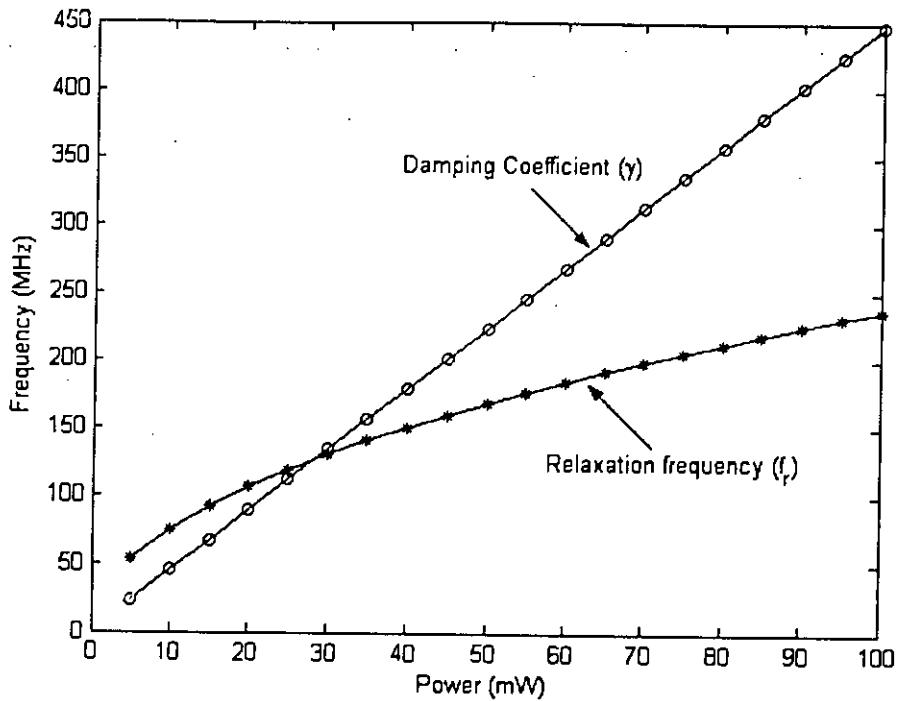
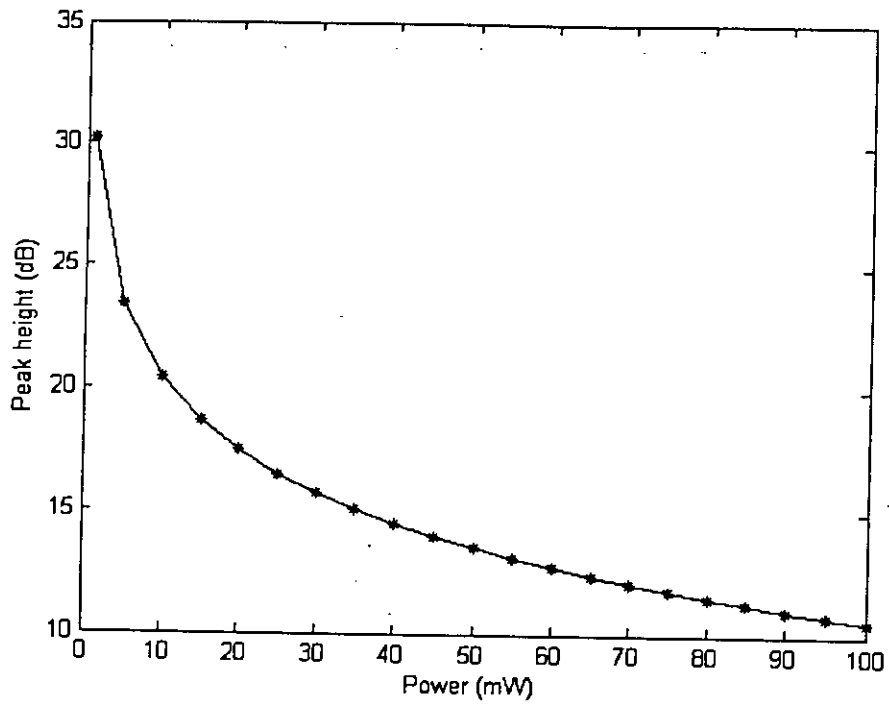


Fig. 5.18 Plot of relaxation frequency ( $f_r$ ) and actual peak frequency of resonance ( $f_p$ ) for different output power.



**Fig. 5.19** Effect of output power on the damping coefficient ( $\gamma$ ) and relaxation resonance frequency ( $f_r$ ).

The effect of power on the damping constant ( $\gamma$ ) and resonance frequency ( $f_r$ ) is shown in Fig. 5.19. From figure, we can see that damping constant increases linearly with the laser output power as derived from Eq<sup>n</sup>.4.59. The variation of peak resonant amplitude with output power is shown in Fig. 5.20. From the figure, we can see that resonant amplitude decreases with increasing output power. This is because amplitude of the resonance peak depends on damping constant. At low output power, this damping is small and the peak height of the response is large. But with the increase of power, the damping rate increases and the peak amplitude decreases.



**Fig. 5.20** Normalized magnitude of the peak of the modulation response as a function of output power.

## 5.6 Transient Characteristics

Fourth-order Runge-Kutta method is used for numerical solutions of the rate equations presented in chapter four. Figs. 5.21 to 5.26 show the numerical plots of the excited erbium atoms and the photon density for different values of drive current. From these figures, we can see that before reaching to the steady-state values, both the excited erbium atoms and photon density undergo a damped oscillation. In each case, we have assumed that excitation current is abruptly increased at  $t = 0$  and then held at steady-state value. Subsequent captures of an electron and hole in the erbium related recombination site releases energy and excites erbium atom from the ground level to the first excited state. Erbium atoms continue to excite due to continuous pumping. Before threshold, population inversion does not occur and little photon density exists only due to spontaneous emission. When excited Er atoms exceed the threshold level, stimulated emission takes place and causes a downward stimulated transition of excited erbium atoms. As Er atoms fall off quickly causing a reduction in the population inversion, gain of the cavity medium reduces from the threshold gain and photon density drops off quickly. This causes the erbium atom to excite again. When the erbium atom exceeds the threshold level, photon density again increases and increases the downward transition rate of erbium atoms. Thus interplay of transition between Er atom and photon density takes place before reaching to the steady-state values. At steady-state, the excited erbium atoms are found to clamp its threshold value. With the increase of excitation, oscillations die out quickly as shown in Figs. 5.22 to 5.25. This is because the decay of the oscillation depends on the damping factor which is large at high excitation.

The numerical simulations shown in the figures also illustrate that time is needed for the Er atom to build up to the threshold value before light is emitted. This build up time is called the turn-on delay of the laser. The turn-on time is found to be smaller if the laser excitation is increased. Because with the increase of excitation, more carriers are available for Er pumping and it then quickly reaches to its threshold level.

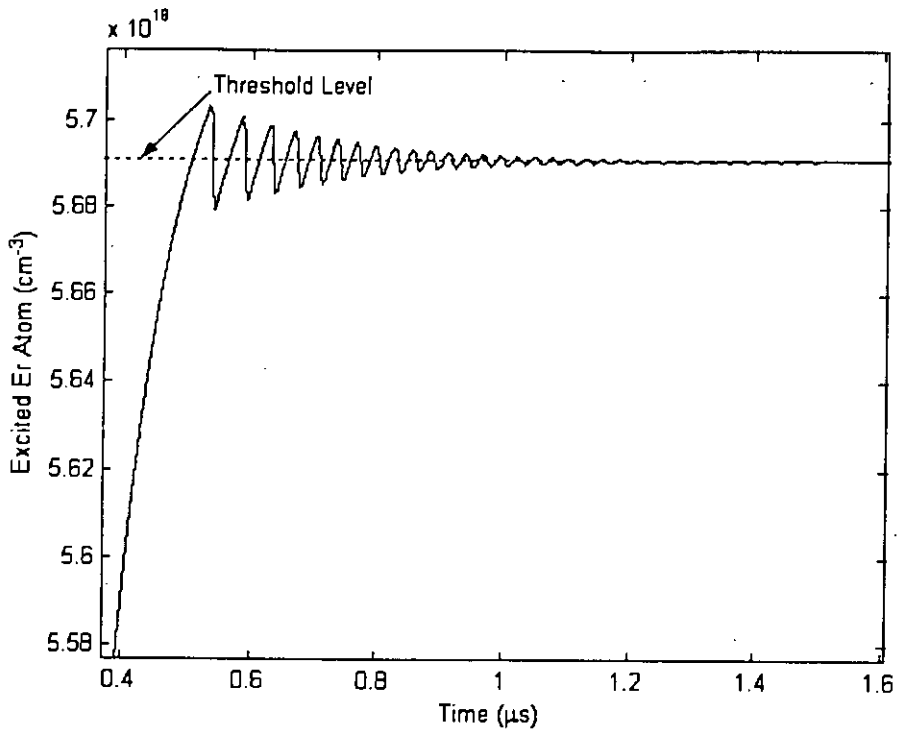


Fig. 5.21 Transient response of excited erbium atoms of EDS laser for step input current density  $J=27.6\text{A/cm}^2$  (carrier concentration  $10^{19}\text{cm}^{-3}$ ). After transient state, the excited erbium atoms clamp to its threshold value  $N_{Erh}^*$ .

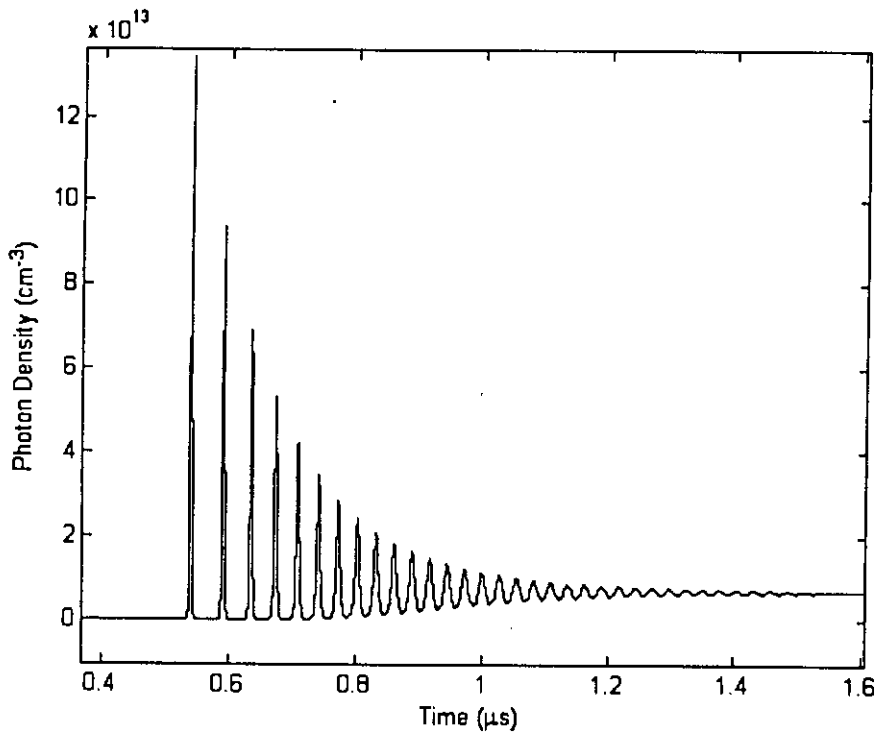
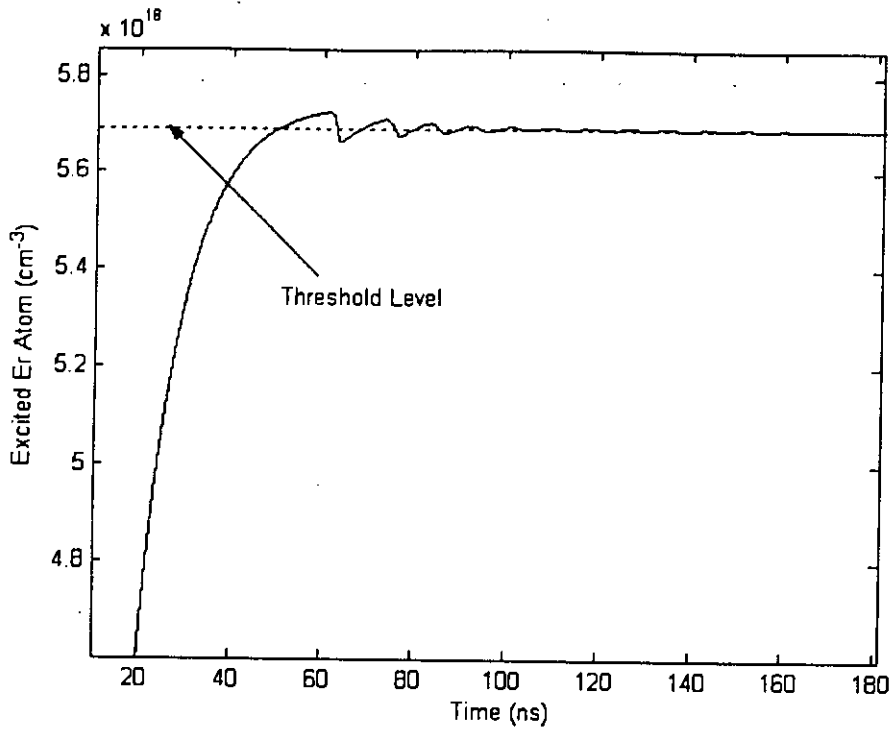
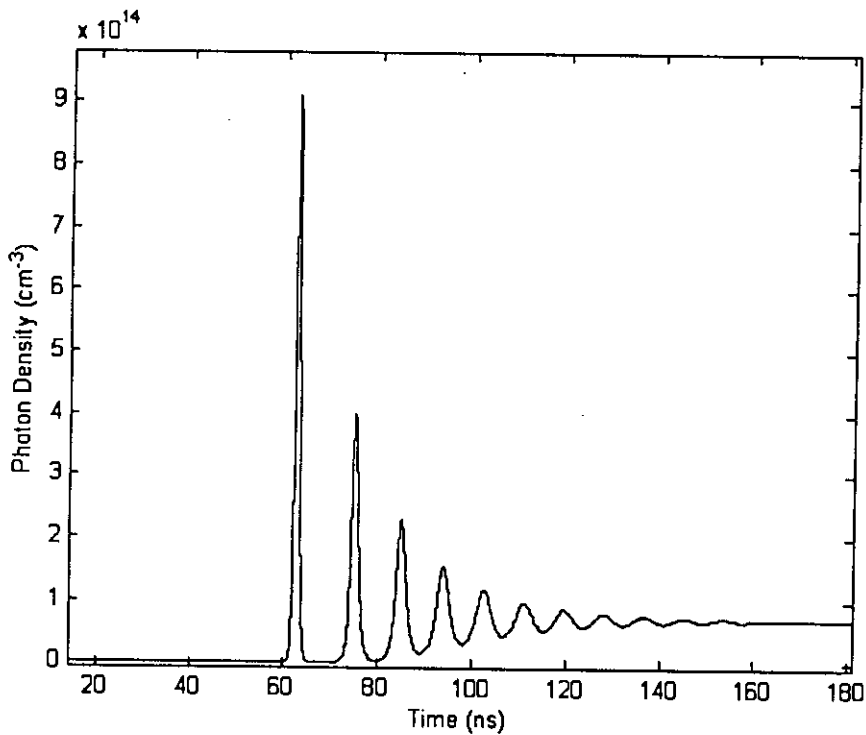


Fig. 5.22 Transient response for photon density of EDS laser for step input current density  $J=27.6\text{A/cm}^2$ .



**Fig. 5.23** Transient response of excited erbium atoms of EDS laser for step input current density  $J=276\text{A}/\text{cm}^2$  (carrier concentration  $10^{20}\text{cm}^{-3}$ ).



**Fig. 5.24** Transient response of photon density of EDS laser for step input current density  $J=276\text{A}/\text{cm}^2$ .



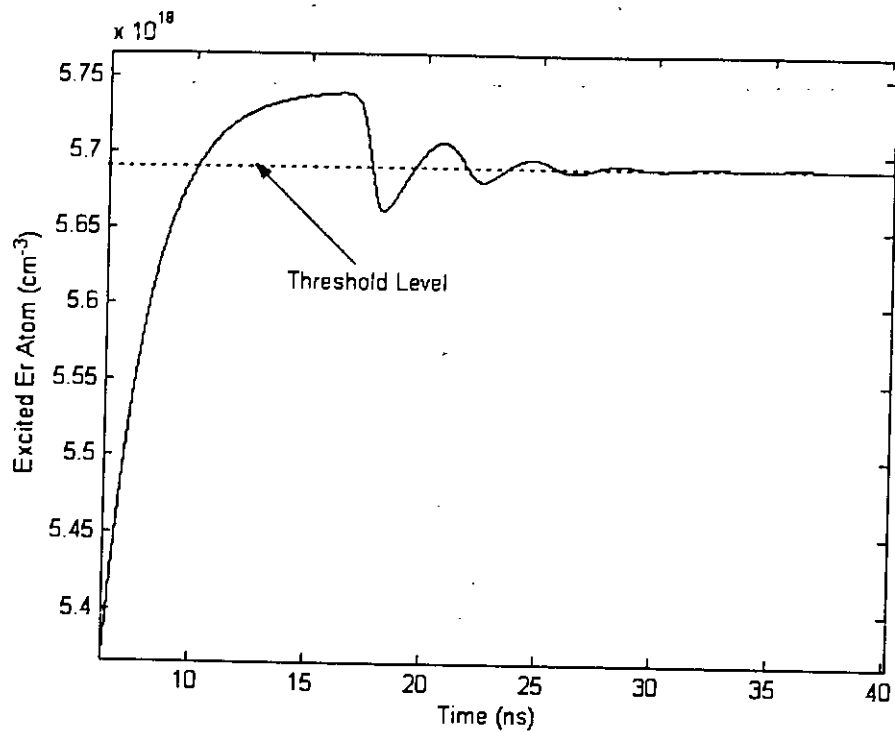


Fig. 5.25 Transient response of excited erbium atoms of EDS laser for step input current density  $J=1380\text{A}/\text{cm}^2$  (carrier concentration  $5 \times 10^{20}\text{cm}^{-3}$ ). Here oscillation dies out quickly.

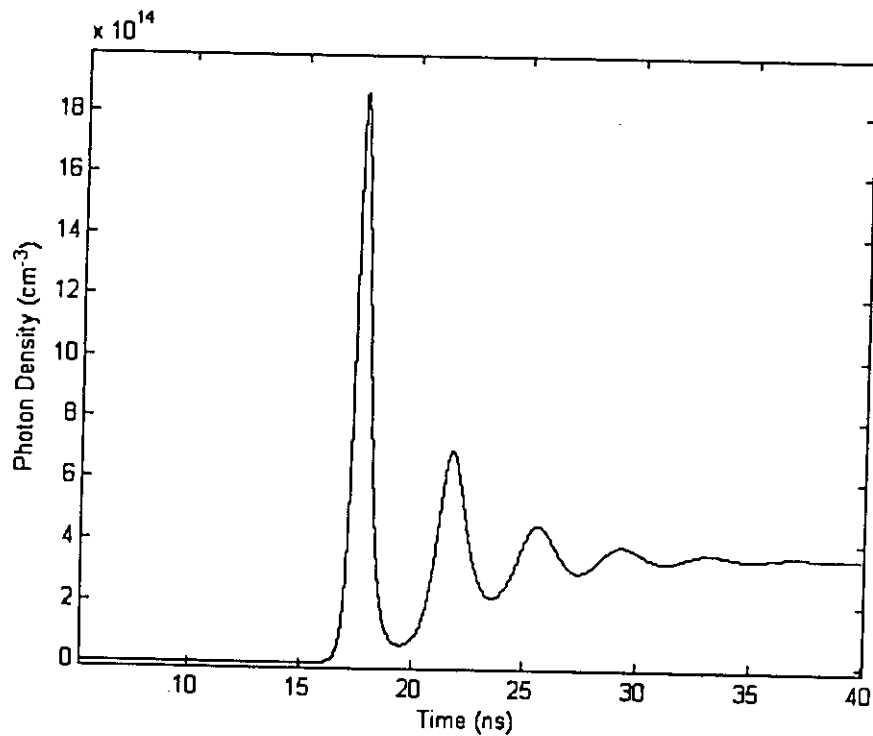


Fig. 5.26 Transient response of photon density of EDS laser for step input current density  $J=1380/\text{cm}^2$ .

# CHAPTER SIX

## Conclusions

In this thesis work, various properties of erbium doped silicon diode laser have been evaluated. Mechanism of erbium excitation through Shockley-Read-Hall (SRH) recombination process has been analyzed for conditions of achieving lasing threshold. Erbium atoms decay from its excited state  $^4I_{13/2}$  through both radiative and non-radiative processes. As we have done our analysis at low temperature (10K), effect of energy back transfer on Er de-excitation has been assumed negligible. The gain needed to compensate all optical losses inside the cavity including mirror losses is called threshold gain and it has been determined. The loss of the light at the end facets has been taken as output power. The effects of erbium concentration, background doping, erbium lifetime, loss coefficient, carrier lifetime etc. have been investigated on light output and discussed these effects with graphical representations. Threshold current density is determined and it is found to vary with the parameters. Below threshold, the output power is due to spontaneous emission which is very small in magnitude (order of few  $\mu\text{W}$ ) and almost same for all cases except the variation for erbium radiative lifetime. When erbium lifetime changes, spontaneous power is found to vary as it is inversely proportional to the lifetime. After threshold, output power is found to increase linearly with the injection current density. For some cases, erbium atoms in the excited state can not exceed the required threshold level and EDS can not lase. But if the erbium concentration is increased, it is found that EDS can lase. In these cases threshold current is reduced with increased output power. Light output for injection dependent loss coefficient has been determined. As  $\alpha$  increases with the carrier injection, the power output no longer remains linear at high level of current injection. This limits the operating region of Si:Er laser. Rate equations for excited erbium atoms and photon density have been solved for small-signal to evaluate the dynamic characteristics of EDS laser. Sinusoidal signal variation has been added with the steady dc current density  $J_0$  and modulation transfer function

has been determined. The transfer function shows resonance peak above which response drops off rapidly. Both the resonance frequency and 3-dB bandwidth increase with the output power level. The rate equations also have been solved numerically for large-signal. The simulation shows that both excited erbium atoms and photon density pass a short period of sinusoidal oscillation before finally reaching to steady-state values. With the increase of excitation current, transient response is found to die out quickly and hence lowers the turn-on time of EDS laser. Finally we can conclude that each characteristic obtained from our prospective Si:Er laser shows very good consistency with the conventional heterojunction laser.

### **6.1 Recommendation for Future Work**

Attainment of light emission from erbium doped silicon material at room temperature is greatly reduced due to temperature quenching effect. So research for reducing the luminescence quenching can be carried out in order to fabricate Si:Er optoelectronic devices operating at room temperature. Achievement of lasing threshold is highly dependent on proper design and processing of the laser structure. If concentration of Er is increased to a high level ( $\sim 10^{20} \text{cm}^{-3}$ ), it is found that EDS can lase for a wide-range variation of the device parameters ( $\alpha$ ,  $\Delta\lambda$ ,  $\tau_{\text{rad}}$  etc.). But Er has limited solid solubility in silicon. So work can be done to increase the concentration of erbium incorporated in silicon.

The direct modulation bandwidth of EDS laser is of the order of hundred MHz range. At very high power, it is also possible to achieve GHz range bandwidth. But low power laser is normally used for optical communication systems in order to avoid fiber non-linearity. So a technique can be exerted to increase the bandwidth even at low output power. In our research, we have performed analysis for amplitude modulation. Similar analysis can also be worked out for frequency modulation. In erbium doped fiber amplifier, erbium is doped in silica. By confining light in EDFA, possibility of laser operation can be investigated.

## APPENDIX – A

### Derivation of Injected Carrier Density at Threshold

$$\text{Excitation rate} = f_i c_p p (N_{Er} - N_{Er}^*)$$

$$\text{De-excitation rate} = \frac{N_{Er}^*}{\tau_{Er}} + v_g g_0 (2N_{Er}^* - N_{Er}) S$$

At steady state, these two rates must be equal. So,

$$f_i c_p p (N_{Er} - N_{Er}^*) = \frac{N_{Er}^*}{\tau_{Er}} + v_g g_0 (2N_{Er}^* - N_{Er}) S$$

Below and at threshold, the value of photon density  $S$  can be neglected as lasing has not yet been started. Under this condition, the above equation becomes

$$f_i c_p p (N_{Er} - N_{Er}^*) = \frac{N_{Er}^*}{\tau_{Er}}$$

$$\Rightarrow f_i c_p p (N_{Er} - N_{Er}^*) = N_{Er}^* \left( \frac{1}{\tau_{rad}} + \frac{1}{\tau_{Af}} + \frac{1}{\tau_{Ab}} + \frac{1}{\tau_{bt}} \right)$$

At low temperature, energy back transfer can be neglected. We have assumed that Er is doped in the p-type silicon then above equation becomes

$$f_i c_p p (N_{Er} - N_{Er}^*) = N_{Er}^* \left( \frac{1}{\tau_{rad}} + C_{Ah} p + C_{Abh} N_A \right)$$

After biasing, equal amount of electrons and holes are injected from the source. In the p-region, the doping concentration is  $N_A$ . So the effective hole concentration is  $p = n + N_A$ . Substituting  $p = n + N_A$ , we obtain

$$f_i c_p (n + N_A) (N_{Er} - N_{Er}^*) = N_{Er}^* \left( \frac{1}{\tau_{rad}} + C_{Ah} (n + N_A) + C_{Abh} N_A \right)$$

$$\Rightarrow f_i c_p (n + N_A) (N_{Er} - N_{Er}^*) = N_{Er}^* \left[ \frac{1}{\tau_{rad}} + C_{Ah} n + (C_{Ah} + C_{Abh}) N_A \right]$$

$$\Rightarrow \frac{(e_p + c_n n)}{e_n + e_p + c_n n + c_p p} c_p (n + N_A) (N_{Er} - N_{Er}^*) = N_{Er}^* \left[ \frac{1}{\tau_{rad}} + C_{Ah} n + (C_{Ah} + C_{Abh}) N_A \right]$$

$$\Rightarrow \frac{(e_p + c_n n)}{e_n + e_p + c_n n + c_p (n + N_A)} c_p (n + N_A) (N_{Er} - N_{Er}^*) = N_{Er}^* \left[ \frac{1}{\tau_{rad}} + C_{Ah} n + (C_{Ah} + C_{Abh}) N_A \right]$$

At the onset of threshold,

$$N_{Er}^* = N_{Erth}^*$$

$$\text{and } n = n_{thrs}$$

Then at threshold, above equation becomes

$$\begin{aligned} & \frac{(e_p + c_n n_{thrs})}{e_n + e_p + c_n n_{thrs} + c_p (n_{thrs} + N_A)} c_p (n_{thrs} + N_A) (N_{Er} - N_{Erth}^*) \\ & = N_{Erth}^* \left[ \frac{1}{\tau_{rad}} + C_{Ah} n_{thrs} + (C_{Ah} + C_{Abh}) N_A \right] \end{aligned}$$

$$\begin{aligned} & \Rightarrow \frac{(e_p + c_n n_{thrs})}{e_n + e_p + N_A c_p + n_{thrs} (c_n + c_p)} c_p (n_{thrs} + N_A) (N_{Er} - N_{Erth}^*) \\ & = N_{Erth}^* \left[ \frac{1}{\tau_{rad}} + (C_{Ah} + C_{Abh}) N_A \right] + N_{Erth}^* C_{Ah} n_{thrs} \end{aligned}$$

$$\Rightarrow \frac{(e_p + c_n n_{thrs})}{H_4 + n_{thrs} H_5} (n_{thrs} + N_A) H_3 = H_1 + H_2 n_{thrs}$$

$$\Rightarrow (e_p + c_n n_{thrs}) (n_{thrs} + N_A) H_3 = (H_1 + H_2 n_{thrs}) (H_4 + H_5 n_{thrs})$$

$$\Rightarrow e_p N_A H_3 + (e_p + c_n N_A) H_3 n_{thrs} + C_n H_3 n_{thrs}^2 = H_1 H_4 + (H_2 H_4 + H_1 H_5) n_{thrs} + H_2 H_5 n_{thrs}^2$$

$$\Rightarrow (H_2 H_5 - c_n H_3) n_{thrs}^2 + (H_2 H_4 + H_1 H_5 - e_p H_3 - c_n N_A H_3) n_{thrs} + (H_1 H_4 - e_p N_A H_3) = 0$$

$$\Rightarrow R_1 n_{thrs}^2 + R_2 n_{thrs} + R_3 = 0$$

$$\Rightarrow n_{thrs} = \frac{-R_2 \pm \sqrt{R_2^2 - 4R_1 R_3}}{2R_1}$$

where

$$H_1 = N_{Erth}^* \left[ \frac{1}{\tau_{rad}} + (C_{Ah} + C_{Abh}) N_A \right]$$

$$H_2 = N_{Erth}^* C_{Ah}$$

$$H_3 = c_p (N_{Er} - N_{Erth}^*)$$

$$H_4 = e_n + e_p + c_p N_A$$

$$H_5 = c_n + c_p$$

$$\begin{aligned} R_1 &= H_2 H_5 - c_n H_3 \\ &= N_{Erth}^* c_{Ah} (c_n + c_p) - c_n c_p (N_{Er} - N_{Erth}^*) \end{aligned}$$

$$\begin{aligned} R_2 &= H_2 H_4 + H_1 H_5 - e_p H_3 - c_n N_A H_3 \\ &= N_{Erth}^* C_{Ah} (e_n + e_p + c_p + N_A) + N_{Erth}^* (c_n + c_p) \left[ \frac{1}{\tau_{rad}} + (C_{Ah} + C_{Abh}) N_A \right] \end{aligned}$$

$$\begin{aligned} R_3 &= H_1 H_4 - e_p N_A H_3 \\ &= N_{Erth}^* (e_n + e_p + c_p N_A) \left[ \frac{1}{\tau_{rad}} + (C_{Ah} + C_{Abh}) N_A \right] - e_p c_p N_A (N_{Er} - N_{Erth}^*) \end{aligned}$$

Therefore the excess or injected carrier density at which excited erbium atom reaches the threshold level of population inversion

$$\begin{aligned} n_{thrs} &= \left[ \frac{\left[ N_{Erth}^* C_{Ah} (e_n + e_p + c_p N_A) + N_{Erth}^* (c_n + c_p) \left\{ \frac{1}{\tau_{rad}} + (C_{Ah} + C_{Abh}) N_A \right\} \right]^2}{4 \left\{ N_{Erth}^* C_{Ah} (c_n + c_p) - c_n c_p (N_{Er} - N_{Erth}^*) \right\} \left[ N_{Erth}^* (e_n + e_p + c_p N_A) \left[ \frac{1}{\tau_{rad}} + (C_{Ah} + C_{Abh}) N_A \right] - e_p c_p N_A (N_{Er} - N_{Erth}^*) \right]} \right. \\ &\quad \left. - \left[ N_{Erth}^* C_{Ah} (e_n + e_p + c_p N_A) + N_{Erth}^* (c_n + c_p) \left\{ \frac{1}{\tau_{rad}} + (C_{Ah} + C_{Abh}) N_A \right\} \right] \right] \\ &\quad \times \frac{1}{2 \left\{ N_{Erth}^* C_{Ah} (c_n + c_p) - c_n c_p (N_{Er} - N_{Erth}^*) \right\}} \end{aligned}$$

The threshold current density is given by

$$J_{th} = \frac{n_{thrs}}{\tau_{si}} L_{eq} q$$

## APPENDIX – B

### Derivation of EDS Laser Output Power

The rate equations for excited erbium atom and photon density are

$$\frac{dN_{Er}^*(t)}{dt} = f_i c_p p (N_{Er} - N_{Er}^*(t)) - \frac{N_{Er}^*(t)}{\tau_{Er}} - v_g g S(t) \quad (B.1)$$

$$\frac{dS(t)}{dt} = v_g g S(t) + \beta \frac{N_{Er}^*(t)}{\tau_{rad}} - \frac{S(t)}{\tau_p} \quad (B.2)$$

Before and at threshold, photon density in the cavity is negligible i.e.,  $S \approx 0$ . At steady state Eq. (B.1) leads to,

$$\begin{aligned} f_i c_p p (N_{Er} - N_{Er}^*) - \frac{N_{Er}^*}{\tau_{Er}} &= 0 \\ \Rightarrow N_{Er}^* &= \frac{f_i c_p p}{f_i c_p p + \frac{1}{\tau_{Er}}} N_{Er} \end{aligned} \quad (B.3)$$

Probability of each Er site occupied by electron is given by [21]

$$f_i = \frac{n_{Er}}{N_{Er}} = \frac{e_p + c_n n}{e_n + e_p + c_n n + c_p p} \quad (B.4)$$

Combining Eqs. (B.3) & (B.4), we get

$$\begin{aligned} N_{Er}^* &= \frac{f_i c_p p}{f_i c_p p + \frac{1}{\tau_{Er}}} N_{Er} \\ &= \frac{\left( \frac{e_p + c_n n}{e_n + e_p + c_n n + c_p p} \right) c_p p}{\left( \frac{e_p + c_n n}{e_n + e_p + c_n n + c_p p} \right) c_p p + \frac{1}{\tau_{rad}} + \frac{1}{\tau_{nonrad}}} N_{Er} \end{aligned}$$

$$\begin{aligned}
&= \frac{(e_p + c_n n)c_p p}{(e_p + c_n n)c_p p + \left(\frac{1}{\tau_{rad}} + \frac{1}{\tau_{nonrad}}\right)(e_n + e_p + c_n n + c_p p)} N_{Er} \\
&= \frac{(e_p + c_n n)c_p p}{(e_p + c_n n)c_p p + \left(\frac{1}{\tau_{rad}} + \frac{1}{\tau_{Af}} + \frac{1}{\tau_{Ab}} + \frac{1}{\tau_{bt}}\right)(e_n + e_p + c_n n + c_p p)} N_{Er} \\
&= \frac{(e_p + c_n n)c_p p}{(e_p + c_n n)c_p p + \left(\frac{1}{\tau_{rad}} + C_{Ah} p + C_{Abh} N_A\right)(e_n + e_p + c_n n + c_p p)} N_{Er} \\
&= \frac{N^R}{D^R} \tag{B.5}
\end{aligned}$$

where

$$\begin{aligned}
N^R &= (e_p + c_n n)c_p p N_{Er} \\
&\quad \text{Putting } p = n + N_A \\
&= (e_p + c_n n)(n + N_A)c_p N_{Er} \\
&= [e_p N_A + (e_p + c_n N_A)n + n^2 c_n] c_p N_{Er} \tag{B.6}
\end{aligned}$$

Carrier density and current density are related by the following expression

$$n = \frac{J \tau_{si}}{L_{eq} q} \tag{B.7}$$

Inserting Eq. (B.7) in Eq. (B.6), we obtain

$$\begin{aligned}
N^R &= \left[ e_p N_A + (e_p + c_n N_A) \frac{J \tau_{si}}{L_{eq} q} + \left( \frac{J \tau_{si}}{L_{eq} q} \right)^2 c_n \right] c_p N_{Er} \\
&= \left[ e_p c_p N_A (L_{eq} q)^2 + \tau_{si} L_{eq} q c_p (e_p + c_n N_A) J + c_n c_p \tau_{si}^2 J^2 \right] \frac{N_{Er}}{(L_{eq} q)^2} \\
&= [P_{01} + P_{02} J + P_{03} J^2] \frac{N_{Er}}{(L_{eq} q)^2} \tag{B.8}
\end{aligned}$$

where

$$\begin{aligned}
P_{01} &= e_p c_p N_A (L_{eq} q)^2 \\
P_{02} &= \tau_{si} L_{eq} q c_p (e_p + c_n N_A) \\
P_{03} &= c_n c_p \tau_{si}^2
\end{aligned}$$



Now

$$\begin{aligned}
D^R &= (e_p + c_n n) c_p p + \left( \frac{1}{\tau_{rad}} + C_{Ah} p + C_{Abh} N_A \right) (e_n + e_p + c_n n + c_p p) \\
&= e_p c_p p + n p c_n c_p + \frac{1}{\tau_{rad}} (e_n + e_p) + \frac{1}{\tau_{rad}} (c_n n + c_p p) + C_{Ah} (e_n + e_p) p + n p c_n C_{Ah} + p^2 C_{Ah} c_p \\
&\quad + C_{Abh} (e_n + e_p) N_A + C_{Abh} N_A c_n n + C_{Abh} N_A c_p p \\
&= e_p c_p (n + N_A) + n (n + N_A) c_n c_p + \frac{1}{\tau_{rad}} (e_n + e_p) + \frac{1}{\tau_{rad}} [c_n n + c_p (n + N_A)] \\
&\quad + C_{Ah} (e_n + e_p) (n + N_A) + n (n + N_A) c_n C_{Ah} + (n + N_A)^2 C_{Ah} c_p + C_{Abh} (e_n + e_p) N_A \\
&\quad + C_{Abh} N_A c_n n + C_{Abh} N_A c_p (n + N_A) \\
&= N_A c_p \left( e_p + \frac{1}{\tau_{rad}} \right) + \frac{1}{\tau_{rad}} (e_n + e_p) + N_A (e_n + e_p) (C_{Ah} + C_{Abh}) + c_p N_A^2 (C_{Ah} + C_{Abh}) \\
&\quad + n \left[ e_p c_n + N_A (c_n c_p + c_n C_{Ah} + 2C_{Ah} c_p) + C_{Abh} N_A (c_n + c_p) + \frac{1}{\tau_{rad}} (c_n + c_p) + C_{Ah} (e_n + e_p) \right] \\
&\quad + n^2 [c_n c_p + C_{Ah} (c_n + c_p)]
\end{aligned} \tag{B.9}$$

Substituting Eq. (B.7) in Eq. (B.9), we get

$$\begin{aligned}
D^R &= N_A c_p \left( e_p + \frac{1}{\tau_{rad}} \right) + \frac{1}{\tau_{rad}} (e_n + e_p) + N_A (e_n + e_p) (C_{Ah} + C_{Abh}) + c_p N_A^2 (C_{Ah} + C_{Abh}) \\
&\quad + \frac{J \tau_{si}}{L_{eq} q} \left[ e_p c_n + N_A (c_n c_p + c_n C_{Ah} + 2C_{Ah} c_p) + C_{Abh} N_A (c_n + c_p) + \frac{1}{\tau_{rad}} (c_n + c_p) + C_{Ah} (e_n + e_p) \right] \\
&\quad + \frac{J^2 \tau_{si}^2}{(L_{eq} q)^2} [c_n c_p + C_{Ah} (c_n + c_p)] \\
&= \left[ \begin{aligned}
&\left\{ N_A c_p \left( e_p + \frac{1}{\tau_{rad}} \right) + \frac{1}{\tau_{rad}} (e_n + e_p) + N_A (e_n + e_p) (C_{Ah} + C_{Abh}) + c_p N_A^2 (C_{Ah} + C_{Abh}) \right\} (L_{eq} q)^2 \\
&\tau_{si} L_{eq} q \left\{ e_p c_n + N_A (c_n c_p + c_n C_{Ah} + 2C_{Ah} c_p) + \right. \\
&\quad \left. C_{Abh} N_A (c_n + c_p) + \frac{1}{\tau_{rad}} (c_n + c_p) + C_{Ah} (e_n + e_p) \right\} J \\
&\tau_{si}^2 [c_n c_p + C_{Ah} (c_n + c_p)] J^2
\end{aligned} \right] \frac{1}{(L_{eq} q)^2} \\
&= [P_{04} + P_{05} J + P_{06} J^2] \frac{1}{(L_{eq} q)^2}
\end{aligned} \tag{B.10}$$

where

$$\begin{aligned}
P_{04} &= \left\{ N_A c_p \left( e_p + \frac{1}{\tau_{rad}} \right) + \frac{1}{\tau_{rad}} (e_n + e_p) + N_A (e_n + e_p) (C_{Ah} + C_{Abh}) + c_p N_A^2 (C_{Ah} + C_{Abh}) \right\} (L_{eq} q)^2 \\
P_{05} &= \tau_{si} L_{eq} q \left\{ e_p c_n + N_A (c_n c_p + c_n C_{Ah} + 2C_{Ah} c_p) + C_{Abh} N_A (c_n + c_p) + \frac{1}{\tau_{rad}} (c_n + c_p) + C_{Ah} (e_n + e_p) \right\} \\
P_{06} &= \tau_{si}^2 \{ c_n c_p + C_{Ah} (c_n + c_p) \}
\end{aligned}$$

From Eqs. (B.5), (B.8) (B.10), we obtain

$$\begin{aligned}
N_{Er}^* &= \frac{[P_{01} + P_{02}J + P_{03}J^2] \frac{N_{Er}}{(L_{eq}q)^2}}{[P_{04} + P_{05}J + P_{06}J^2] \frac{1}{(L_{eq}q)^2}} \\
&= \frac{P_{01} + P_{02}J + P_{03}J^2}{P_{04} + P_{05}J + P_{06}J^2} N_{Er}
\end{aligned} \tag{B.11}$$

Neglecting the stimulated transition term from Eq. (B.2) at steady state we get,

$$\begin{aligned}
\beta \frac{N_{Er}^*}{\tau_{rad}} - \frac{S}{\tau_p} &= 0 \\
\Rightarrow S &= \beta \frac{\tau_p}{\tau_{rad}} N_{Er}^* \quad (J < J_{th})
\end{aligned} \tag{B.12}$$

This is the photon density inside the cavity before threshold due to spontaneous emission. So the output power due to spontaneous emission is

$$\begin{aligned}
P_{spont} &= h\nu\beta \frac{\tau_p}{\tau_{rad}} N_{Er}^* (Vol^m) v_g \alpha_m \\
&= h\nu\beta \frac{1}{v_g (\alpha_i + \alpha_m) \tau_{rad}} \left( \frac{P_{01} + P_{02}J + P_{03}J^2}{P_{04} + P_{05}J + P_{06}J^2} \right) N_{Er} (Vol^m) v_g \alpha_m \\
&= \frac{\alpha_m}{(\alpha_i + \alpha_m)} h\nu \frac{\beta}{\tau_{rad}} N_{Er} (Vol^m) \left( \frac{P_{01} + P_{02}J + P_{03}J^2}{P_{04} + P_{05}J + P_{06}J^2} \right) \\
&= H_{spont} \left( \frac{P_{01} + P_{02}J + P_{03}J^2}{P_{04} + P_{05}J + P_{06}J^2} \right)
\end{aligned} \tag{B.13}$$

where

$$H_{spont} = \frac{\alpha_m}{(\alpha_i + \alpha_m)} h\nu \frac{\beta}{\tau_{rad}} N_{Er} (Vol^m)$$

After threshold, at steady state, from Eq. (B.1) we get

$$\begin{aligned} f_i c_p P (N_{Er} - N_{Erth}^*) - \frac{N_{Erth}^*}{\tau_{Er}} - v_g g_{th} S &= 0 \\ \Rightarrow S &= \frac{f_i c_p P (N_{Er} - N_{Erth}^*) - \frac{N_{Erth}^*}{\tau_{Er}}}{v_g g_{th}} \end{aligned} \quad (B.14)$$

Now

$$f_i c_p P = \frac{(e_p + c_n n) c_p P}{e_n + e_p + c_n n + c_p P} \quad (B.15)$$

Putting  $p = n + N_A$ , Eq. (B.15) leads to

$$\begin{aligned} f_i c_p P &= \frac{(e_p + c_n n) c_p (n + N_A)}{e_n + e_p + c_n n + c_p (n + N_A)} \\ &= \frac{(e_p + c_n n)(n + N_A) c_p}{e_n + e_p + n(c_n + c_p) + N_A c_p} \\ &= \frac{e_p c_p N_A + n(e_p + c_n N_A) c_p + n^2 c_n c_p}{e_n + e_p + N_A c_p + n(c_n + c_p)} \end{aligned} \quad (B.16)$$

Inserting Eq. (B.7) in Eq. (B.16), we obtain

$$\begin{aligned} f_i c_p P &= \frac{e_p c_p N_A + \frac{J \tau_{si}}{L_{eq} q} (e_p + c_n N_A) c_p + c_n c_p \left( \frac{J \tau_{si}}{L_{eq} q} \right)^2}{e_n + e_p + N_A c_p + (c_n + c_p) \frac{J \tau_{si}}{L_{eq} q}} \\ &= \frac{e_p c_p N_A L_{eq}^2 q^2 + \tau_{si} L_{eq} q c_p (e_p + c_n N_A) J + c_n c_p \tau_{si}^2 J^2}{L_{eq}^2 q^2 (e_n + e_p + N_A c_p) + \tau_{si} L_{eq} q (c_n + c_p) J} \\ &= \frac{P_{07} + P_{08} J + P_{09} J^2}{P_{10} + P_{11} J} \end{aligned} \quad (B.17)$$

where

$$\begin{aligned} P_{07} &= e_p c_p N_A L_{eq}^2 q^2 \\ P_{08} &= \tau_{si} L_{eq} q c_p (e_p + c_n N_A) \end{aligned}$$

$$P_{09} = c_n c_p \tau_{si}^2$$

$$P_{10} = L_{eq}^2 q^2 (e_n + e_p + N_A c_p)$$

$$P_{11} = \tau_{si} L_{eq} q (c_n + c_p)$$

Erbium (Er) life time:

$$\begin{aligned} \frac{1}{\tau_{Er}} &= \frac{1}{\tau_{rad}} + \frac{1}{\tau_{nonrad}} \\ &= \frac{1}{\tau_{rad}} + \frac{1}{\tau_{Af}} + \frac{1}{\tau_{Ab}} + \frac{1}{\tau_{bt}} \\ &= \frac{1}{\tau_{rad}} + C_{Ah} P + C_{Abh} N_A \\ &= \frac{1}{\tau_{rad}} + C_{Ah} (n + N_A) + C_{Abh} N_A \\ &= \frac{1}{\tau_{rad}} + N_A (C_{Ah} + C_{Abh}) + C_{Ah} n \\ &= \frac{1}{\tau_{rad}} + N_A (C_{Ah} + C_{Abh}) + \frac{C_{Ah} \tau_{si}}{L_{eq} q} J \\ &= P_{12} + P_{13} J \end{aligned} \tag{B.18}$$

where

$$P_{12} = \frac{1}{\tau_{rad}} + N_A (C_{Ah} + C_{Abh})$$

$$P_{13} = \frac{C_{Ah} \tau_{si}}{L_{eq} q}$$

Using Eqs. (B.14), (B.17), (B.18), we obtain

$$S = \frac{P_{07} + P_{08} J + P_{09} J^2 (N_{Er} - N_{Erh}^*) - N_{Erh}^* (P_{12} + P_{13} J)}{v_g g_{th}}$$

So the photon density inside the cavity after threshold is

$$S = \frac{(P_{07} + P_{08} J + P_{09} J^2) (N_{Er} - N_{Erh}^*) - N_{Erh}^* (P_{10} + P_{11} J) (P_{12} + P_{13} J)}{v_g g_{th} (P_{10} + P_{11} J)} \tag{B.19}$$

or,

$$S = \left[ \begin{aligned} & \left\{ e_p c_p N_A L_{eq}^2 q^2 + \tau_{st} L_{eq} q c_p (e_p + c_n N_A) J + c_n c_p \tau_{st}^2 J^2 \right\} (N_{Er} - N_{Erth}^*) \\ & - N_{Erth}^* \left\{ L_{eq}^2 q^2 (e_n + e_p + N_A c_p) + \tau_{st} L_{eq} q (c_n + c_p) \right\} \left( \frac{1}{\tau_{rad}} + N_A (C_{Ah} + C_{Abh}) + \frac{C_{Ah} \tau_{st}}{L_{eq} q} J \right) \end{aligned} \right] \\ \times \left[ \frac{1}{v_g g_{th} \left[ L_{eq}^2 q^2 (e_n + e_p + N_A c_p) + \tau_{st} L_{eq} q (c_n + c_p) \right] J} \right] \quad (B.20)$$

Therefore, the laser output power after threshold is

$$P_{out} = S * v_g * \alpha_m * h\nu * Vol \quad (B.21)$$

## APPENDIX - C

### EDS Laser Frequency Response

The rate equations for excited erbium atom and photon density are

$$\frac{dN_{Er}^*(t)}{dt} = f_i c_p p (N_{Er} - N_{Er}^*(t)) - \frac{N_{Er}^*(t)}{\tau_{Er}} - \nu_g g(N_{Er}^*) S(t) \quad (C.1)$$

$$\frac{dS(t)}{dt} = \nu_g g(N_{Er}^*) S(t) + \beta \frac{N_{Er}^*(t)}{\tau_{rad}} - \frac{S(t)}{\tau_p} \quad (C.2)$$

The gain of the cavity medium depends on excited erbium atom and is given by [1]

$$g(N_{Er}^*) = g_0 (2N_{Er}^* - N_{Er}) \quad (C.3)$$

where  $g_0$  is the gain cross-section. It is an intrinsic property of EDS and given by

$$g_0 = \frac{\lambda^4}{8\pi N_r^2 \tau_{rad} c \Delta\lambda} \quad (C.4)$$

From Eq. (C.1)

$$\begin{aligned} \frac{dN_{Er}^*(t)}{dt} &= f_i c_p p (N_{Er} - N_{Er}^*(t)) - \frac{N_{Er}^*(t)}{\tau_{Er}} - \nu_g g(N_{Er}^*) S(t) \\ &= f_i c_p p (N_{Er} - N_{Er}^*(t)) - N_{Er}^*(t) \left( \frac{1}{\tau_{rad}} + \frac{1}{\tau_{Af}} + \frac{1}{\tau_{Ab}} + \frac{1}{\tau_{bt}} \right) - \nu_g g_0 (2N_{Er}^*(t) - N_{Er}) S(t) \end{aligned} \quad (C.5)$$

At low temperature, energy back transfer can be neglected i.e.,  $\frac{1}{\tau_{bt}} \approx 0$ . Then above

equation becomes

$$\begin{aligned} \frac{dN_{Er}^*(t)}{dt} &= f_i c_p p (N_{Er} - N_{Er}^*(t)) - N_{Er}^*(t) \left( \frac{1}{\tau_{rad}} + \frac{1}{\tau_{Af}} + \frac{1}{\tau_{Ab}} \right) - \nu_g g_0 (2N_{Er}^*(t) - N_{Er}) S(t) \\ &= f_i c_p p (N_{Er} - N_{Er}^*(t)) - N_{Er}^*(t) \frac{1}{\tau_{Af}} - N_{Er}^*(t) \left( \frac{1}{\tau_{rad}} + \frac{1}{\tau_{Ab}} \right) - \nu_g g_0 (2N_{Er}^*(t) - N_{Er}) S(t) \end{aligned} \quad (C.6)$$

We assume that Er is doped into the p-type silicon. Then

$$\frac{1}{\tau_{Af}} = C_{Ah}p \quad \text{and} \quad \frac{1}{\tau_{Ab}} = C_{Abh}N_A$$

Eq. (C.6) then becomes

$$\frac{dN_{Er}^*(t)}{dt} = f_i c_p p (N_{Er} - N_{Er}^*(t)) - N_{Er}^*(t) C_{Ah} p - N_{Er}^*(t) \left( \frac{1}{\tau_{rad}} + \frac{1}{\tau_{Ab}} \right) - v_g g_0 (2N_{Er}^*(t) - N_{Er}) S(t) \quad (C.7)$$

At high level of excitation, we can assume  $n \approx p$ . Converting carrier density into current

density using  $n = \frac{\tau_{si}}{L_{eq}q} J$ , we get

$$\begin{aligned} \frac{dN_{Er}^*(t)}{dt} &= f_i c_p \frac{\tau_{si}}{L_{eq}q} J (N_{Er} - N_{Er}^*(t)) - N_{Er}^*(t) C_{Ah} \frac{\tau_{si}}{L_{eq}q} J - N_{Er}^*(t) \left( \frac{1}{\tau_{rad}} + \frac{1}{\tau_{Ab}} \right) - v_g g_0 (2N_{Er}^*(t) - N_{Er}) S(t) \\ &= A_{01} J (N_{Er} - N_{Er}^*(t)) - A_{02} J N_{Er}^*(t) - A_{03} N_{Er}^*(t) - v_g g_0 (2N_{Er}^*(t) - N_{Er}) S(t) \end{aligned} \quad (C.8)$$

where,

$$A_{01} = f_i c_p \frac{\tau_{si}}{L_{eq}q}$$

$$A_{02} = \frac{C_{Ah} \tau_{si}}{L_{eq}q}$$

$$A_{03} = \left( \frac{1}{\tau_{rad}} + \frac{1}{\tau_{Ab}} \right)$$

At steady state,

$$\frac{dN_{Er}^*(t)}{dt} = 0$$

$$\Rightarrow A_{01} J_0 (N_{Er} - N_{Er}^*) - A_{02} J_0 N_{Er}^* - A_{03} N_{Er}^* - v_g g_0 (2N_{Er}^* - N_{Er}) S_0 = 0$$

$$\Rightarrow A_{01} J_0 (N_{Er} - N_{Er}^*) = A_{02} J_0 N_{Er}^* + A_{03} N_{Er}^* + v_g g_0 (2N_{Er}^* - N_{Er}) S_0 \quad (C.9)$$

$$\Rightarrow N_{Er}^* (A_{01} J_0 + A_{02} J_0 + A_{03} + 2v_g g_0 S_0) = (A_{01} J_0 + v_g g_0 S_0) N_{Er}$$

$$\Rightarrow N_{Er}^* ((A_{01} + A_{02}) J_0 + A_{03} + 2v_g g_0 S_0) = (A_{01} J_0 + v_g g_0 S_0) N_{Er} \quad (C.10)$$

From eqn. (C.2)

$$\frac{dS(t)}{dt} = v_g g (N_{Er}^*(t)) S(t) + \beta \frac{N_{Er}^*(t)}{\tau_{rad}} - \frac{S(t)}{\tau_p}$$

$$= v_g g_0 (2N_{lir}^*(t) - N_{lir}) S(t) + \beta \frac{N_{lir}^*(t)}{\tau_{rad}} - \frac{S(t)}{\tau_p} \quad (C.11)$$

At steady state, we get from Eq. (C.11)

$$\begin{aligned} \frac{dS(t)}{dt} &= 0 \\ \Rightarrow v_g g_0 (2N_{Erh}^* - N_{lir}) S_0 + \beta \frac{N_{Erh}^*}{\tau_{rad}} - \frac{S_0}{\tau_p} &= 0 \\ \Rightarrow v_g g_0 (2N_{Erh}^* - N_{Er}) S_0 &= \frac{S_0}{\tau_p} - \beta \frac{N_{Erh}^*}{\tau_{rad}} \end{aligned} \quad (C.12)$$

$$\begin{aligned} \Rightarrow 2v_g g_0 N_{Erh}^* S_0 &= \frac{S_0}{\tau_p} + v_g g_0 N_{Er} S_0 - \beta \frac{N_{Erh}^*}{\tau_{rad}} \\ \Rightarrow 2v_g g_0 N_{Erh}^* &= \frac{1}{\tau_p} + v_g g_0 N_{Er} - \beta \frac{N_{Erh}^*}{\tau_{rad} S_0} \end{aligned} \quad (C.13)$$

### Small Signal Analysis:

$$\text{Let,} \quad J(t) = J_0 + \Delta J(t) \quad (C.14a)$$

$$N_{Er}^*(t) = N_{Er}^* + \Delta N_{Er}^*(t) \quad (C.14b)$$

$$S(t) = S_0 + \Delta S(t) \quad (C.14c)$$

Substituting these in the Eq. (C.8)

$$\begin{aligned} \frac{d}{dt} [N_{Erh}^* + \Delta N_{Er}^*(t)] &= A_{01} [J_0 + \Delta J(t)] [N_{Er} - N_{Erh}^* - \Delta N_{Er}^*(t)] - A_{02} [J_0 + \Delta J(t)] [N_{Erh}^* + \Delta N_{Er}^*(t)] \\ &\quad - v_g g_0 [2N_{Erh}^* + 2\Delta N_{Er}^*(t) - N_{Er}] [S_0 + \Delta S(t)] - A_{03} [N_{Erh}^* + \Delta N_{Er}^*(t)] \\ \Rightarrow \frac{d}{dt} [\Delta N_{Er}^*(t)] &= A_{01} [J_0 N_{Er} + N_{Er} \Delta J(t) - J_0 N_{Erh}^* - N_{Erh}^* \Delta J(t) - J_0 \Delta N_{Er}^*(t) - \Delta J(t) \Delta N_{Er}^*(t)] \\ &\quad - A_{02} [J_0 \Delta N_{Erh}^* + J_0 \Delta N_{Er}^*(t) + N_{Erh}^* \Delta J(t) + \Delta J(t) \Delta N_{Er}^*(t)] - A_{03} N_{Erh}^* - A_{03} \Delta N_{Er}^*(t) \\ &\quad - v_g g_0 [(2N_{Erh}^* - N_{Er}) S_0 + 2S_0 \Delta N_{Er}^*(t) + (2N_{Erh}^* - N_{Er}) \Delta S(t) + 2\Delta S(t) \Delta N_{Er}^*(t)] \end{aligned} \quad (C.15)$$

Assuming,

$$\Delta J(t) \Delta N_{Er}^*(t) \approx 0 \quad \text{and}$$

$$\Delta S(t) \Delta N_{Er}^*(t) \approx 0$$

Then we get,



$$\begin{aligned}
\frac{d}{dt} [\Delta N_{Er}^*(t)] &= A_{01} [J_0 N_{Er} + N_{Er} \Delta J(t) - J_0 N_{Erth}^* - N_{Erth}^* \Delta J(t) - J_0 \Delta N_{Er}^*(t)] \\
&\quad - A_{02} [J_0 N_{Erth}^* + J_0 \Delta N_{Er}^*(t) + N_{Erth}^* \Delta J(t)] - A_{03} N_{Erth}^* - A_{03} \Delta N_{Er}^*(t) \\
&\quad - v_g g_0 [(2N_{Erth}^* - N_{Er}) S_0 + 2S_0 \Delta N_{Er}^*(t) + (2N_{Erth}^* - N_{Er}) \Delta S(t)] \\
&= A_{01} [J_0 (N_{Er} - N_{Erth}^*) + (N_{Er} - N_{Erth}^*) \Delta J(t) - J_0 \Delta N_{Er}^*(t)] \\
&\quad - A_{02} [J_0 N_{Erth}^* + J_0 \Delta N_{Er}^*(t) + N_{Erth}^* \Delta J(t)] - A_{03} N_{Erth}^* - A_{03} \Delta N_{Er}^*(t) \\
&\quad - v_g g_0 [(2N_{Erth}^* - N_{Er}) S_0 + 2S_0 \Delta N_{Er}^*(t) + (2N_{Erth}^* - N_{Er}) \Delta S(t)] \\
&= A_{01} [A_{05} J_0 + A_{05} \Delta J(t) - J_0 \Delta N_{Er}^*(t)] - A_{02} [J_0 N_{Erth}^* + J_0 \Delta N_{Er}^*(t) + N_{Erth}^* \Delta J(t)] \\
&\quad - v_g g_0 [A_{06} S_0 + 2S_0 \Delta N_{Er}^*(t) + A_{06} \Delta S(t)] - A_{03} N_{Erth}^* - A_{03} \Delta N_{Er}^*(t) \\
&= A_{01} A_{05} J_0 + A_{01} A_{05} \Delta J(t) - A_{01} J_0 \Delta N_{Er}^*(t) - A_{02} J_0 N_{Erth}^* - A_{02} J_0 \Delta N_{Er}^*(t) - A_{02} N_{Erth}^* \Delta J(t) \\
&\quad - A_{06} v_g g_0 S_0 - 2v_g g_0 S_0 \Delta N_{Er}^*(t) - A_{06} v_g g_0 \Delta S(t) - A_{03} N_{Erth}^* - A_{03} \Delta N_{Er}^*(t)
\end{aligned} \tag{C.16}$$

where

$$\begin{aligned}
A_{05} &= N_{Er} - N_{Erth}^* \\
A_{06} &= 2N_{Erth}^* - N_{Er}
\end{aligned}$$

From eqn (C.9)

$$\begin{aligned}
A_{01} J_0 (N_{Er} - N_{Erth}^*) &= A_{02} J_0 N_{Erth}^* + A_{03} N_{Erth}^* + v_g g_0 (2N_{Erth}^* - N_{Er}) S_0 \\
\Rightarrow A_{01} A_{05} J_0 &= A_{02} J_0 N_{Erth}^* + A_{03} N_{Erth}^* + A_{06} v_g g_0 S_0
\end{aligned} \tag{C.17}$$

From eqn (C.16) and (C.17)

$$\begin{aligned}
\frac{d}{dt} [\Delta N_{Er}^*(t)] &= A_{02} J_0 N_{Erth}^* + A_{03} N_{Erth}^* + A_{06} v_g g_0 S_0 + A_{01} A_{05} \Delta J(t) - A_{01} J_0 \Delta N_{Er}^*(t) - A_{02} J_0 N_{Erth}^* \\
&\quad - A_{02} J_0 \Delta N_{Er}^*(t) - A_{02} N_{Erth}^* \Delta J(t) - A_{06} v_g g_0 S_0 - 2v_g g_0 S_0 \Delta N_{Er}^*(t) \\
&\quad - A_{06} v_g g_0 \Delta S(t) - A_{03} N_{Erth}^* - A_{03} \Delta N_{Er}^*(t) \\
&= A_{01} A_{05} \Delta J(t) - A_{01} J_0 \Delta N_{Er}^*(t) - A_{02} J_0 \Delta N_{Er}^*(t) - A_{02} N_{Erth}^* \Delta J(t) - 2v_g g_0 S_0 \Delta N_{Er}^*(t) \\
&\quad - A_{06} v_g g_0 \Delta S(t) - A_{03} \Delta N_{Er}^*(t) \\
&= A_{01} A_{05} \Delta J(t) - A_{01} J_0 \Delta N_{Er}^*(t) - A_{02} J_0 \Delta N_{Er}^*(t) - A_{02} N_{Erth}^* \Delta J(t) - 2v_g g_0 S_0 \Delta N_{Er}^*(t) \\
&\quad - A_{06} v_g g_0 \Delta S(t) - A_{03} \Delta N_{Er}^*(t) \\
&= [A_{01} A_{05} - A_{02} N_{Erth}^*] \Delta J(t) - A_{06} v_g g_0 \Delta S(t) - [2v_g g_0 S_0 + (A_{01} + A_{02}) J_0 + A_{03}] \Delta N_{Er}^*(t) \\
&= A_{07} \Delta J(t) - A_{08} \Delta S(t) - A_{09} \Delta N_{Er}^*(t)
\end{aligned} \tag{C.18}$$

where

$$A_{07} = A_{01}A_{05} - A_{02}N_{Erth}^*$$

$$A_{08} = A_{06}v_g g_0$$

$$A_{09} = 2v_g g_0 S_0 + (A_{01} + A_{02})J_0 + A_{03}$$

From Eqs. (C.11) and (C.14), we obtain

$$\begin{aligned} \frac{d}{dt}[S_0 + \Delta S(t)] &= v_g g_0 [2N_{Erth}^* + 2\Delta N_{Er}^*(t) - N_{Er}][S_0 + \Delta S(t)] + \frac{\beta}{\tau_{rad}} [N_{Erth}^* + \Delta N_{Er}^*(t)] - \frac{1}{\tau_p} [S_0 + \Delta S(t)] \\ \Rightarrow \frac{d}{dt}[\Delta S(t)] &= v_g g_0 [(2N_{Erth}^* - N_{Er})S_0 + 2S_0\Delta N_{Er}^*(t) + 2\Delta S(t)\Delta N_{Er}^*(t) + (2N_{Erth}^* - N_{Er})\Delta S(t)] \\ &\quad + \frac{\beta}{\tau_{rad}} N_{Erth}^* + \frac{\beta}{\tau_{rad}} \Delta N_{Er}^*(t) - \frac{1}{\tau_p} S_0 - \frac{1}{\tau_p} \Delta S(t) \end{aligned} \quad (C.19)$$

Assuming  $\Delta S(t)\Delta N_{Er}^*(t) \approx 0$ , we get

$$\begin{aligned} \frac{d}{dt}[\Delta S(t)] &= v_g g_0 [(2N_{Erth}^* - N_{Er})S_0 + 2S_0\Delta N_{Er}^*(t) + (2N_{Erth}^* - N_{Er})\Delta S(t)] + \frac{\beta}{\tau_{rad}} N_{Erth}^* + \frac{\beta}{\tau_{rad}} \Delta N_{Er}^*(t) \\ &\quad - \frac{1}{\tau_p} S_0 - \frac{1}{\tau_p} \Delta S(t) \\ &= v_g g_0 (2N_{Erth}^* - N_{Er})S_0 + 2v_g g_0 S_0 \Delta N_{Er}^*(t) + v_g g_0 (2N_{Erth}^* - N_{Er})\Delta S(t) + \frac{\beta}{\tau_{rad}} N_{Erth}^* \\ &\quad + \frac{\beta}{\tau_{rad}} \Delta N_{Er}^*(t) - \frac{1}{\tau_p} S_0 - \frac{1}{\tau_p} \Delta S(t) \end{aligned} \quad (C.20)$$

From Eq. (C.12) and (C.20),

$$\begin{aligned} \frac{d}{dt}[\Delta S(t)] &= \frac{S_0}{\tau_p} - \beta \frac{N_{Erth}^*}{\tau_{rad}} + 2v_g g_0 S_0 \Delta N_{Er}^*(t) + v_g g_0 (2N_{Erth}^* - N_{Er})\Delta S(t) + \frac{\beta}{\tau_{rad}} N_{Erth}^* + \frac{\beta}{\tau_{rad}} \Delta N_{Er}^*(t) \\ &\quad - \frac{1}{\tau_p} S_0 - \frac{1}{\tau_p} \Delta S(t) \\ &= 2v_g g_0 S_0 \Delta N_{Er}^*(t) + v_g g_0 (2N_{Erth}^* - N_{Er})\Delta S(t) + \frac{\beta}{\tau_{rad}} N_{Erth}^* + \frac{\beta}{\tau_{rad}} \Delta N_{Er}^*(t) - \frac{1}{\tau_p} \Delta S(t) \\ &= \left[ \frac{\beta}{\tau_{rad}} + 2v_g g_0 S_0 \right] \Delta N_{Er}^*(t) + \left[ A_{06}v_g g_0 - \frac{1}{\tau_p} \right] \Delta S(t) \\ &= A_{10} \Delta N_{Er}^*(t) + A_{11} \Delta S(t) \end{aligned} \quad (C.21)$$

where

$$A_{10} = \frac{\beta}{\tau_{rad}} + 2v_g g_0 S_0$$

$$\text{and } A_{11} = A_{06} v_k g_0 - \frac{1}{\tau_p}$$

Differentiating Eq. (C.21) again

$$\begin{aligned} \frac{d^2}{dt^2} [\Delta S(t)] &= A_{10} \frac{d}{dt} [\Delta N_{Er}^*(t)] + A_{11} \frac{d}{dt} [\Delta S(t)] \\ &= A_{10} [A_{07} \Delta J(t) - A_{08} \Delta S(t) - A_{09} \Delta N_{Er}^*(t)] + A_{11} \frac{d}{dt} [\Delta S(t)] \\ &= A_{07} A_{10} \Delta J(t) - A_{08} A_{10} \Delta S(t) - A_{09} A_{10} \Delta N_{Er}^*(t) + A_{11} \frac{d}{dt} [\Delta S(t)] \end{aligned} \quad (\text{C.22})$$

Substitute the value of  $N_{Er}^*(t)$  from Eq. (C.21) into Eq. (C.22), we obtain

$$\begin{aligned} \frac{d^2}{dt^2} [\Delta S(t)] &= A_{07} A_{10} \Delta J(t) - A_{08} A_{10} \Delta S(t) - A_{09} \left[ \frac{d}{dt} \{ \Delta S(t) \} - A_{11} \Delta S(t) \right] + A_{11} \frac{d}{dt} [\Delta S(t)] \\ \Rightarrow \frac{d^2}{dt^2} [\Delta S(t)] &= A_{07} A_{10} \Delta J(t) - (A_{09} - A_{11}) \frac{d}{dt} [\Delta S(t)] - (A_{08} A_{10} - A_{09} A_{11}) \Delta S(t) \\ \Rightarrow \frac{d^2}{dt^2} [\Delta S(t)] + (A_{09} - A_{11}) \frac{d}{dt} [\Delta S(t)] + (A_{08} A_{10} - A_{09} A_{11}) \Delta S(t) &= A_{07} A_{10} \Delta J(t) \\ \Rightarrow \frac{d^2}{dt^2} [\Delta S(t)] + A_{12} \frac{d}{dt} [\Delta S(t)] + A_{13} \Delta S(t) &= A_{14} \Delta J(t) \end{aligned} \quad (\text{C.23})$$

where

$$A_{12} = A_{09} - A_{11}$$

$$A_{13} = A_{08} A_{10} - A_{09} A_{11}$$

$$A_{14} = A_{07} A_{10}$$

Let

$$\Delta S(t) = \Delta S(\omega) e^{j\omega t} \quad (\text{C.24a})$$

$$\text{and } \Delta J(t) = \Delta J(\omega) e^{j\omega t} \quad (\text{C.24b})$$

Putting these in Eq. (C.23)

$$\begin{aligned} \frac{d^2}{dt^2} [\Delta S(\omega) e^{j\omega t}] + A_{12} \frac{d}{dt} [\Delta S(\omega) e^{j\omega t}] + A_{13} \Delta S(\omega) e^{j\omega t} &= A_{14} \Delta J(\omega) e^{j\omega t} \\ \Rightarrow -\omega^2 \Delta S(\omega) e^{j\omega t} + j\omega A_{12} \Delta S(\omega) e^{j\omega t} + A_{13} \Delta S(\omega) e^{j\omega t} &= A_{14} \Delta J(\omega) e^{j\omega t} \\ \Rightarrow \left[ (A_{13} - \omega^2) + j\omega A_{12} \right] \Delta S(\omega) &= A_{14} \Delta J(\omega) \end{aligned}$$

Therefore, small signal transfer function is

$$M(\omega) = \frac{\Delta S(\omega)}{\Delta J(\omega)} = \frac{A_{14}}{(A_{13} - \omega^2) + j\omega A_{12}} \quad (C.25)$$

At  $\omega = 0$ ,

$$M(0) = \frac{A_{14}}{A_{13}} \quad (C.26)$$

Normalized Transfer function

$$\begin{aligned} H(\omega) &= \frac{M(\omega)}{M(0)} = \frac{A_{13}}{(A_{13} - \omega^2) + j\omega A_{12}} \\ &= \frac{\omega_r^2}{(\omega_r^2 - \omega^2) + j\omega\gamma} \end{aligned} \quad (C.27)$$

Now

$$\begin{aligned} A_{13} &= A_{08}A_{10} - A_{09}A_{11} \\ &= A_{08}A_{10} - A_{09}A_{11} \\ &= A_{06}v_g g_0 \left[ \frac{\beta}{\tau_{rad}} + 2v_g g_0 S_0 \right] - \left[ 2v_g g_0 S_0 + (A_{01} + A_{02})J_0 + A_{03} \right] \left[ A_{06}v_g g_0 - \frac{1}{\tau_p} \right] \\ &= v_g g_0 (2N_{Erh}^* - N_{Er}) \left[ \frac{\beta}{\tau_{rad}} + 2v_g g_0 S_0 \right] - \left[ 2v_g g_0 S_0 + (A_{01} + A_{02})J_0 + A_{03} \right] \left[ v_g g_0 (2N_{Erh}^* - N_{Er}) - \frac{1}{\tau_p} \right] \\ &= v_g g_0 (2N_{Erh}^* - N_{Er}) \left[ \frac{\beta}{\tau_{rad}} + 2v_g g_0 S_0 \right] - \left[ 2v_g g_0 S_0 + (f_i c_p + C_{Ah}) \frac{\tau_{si}}{L_{eq} q} J_0 + \frac{1}{\tau_{rad}} + \frac{1}{\tau_{Ab}} \right] \left[ v_g g_0 (2N_{Erh}^* - N_{Er}) - \frac{1}{\tau_p} \right] \end{aligned} \quad (C.28)$$

From Eq. (C.9)

$$\begin{aligned} A_{01}J_0(N_{Er} - N_{Erh}^*) &= A_{02}J_0N_{Erh}^* + A_{03}N_{Erh}^* + v_g g_0 (2N_{Erh}^* - N_{Er})S_0 \\ \Rightarrow J_0 &= \frac{A_{03}N_{Erh}^* + v_g g_0 (2N_{Erh}^* - N_{Er})S_0}{A_{01}(N_{Er} - N_{Erh}^*) - A_{02}N_{Erh}^*} \\ &= \frac{\left( \frac{1}{\tau_{rad}} + \frac{1}{\tau_{Ab}} \right) N_{Erh}^* + v_g g_0 (2N_{Erh}^* - N_{Er})S_0}{f_i c_p \frac{\tau_{si}}{L_{eq} q} (N_{Er} - N_{Erh}^*) - \frac{C_{Ah} \tau_{si}}{L_{eq} q} N_{Erh}^*} \end{aligned} \quad (C.29)$$

Substituting the value of  $J_0$  into Eq. (C.28), we obtain

$$\begin{aligned}
A_{13} &= v_g g_0 (2N_{Erth}^* - N_{Er}) \left[ \frac{\beta}{\tau_{rad}} + 2v_g g_0 S_0 \right] \\
&- \left[ 2v_g g_0 S_0 + (f_i c_p + C_{Ah}) \frac{\tau_{si}}{L_{eq} q} \left\{ \frac{\left( \frac{1}{\tau_{rad}} + \frac{1}{\tau_{Ab}} \right) N_{Erth}^* + v_g g_0 (2N_{Erth}^* - N_{Er}) S_0}{f_i c_p \frac{\tau_{si}}{L_{eq} q} (N_{Er} - N_{Erth}^*) - \frac{C_{Ah} \tau_{si}}{L_{eq} q} N_{Erth}^*} \right\} + \frac{1}{\tau_{rad}} + \frac{1}{\tau_{Ab}} \right] \\
&\times \left[ v_g g_0 (2N_{Erth}^* - N_{Er}) - \frac{1}{\tau_p} \right] \\
&= v_g g_0 (2N_{Erth}^* - N_{Er}) \left[ \frac{\beta}{\tau_{rad}} + 2v_g g_0 S_0 \right] - \left[ v_g g_0 (2N_{Erth}^* - N_{Er}) - \frac{1}{\tau_p} \right] \\
&\times \left[ 2v_g g_0 S_0 + \frac{1}{\tau_{rad}} + \frac{1}{\tau_{Ab}} + (f_i c_p + C_{Ah}) \left\{ \frac{\left( \frac{1}{\tau_{rad}} + \frac{1}{\tau_{Ab}} \right) N_{Erth}^* + v_g g_0 (2N_{Erth}^* - N_{Er}) S_0}{f_i c_p (N_{Er} - N_{Erth}^*) - C_{Ah} N_{Erth}^*} \right\} \right]
\end{aligned} \tag{C.30}$$

So the relaxation oscillation frequency

$$\omega_r = \sqrt{A_{13}}$$

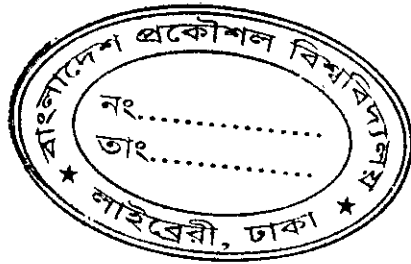
$$\begin{aligned}
&\left[ v_g g_0 (2N_{Erth}^* - N_{Er}) \left\{ \frac{\beta}{\tau_{rad}} + 2v_g g_0 S_0 \right\} - \left\{ v_g g_0 (2N_{Erth}^* - N_{Er}) - \frac{1}{\tau_p} \right\} \right]^{\frac{1}{2}} \\
&= \left[ \left\{ 2v_g g_0 S_0 + \frac{1}{\tau_{rad}} + \frac{1}{\tau_{Ab}} + (f_i c_p + C_{Ah}) \left\{ \frac{\left( \frac{1}{\tau_{rad}} + \frac{1}{\tau_{Ab}} \right) N_{Erth}^* + v_g g_0 (2N_{Erth}^* - N_{Er}) S_0}{f_i c_p (N_{Er} - N_{Erth}^*) - C_{Ah} N_{Erth}^*} \right\} \right\} \right]^{\frac{1}{2}}
\end{aligned} \tag{C.31}$$

Damping coefficient:

$$\begin{aligned}
\gamma &= A_{12} \\
&= A_{09} - A_{11} \\
&= 2v_g g_0 S_0 + (A_{01} + A_{02}) J_0 + A_{03} - A_{06} v_g g_0 + \frac{1}{\tau_p} \\
&= 2v_g g_0 S_0 + (f_i c_p + C_{Ah}) \frac{\tau_{si}}{L_{eq} q} J_0 + \frac{1}{\tau_{rad}} + \frac{1}{\tau_{Ab}} - v_g g_0 (2N_{Erth}^* - N_{Er}) + \frac{1}{\tau_p}
\end{aligned}$$

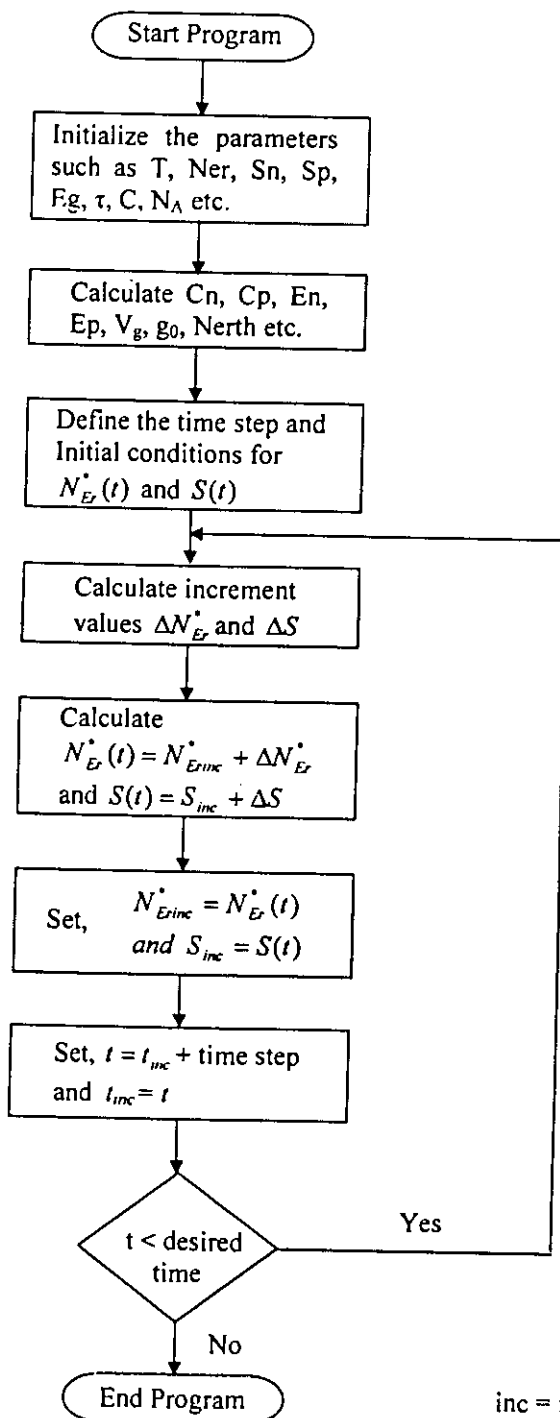
$$\begin{aligned}
&= 2v_g g_0 S_0 - v_g g_0 (2N_{Erth}^* - N_{Er}) + \frac{1}{\tau_{rad}} + \frac{1}{\tau_{Ab}} + \frac{1}{\tau_p} \\
&\quad + (f_i c_p + C_{Ah}) \frac{\tau_{st}}{L_{eq} q} \left[ \frac{\left( \frac{1}{\tau_{rad}} + \frac{1}{\tau_{Ab}} \right) N_{Erth}^* + v_g g_0 (2N_{Erth}^* - N_{Er}) S_0}{f_i c_p \frac{\tau_{st}}{L_{eq} q} (N_{Er} - N_{Erth}^*) - \frac{C_{Ah} \tau_{st}}{L_{eq} q} N_{Erth}^*} \right] \\
&= 2v_g g_0 S_0 - v_g g_0 (2N_{Erth}^* - N_{Er}) + \frac{1}{\tau_{rad}} + \frac{1}{\tau_{Ab}} + \frac{1}{\tau_p} \\
&\quad + (f_i c_p + C_{Ah}) \left[ \frac{\left( \frac{1}{\tau_{rad}} + \frac{1}{\tau_{Ab}} \right) N_{Erth}^* + v_g g_0 (2N_{Erth}^* - N_{Er}) S_0}{f_i c_p (N_{Er} - N_{Erth}^*) - C_{Ah} N_{Erth}^*} \right]
\end{aligned}$$

(C.32)



## APPENDIX – D

### Flowchart for Transient Characteristics of Excited Er atom and Photon Density for Step Input



inc = initial condition

## REFERENCES

- [1] Y. H. Xie, E. A. Fitzgerald and Y. J. Mii, "Evaluation of erbium-doped silicon for optoelectronic applications," *J. Appl. Phys.*, Vol. 70, p. 3223, 1991.
- [2] A. Polman, J. S. Custer, E. Snokes, and G. N. Van den Hoven, "Incorporation of high concentrations of erbium in crystal silicon," *Appl. Phys. Lett.*, Vol. 62, pp. 507-509, 1993.
- [3] J. Michel, J. L. Benton, R. F. Farante, D. C. Jacobson, D. J. Eaglesham, E. A. Fitzgerald, Y. H. Xie, J. M. Poate, and L. C. Kimerling, "Impurity enhancement of the 1.54- $\mu\text{m}$   $\text{Er}^{3+}$  luminescence in silicon," *J. Appl. Phys.*, Vol. 70, p. 2672, 1991.
- [4] G. Franzo, F. Priolo, S. Coffa, A. Polman, and A. Carnera, "Room-temperature electroluminescence from Er-doped crystalline Si," *Appl. Phys. Lett.*, Vol. 64, p. 2235, 1994.
- [5] H. Ennen, J. Schneider, G. Pomrenke, and A. Axmann, "1.54- $\mu\text{m}$  luminescence of erbium-implanted III-V semiconductors and silicon," *Appl. Phys. Lett.*, Vol. 43, p. 943, 1983.
- [6] H. Ennen, J. Wagner, H. D. Muller, and R. S. Smith, "Photoluminescence excitation measurements on GaAs:Er grown by molecular-beam epitaxy," *J. Appl. Phys.*, Vol. 61, p. 4877, 1987.
- [7] Y. S. Tang, K. C. Heasman, W. P. Gillin, and B. J. Sealy, "Characteristics of rare-earth element implanted in silicon," *Appl. Phys. Lett.*, Vol. 55, p. 432, 1989.
- [8] D. L. Alder, D. C. Jacobson, D. J. Eaglesham, M. A. Marcus, J. L. Benton, J. M. Poate, and P. H. Citrin, "Local structure of 1.54- $\mu\text{m}$  luminescence  $\text{Er}^{3+}$  implanted in Si," *Appl. Phys. Lett.*, Vol. 61, p. 2181, 1992.
- [9] J. L. Benton, J. Michel, L. C. Kimerling, D. C. Jacobson, Y. H. Xie, D. J. Eaglesham, E. A. Fitzgerald, and J. M. Poate, "The electrical and defect properties of erbium-implanted silicon," *J. Appl. Phys.*, Vol. 70, p. 2667, 1991.
- [10] S. Libertino, S. Coffa, G. Franzo, and F. Priolo, "The effects of oxygen and defects on the deep trap level properties of Er in crystalline Si," *Appl. Phys. Lett.*, Vol. 78, p. 3867, 1995.



- [11] F. Priolo, S. Coffa, G. Franzo, C. Spinella, A. Carnera and V. Bellani, "Electrical and optical characterization of Er-implanted Si: The role of impurities and defects," *J. Appl. Phys.*, Vol. 74, p. 4936, 1993.
- [12] S. Coffa, G. Franzo, F. Priolo, A. Polman, and R. Serna, "Temperature dependence and quenching processes of the intra-4f luminescence of Er in crystalline Si," *Phys. Rev. B*, Vol. 49, p.16313, 1993.
- [13] S. Lombardo, S. U. Campisano, G. N. van den Hoven, and A. Polman, "Erbium in oxygen-doped silicon: Electroluminescence," *J. Appl. Phys.*, Vol. 77, p. 6504, 1995.
- [14] F. Priolo, G. Franzo, S. Coffa, A. Polman, S. Libertino, R. Barklie, and D. Carey, "The erbium-impurity interaction and its effect on the 1.54  $\mu\text{m}$  luminescence of  $\text{Er}^{3+}$  in crystalline silicon," *Appl. Phys. Lett.*, Vol. 78, p. 3874, 1995.
- [15] P. G. Kik, M. J. A. de Dood, K. Kikoin, and A. Polman, "Excitation and deexcitation of  $\text{Er}^{3+}$  in crystalline silicon," *Appl. Phys. Lett.*, Vol. 70, p. 1721, 1997.
- [16] Jung H. Shin, G. N. van den Hoven, and A. Polman, "Direct experimental evidence for trap-state mediated excitation of  $\text{Er}^{3+}$  in silicon," *Appl. Phys. Lett.*, Vol. 67, p. 377, 1995.
- [17] Francesco Priolo, Giorgia Franzo, Salvatore Coffa and Alberta Carnera, "Excitation and nonradiative deexcitation processes of  $\text{Er}^{3+}$  in crystalline Si," *Phys. Rev. B*, Vol. 57, p. 4443, 1998.
- [18] D. T. X Thao, C. A. J. Ammerlaan, and T. Gregorkiewicz, "Photoluminescence of erbium-doped silicon: Excitation power and temperature dependence," *J. Appl. Phys.*, Vol. 88, p. 1443, 2000.
- [19] J. Palm, F. Gan, B. Zheng, J. Michel, and L. C. Kimerling, "Electroluminescence of erbium-doped silicon," *Phys. Rev. B*, Vol. 54, p.17603, 1996.
- [20] S.Coffa, F. Priolo, G. Franzo, A. Carnera, and C. Spinella, "Optical activation and excitation mechanism of Er implanted in Si," *Phys. Rev. B*, Vol. 48, p.11782, 1993.
- [21] M. Q. Huda, S. A. Siddiqui, and M. S. Islam, "Explaining the erbium luminescence profile in silicon under short excitation pulses," *Solid State Communications*, Vol. 118, p. 235, 2001.
- [22] Giorgia Franzo, Salvatore Coffa, Francesco Priolo, and Corrado Spinella, "Mechanism and performance of forward and reverse bias electroluminescence at 1.54  $\mu\text{m}$  from Er-doped Si diodes," *J. Appl. Phys.*, Vol. 81, p. 2784, 1997
- [23] Shun Lien Chuang, *Physics of Optoelectronic Devices*, Second edition, John Willy & Sons, New York, 1995.

- [24] J. Wilson and J. F. B. Hawkes, *Optoelectronics An Introduction*, Second edition, Prentice-Hall International (UK) Limited, 1996.
- [25] M. Q. Huda, and S. I. Ali, "A study on stimulated emission from erbium in silicon," *Materials Science & Engineering B105* (2003), p-p146-149.
- [26] L. A. Coldren, and S. W. Corzine, *Diode Lasers and Photonic Integrated Circuits*, John Wiley & Sons, Newyork, 1995.
- [28] Joseph T. Verdeyen, *Laser Electronics*, Second Edition, Prentice Hall, 1989.
- [27] K. Y. Lau, and A. Yariv, "Ultra-high speed semiconductor lasers," *IEEE J. Quantum Electronics*, Vol. QE-21, pp. 121-137, 1985.
- [28] Rodney S. Tucker, "High-speed Modulation of Semiconductor Lasers," *J. of Lightwave Technology*, Vol. LT-3, No. 6, 1985.
- [29] K. A. Black, E. S. Bjorlin, J. Piprek, E. L. Hu, and J. E. Bowers, "Small-signal frequency response of long-wavelength vertical-cavity lasers," *IEEE Photonics Technology Letters*, Vol. 13, No. 10, 2001.
- [30] J. Wang, M. K. Haldar, L. Li., and F. V. C. Mendis, "Enhancement of modulation bandwidth of laser diodes by injection locking," *IEEE Photonics Technology Letters*, Vol. 8, No. 1, 1996.
- [31] G. Morthier, and B. Moeyersoon, "Improvement of direct modulation behavior of semiconductor lasers by using a holding beam," *IEEE Photonics Technology Letters*, Vol. 16, No. 7, 2004.

